Tectonophysics 658 (2015) 14–45

Contents lists available at ScienceDirect

Tectonophysics

journal homepage: www.elsevier.com/locate/tecto

Invited Review

# Mantle structure and tectonic history of SE Asia

Robert Hall [a,*], Wim Spakman [b,c]

[a] SE Asia Research Group, Department of Earth Sciences, Royal Holloway University of London, Egham, Surrey TW20 0EX, United Kingdom
[b] Department of Earth Sciences, Utrecht University, Budapestlaan 4, 3584CD Utrecht, The Netherlands
[c] Centre for Earth Evolution and Dynamics — CEED, University of Oslo, Norway

ARTICLE INFO

*Article history:*
Received 27 April 2015
Accepted 6 July 2015
Available online 26 July 2015

*Keywords:*
Subduction
Tomography
Tectonic reconstructions
Indonesia

ABSTRACT

Seismic travel-time tomography of the mantle under SE Asia reveals patterns of subduction-related seismic P-wave velocity anomalies that are of great value in helping to understand the region's tectonic development. We discuss tomography and tectonic interpretations of an area centred on Indonesia and including Malaysia, parts of the Philippines, New Guinea and northern Australia. We begin with an explanation of seismic tomography and causes of velocity anomalies in the mantle, and discuss assessment of model quality for tomographic models created from P-wave travel times. We then introduce the global P-wave velocity anomaly model UU-P07 and the tectonic model used in this paper and give an overview of previous interpretations of mantle structure. The slab-related velocity anomalies we identify in the upper and lower mantle based on the UU-P07 model are interpreted in terms of the tectonic model and illustrated with figures and movies. Finally, we discuss where tomographic and tectonic models for SE Asia converge or diverge, and identify the most important conclusions concerning the history of the region. The tomographic images of the mantle record subduction beneath the SE Asian region to depths of approximately 1600 km. In the upper mantle anomalies mainly record subduction during the last 10 to 25 Ma, depending on the region considered. We interpret a vertical slab tear crossing the entire upper mantle north of west Sumatra where there is a strong lateral kink in slab morphology, slab holes between c.200–400 km below East Java and Sumbawa, and offer a new three-slab explanation for subduction in the North Sulawesi region. There is a different structure in the lower mantle compared to the upper mantle and the deep structure changes from west to east. What was imaged in earlier models as a broad and deep anomaly below SE Asia has a clear internal structure and we argue that many features can be identified as older subduction zones. We identify remnants of slabs that detached in the Early Miocene such as the Sula slab, now found in the lower mantle north of Lombok, and the Proto-South China Sea slab now at depths below 700 km curving from northern Borneo to the Philippines. Based on our tectonic model we interpret virtually all features seen in upper mantle and lower mantle to depths of at least 1200 km to be the result of Cenozoic subduction.



**Contents**



* Corresponding author at: Department of Earth Sciences, Royal Holloway University of London, Egham, Surrey TW20 0EX, United Kingdom. Tel.: +44 1784 443897.
*E-mail address:* robert.hall@rhul.ac.uk (R. Hall).

http://dx.doi.org/10.1016/j.tecto.2015.07.003
0040-1951/

## 1. Introduction

In this paper our focus is an assessment of independent models of tectonic evolution and mantle structure concerned with SE Asia. We discuss tomography and tectonic interpretations of the region centred on Indonesia and including Malaysia, parts of the Philippines, New Guinea and northern Australia (Fig. 1).

At present much of the SE Asia region can be considered part of the Eurasian plate, and for some a separate sub-plate, given various names such as the SE Asia plate or the Sunda block, at a boundary that varies in position according to author (e.g. Bird, 2003; McCaffrey, 1996; Rangin et al., 1999; Simons et al., 2007). SE Asia is bounded largely by subduction zones and is situated in a position where major plates are converging from the south and east (India, Australia, Pacific, Philippine Sea). Subducted slabs are mainly well defined by seismicity down to depths of about 660 km (Fig. 1B) and by volcanoes (Fig. 1A). The region has a particularly complicated geology and plate tectonic history which has been dominated by subduction (e.g. Audley-Charles et al., 1988; Haile, 1973; Hall, 1996, 2002, 2012; Hamilton, 1979; Hutchison, 1989; Katili, 1973, 1975; Lee and Lawver, 1995; Metcalfe, 1990, 2011, 2013). The SE Asian promontory has grown primarily as a result of subduction and there have been thousands of kilometres of lithosphere subducted during the Mesozoic as Tethyan oceans were subducted, and during the Cenozoic as Australia moved northwards and the Pacific plates moved westwards.

It is now accepted that the mantle contains a record of subduction that can be imaged because subducted lithosphere produces a strong temperature anomaly which allows slabs to be detected as regions with relatively high seismic velocities. High-resolution (P-wave) seismic tomography reveals such anomalies although the images are blurred representations of mantle structure. Interpretation of subducted slabs is uncontroversial in regions which are seismically active and the combination of seismicity and tomography can reveal details of slab morphology and structure that may be used to understand the history of subduction. Anomalies in aseismic regions can be more problematic to interpret since they may result from processes, as yet unidentified, other than subduction. Nonetheless, seismic tomography should be of great value in helping to understand the tectonic development of SE Asia because its active margins are characterised by intense seismicity and volcanic activity and there are obvious, relatively simple, seismic velocity anomalies in the upper mantle which are clearly subduction-related.

Global Positioning System (GPS) measurements (Bock et al., 2003; Simons et al., 2007) and other kinematic data (DeMets et al., 1990, 2010) indicate very high rates of relative motions between plates and smaller tectonic fragments in the region. The rates of subduction at the margins of SE Asia are high, typically between 5 and 10 cm/year, and locally even higher. The lengths of slabs in the upper mantle identified by seismicity to depths of c. 660 km can therefore record only a limited period of time, of the order of 10 to 25 Ma, depending on rates of subduction. A longer subduction history may be recorded in the lower mantle. Like many other workers, but not all (e.g. Anderson, 2007; Hamilton, 2007), we consider that parts, or all, of subducted slabs often enter the lower mantle. Positive velocity anomalies below 660 km have been interpreted to record subduction that occurred as early as ~250 Ma (e.g. van der Meer et al., 2010). A good example of subduction history recorded in the lower mantle is seen in the Indonesian region between Java and the Banda arc (Fig. 2). In the east none of the slab subducted at the former Banda trench penetrates into the lower mantle and there is a large flat lying portion of the slab resting on the 660-km discontinuity (Spakman and Hall, 2010), whereas further west the subducted slab becomes almost vertical below about 300 km and the positive velocity anomaly can be traced well into the lower mantle to depths of c. 1500 km (Fukao et al., 1992; Puspito and Shimazaki, 1995; Widiyantoro and van der Hilst, 1997). This is not an artefact of tomographic methodology and we consider it to be lithosphere that was subducted before the slab now imaged in the upper mantle.

Interpreting tectonic history from seismic tomography is not straightforward, even for the upper mantle, and even if it is entirely the result of subduction. Anomalies at the same depth may correspond to subduction of lithosphere of different ages, at different rates, may result from subduction oblique to the trench, and slabs may deform during subduction. Furthermore, we cannot exclude seismic heterogeneities resulting from other processes or inherited in different ways, and some anomalies are simply artefacts of the tomographic imaging. These problems become even greater for the lower mantle where the interpreted subducted slabs are less plate-like and more amorphous, perhaps owing to folding and thickening in the more viscous lower mantle. Thus, linking imaged anomalies to past tectonic evolution becomes less well constrained. Despite the difficulties, there are now many parts of the globe where imaged upper and lower mantle structure has been convincingly interpreted in terms of tectonic history. A tectonic reconstruction model can be used to predict where lithosphere has been subducted and how much has been consumed in plate convergence zones. The predictions can be compared to the mantle structure interpreted by seismic tomography and if the two are independent (i.e. the tomographic model has not been used in making the reconstruction) the tomography provides an independent test of the tectonic reconstruction, and conversely the plate tectonic model may suggest interpretations of mantle structure. This analysis may then result in changes of the tectonic reconstruction, particularly if remnants of proposed subduction are not detected or if remnants of subduction are found in a different location than predicted.

We begin with an explanation of seismic tomography, assessment of tomographic model quality for tomography models created from seismic P-wave travel times and causes of velocity anomalies in the mantle. Then we introduce the detailed global P-wave velocity anomaly model UU-P07 used in the paper and explain how the imaged mantle

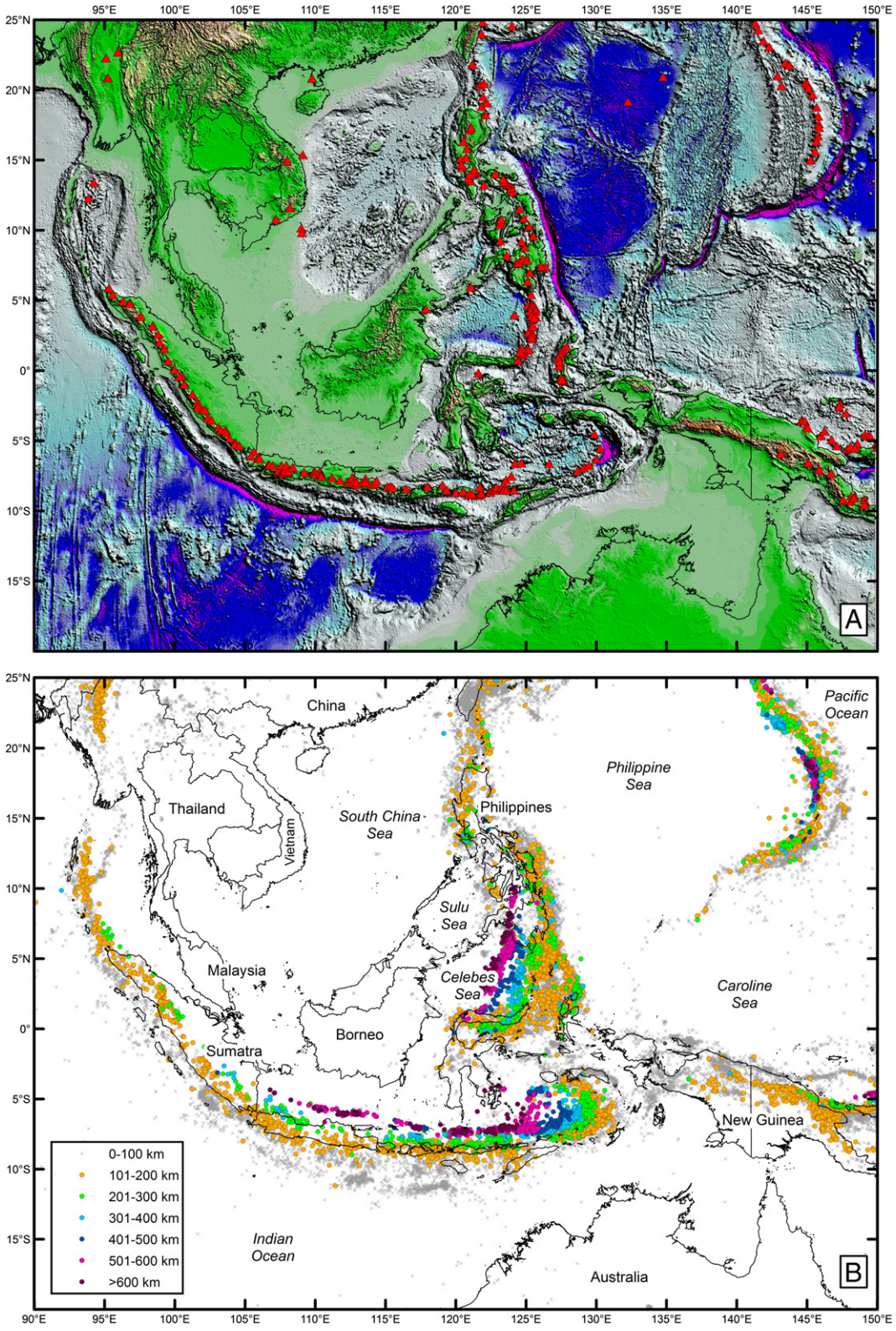


**Fig. 1.** A. DEM of the region including SE Asia, the Western Pacific, eastern Indian Ocean and northern Australia from satellite gravity-derived bathymetry combined with SRTM topography (Sandwell and Smith, 2009). Red filled triangles are volcanoes from the Smithsonian Institution Global Volcanism Program (Siebert and Simkin, 2002). B. Seismicity in and around SE Asia with hypocentre depths (Engdahl et al., 1998).

structure of SE Asia mantle structure will be presented in figures and movies, followed by an overview of previous interpretations of mantle structure. Next we introduce the tectonic model used in this paper, and continue with an assessment of velocity anomalies in the upper, and then lower, mantle and our interpretation of them in terms of the tectonic model. Finally, we discuss where tomographic and tectonic models for SE Asia converge or diverge, and identify the most important conclusions concerning the history of the region.

## 2. Introduction to seismic tomography models based on travel-times

### 2.1. A summary of travel-time tomography

Most of the three-dimensional models of SE Asian mantle structure have been created with seismic travel-time tomography using P-wave data and adopting the seismic ray approximation (e.g. Fukao et al., 1992; Puspito et al., 1993; Widyantoro and van der Hilst, 1996). Seismic travel-time tomography is a geophysical inversion method that converts observed travel times of seismic waves into a three-dimensional (3-D) model of the seismic velocity structure of the mantle (e.g. Spakman et al., 1993). Usually, tomographic models are presented as colour maps displaying seismic velocity anomalies as percentages of a used 1-D background, or reference model, of seismic velocity (e.g. Fig. 2). Travel-time tomography developed from the pioneering work of Aki et al. (1977). Other developments have meanwhile led to many different tomographic methods for different data extracted from seismograms such as classical travel-time picks of seismic waves, arrival times determined from waveforms of body ways or surface waves, or even large portions of a seismogram (e.g. Fichtner et al., 2013; Zhu et al., 2012). For an overview of the various tomographic methods we refer to Nolet (2008). A summary of travel-time tomography, particularly relevant to most of the models shown here, follows below.

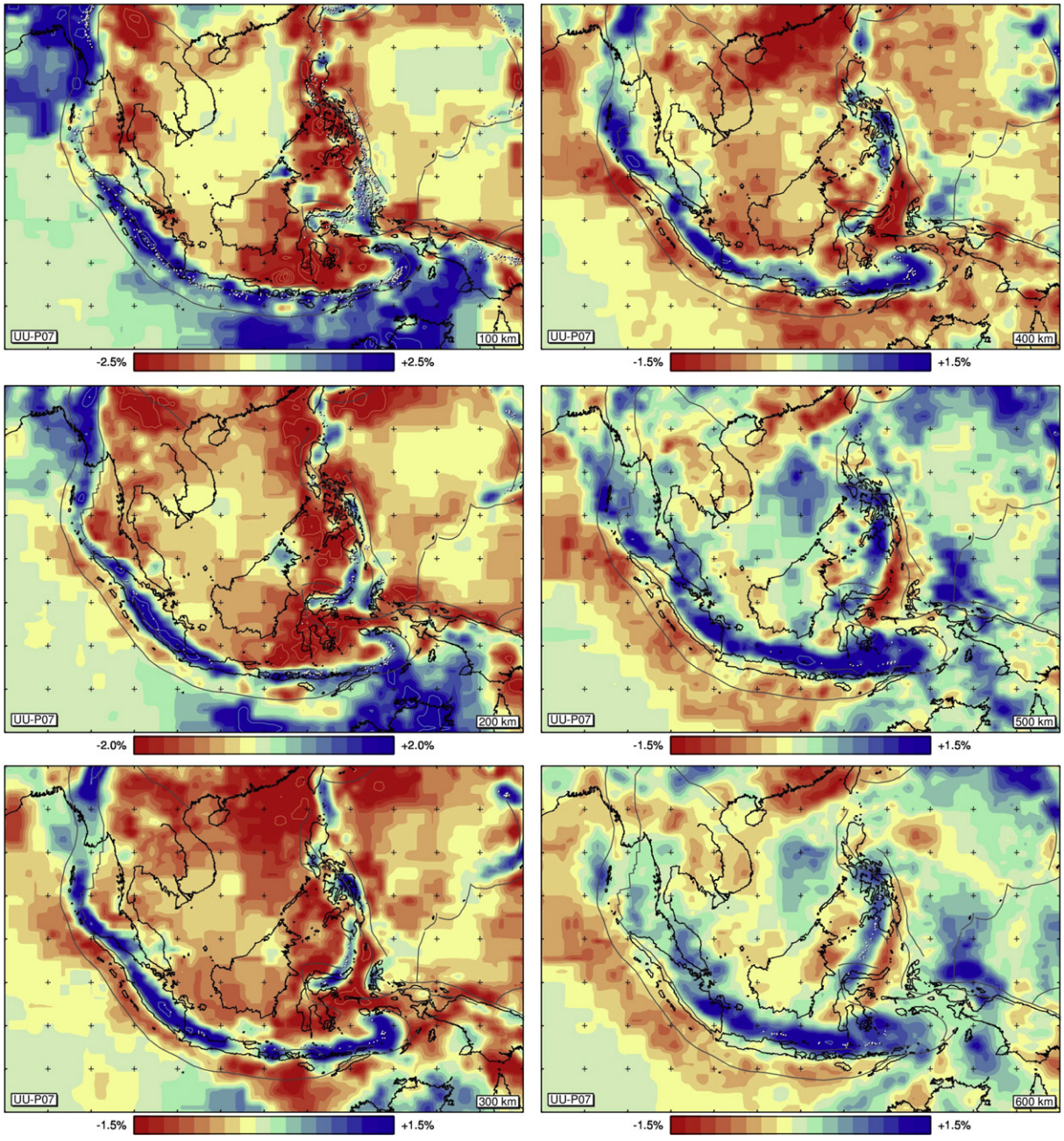


**Fig. 2.** Tomographic slices through model UU-P07 (Amaru, 2007) at selected depths. Colours indicate the P-wave wave-speed anomalies relative to the radial reference model ak135 of Kennett et al. (1995). Notice that the limits of the wave-speed anomaly scale change with depth. This depth variation follows the scaling between temperature and wave-speed anomalies as used in Goes et al. (2005). Blue colours correspond to positive and red to negative wave-speed anomalies. Extra contour lines indicate regions where anomalies are in excess of the colour contour limits by multiples of 1%. White dots denote earthquake hypocentres from the EHB data set (Engdahl et al., 1998) used in tomography. Only events within 5 km of the depth of the tomographic slice are plotted. Small crosses denote the longitude–latitude grid at 5° intervals. Solid lines indicate coastlines, plate boundaries or other major tectonic lineaments in the region.

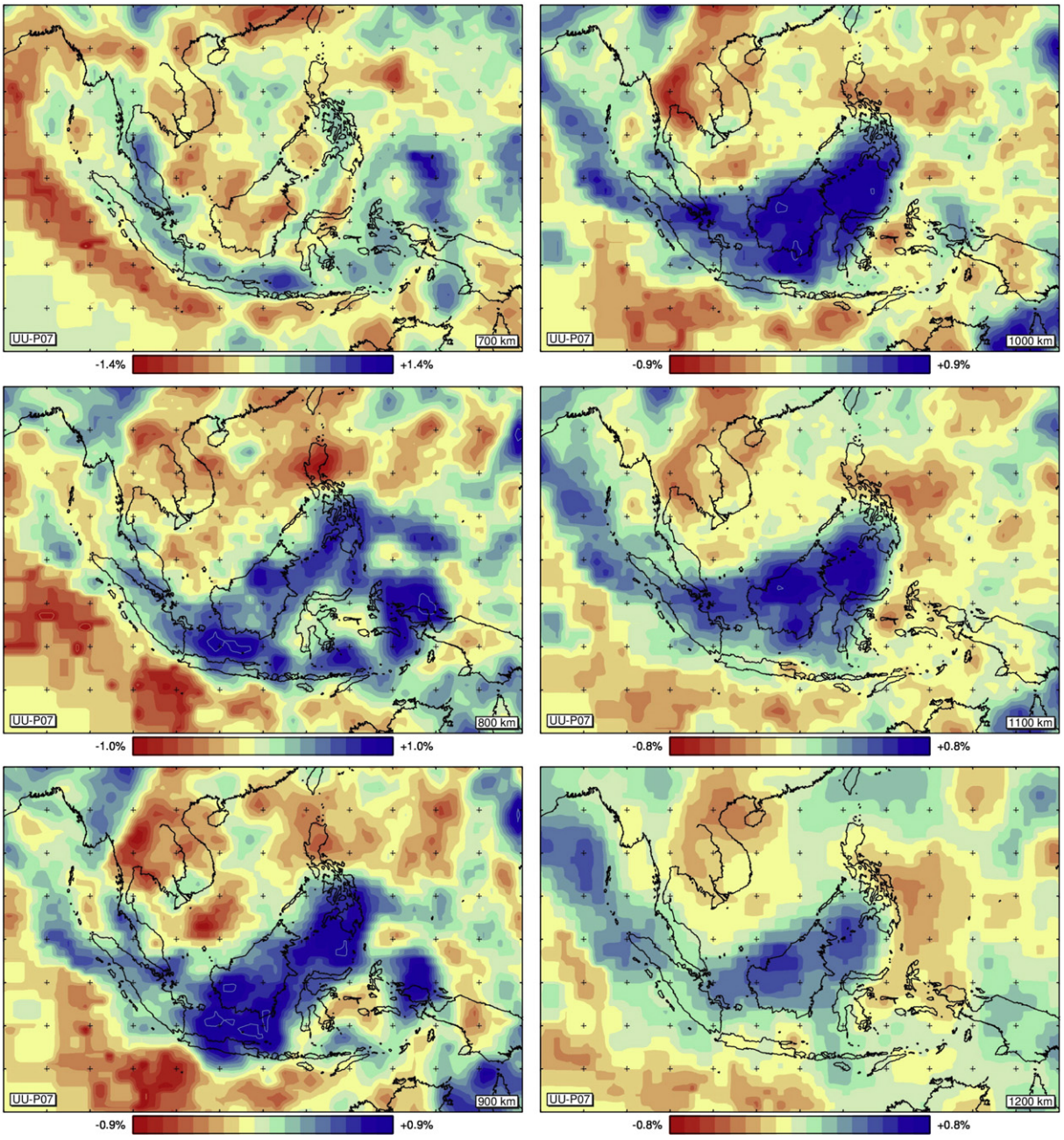


**Fig. 2** (*continued*).

Travel-time tomography based on the ray approximation combines seismic rays with travel time picks of short-period (~1 s) P-waves. A seismic ray is a high frequency representation of wave propagation and constitutes the particular path through the mantle along which a seismic wave travels from an earthquake hypocentre to a seismological station. The ray geometry $L$ is fully determined by the seismic velocity structure $v(\boldsymbol{r})$ of the mantle. The observed travel time $T$ is interpreted as an integrated measure of all seismic velocities encountered along the ray path. Mathematically this is expressed as the integral $T = \int_L 1/v(\boldsymbol{r})dl$. This travel-time integral forms the basis of travel-time tomography. Global travel-time tomography problems are based on a data set consisting of many millions of these integral equations. The tomographic inversion focuses on estimating the 3-D seismic velocity anomaly field $\Delta v(\boldsymbol{r})$ with respect to a laterally averaged seismic velocity $v_o(r)$ such as the radial reference model *ak135* of Kennett et al. (1995) which is often used for global travel-time tomography.

A reference model plays an important role in the formulation of the tomographic problem. It facilitates the computation of approximations $L_o$ of seismic rays $L$, of the estimation of earthquake hypocentres from which $L_o$ starts, and of reference model travel times $T_o = \int_{L_o} \frac{1}{v_o} dl_o$. This information is used to formulate a mathematical linearization of the delay time integral equations $d = T - T_o = \int_L \frac{1}{(v_o + \Delta v)} dl - \int_{L_o} \frac{1}{v_o} dl_o$ relative to these reference model quantities. The delay-time $d$ is the difference between observed travel time $T$, acquired along the true ray $L$, and reference travel-time $T_o$ computed along the reference model ray geometry $L_o$.

As a next step towards inversion, the Earth's mantle is usually subdivided into 3-D network of non-overlapping cells which can be of variable size (e.g. Bijwaard et al., 1998; Fukao et al., 1992; Spakman and Bijwaard, 2001; Widiyantoro and van der Hilst, 1997), or for

instance a prescribed network of velocity nodes between which velocity is interpolated (e.g. Montelli et al., 2006). The cell model is the basis of a mathematical parameterization of the unknown seismic velocity anomaly structure $\Delta v(\boldsymbol{r})$ of the mantle and is used to convert the integral equations into a linear algebraic set of observation equations $\boldsymbol{d_{obs}} = \boldsymbol{Am} + \epsilon$, which renders the tomographic inverse problem suitable for solving on computers. $\boldsymbol{d_{obs}}$ is the data vector consisting of millions of delay times; $\boldsymbol{m}$ is the model vector from which all velocity anomaly values in the cell model are obtained while $\boldsymbol{m}$ also incorporates parameters associated with hypocentre mislocation and station corrections; $\boldsymbol{A}$ is the matrix constructed from ray path intersections with cells and from coefficients related to hypocentre mislocation and seismological stations (e.g. Bijwaard et al., 1998; Spakman et al., 1993). The unknown vector of errors $\epsilon$ absorbs all inconsistencies between the data $\boldsymbol{d_{obs}}$ and $\boldsymbol{Am}$. Clearly, the solution sought is the true mantle model $\boldsymbol{m_{true}}$ constituting the true anomalous mantle cell structure. By writing $\boldsymbol{d_{obs}} = \boldsymbol{Am_{true}} + \epsilon$, the error vector $\epsilon$ can be interpreted to comprise not only travel-time observation errors but also implicit errors due to using approximate ray theory, due to linearization of the observation equation relative to reference model quantities, and due to the approximation of true anomalous mantle structure by the adopted model parameterization. There are several ways to minimize the different sources of implicit data errors, for instance by using adaptive cell parameterization (Bijwaard et al., 1998; Spakman and Bijwaard, 2001), by using iterative approaches with repeated 3-D ray tracing and earthquake relocation (Bijwaard and Spakman, 2000), or by starting from different 1-D reference models (Spakman et al., 1993; van der Hilst and Spakman, 1989) or even from 3-D reference models (Amaru, 2007; Widiyantoro et al., 2000).

Due to insufficient data and data errors $\epsilon$ the linear equation $\boldsymbol{d_{obs}} = \boldsymbol{Am} + \epsilon$ has no unique solution and many different models may fit the observations equally well. A general strategy towards determining solutions is to find models $\hat{\boldsymbol{m}}$ with data predictions $\boldsymbol{d_{pred}} = \boldsymbol{A}\hat{\boldsymbol{m}}$ that minimize the difference $\epsilon = \boldsymbol{d_{obs}} - \boldsymbol{d_{pred}}$, e.g. by using least squares methods, to some acceptable level guided by whatever is known, or perceived, about error variances and error correlations. An additional complicating factor is that there are usually insufficient data to uniquely resolve mantle structure on the cell model. To find acceptable solutions there are basically two strategies. The first is to search the model space for suitable models, compute for each the data prediction $\boldsymbol{d_{pred}}$, and devise search strategies to select the model best fitting the data using a predefined data fit measure. This approach has so far only been applied in mantle tomography using rather coarse model parameterizations involving relatively few model parameters (e.g. Rawlinson et al., 2014; Trampert et al., 2004). For obtaining detailed mantle models this strategy is too demanding of computer time. The second strategy is based on assuming additional information on general aspects of model geometry, for instance by putting restrictions on model amplitudes and/or requiring the model to be spatially flat and/or smooth. This can be implemented in several ways depending on the inversion approach (e.g. Nolet, 2008) and regularises the inverse problem such that selected solutions can be computed. The importance of these additional constraints for selecting a solution can be tuned. Finding an acceptable model always requires making a subjective choice between fitting the data and fitting the additional constraints on model geometry.

Formally the entire data inversion step can be written, independent of methodology, as $\hat{\boldsymbol{m}} = \boldsymbol{G}^{-}\boldsymbol{d}$ leading to the estimated tomographic model $\hat{\boldsymbol{m}}$. The matrix $\boldsymbol{G}^{-}$ is called the generalized inverse and is not unique as it depends on the imposed model regularisation and on estimates of data errors and their correlations. The generalized inverse can be explicitly computed in small inverse problems, but for many practical problems with a large number of model parameters $\boldsymbol{G}^{-}$ cannot be computed explicitly. Instead, the multiplication $\boldsymbol{G}^{-}\boldsymbol{d}$ is implicitly constructed by iterative solution techniques (e.g. Spakman and Nolet, 1988) leading to an approximated solution $\hat{\boldsymbol{m}}$ from which estimates of the velocity anomaly in each cell, as well as hypocentre and station parameters, can be readily obtained.

Due to the assumptions and approximations described above, the tomography model $\hat{\boldsymbol{m}}$ is obtained as an approximation of real mantle structure $\boldsymbol{m_{true}}$ and is usually presented in percentages $\Delta v/v_o(r)$ of the reference velocity at radius $r$. The preference for a particular model $\hat{\boldsymbol{m}}$ created is that of the tomographer who makes the choices of applicable theory, reference model, model parameterisation, estimates of data errors, and the inversion strategy, the latter being crucially based on the adopted data fit measure and on the additional regularisation constraints imposed.

### 2.2. Model quality assessment

Without measures of model quality a tomographic model cannot be reasonably interpreted. For very large inverse problems with many tens to hundreds of thousands of model parameters, assessment of the spatial resolution and model amplitude errors is usually performed with sensitivity analysis based on imaging synthetic seismic velocity models $\boldsymbol{m}$ (Humphreys and Clayton, 1988; Rawlinson et al., 2014; Spakman and Nolet, 1988). Synthetic data $\boldsymbol{d_{syn}}$ are first generated from a synthetic seismic velocity model using the same ray paths as in the real data inversion, i.e., by forward computation $\boldsymbol{Am_{syn}} = \boldsymbol{d_{syn}}$. A synthetic model usually consists of an alternating pattern of negative and positive anomalies, e.g. isolated cells of different sizes (Spakman and Nolet, 1988) or checkerboard structures of different cell sizes (Fukao et al., 1992). The synthetic data are inverted in the same manner as the actual data. This leads to the solution $\hat{\boldsymbol{m}}_{syn} = \boldsymbol{G}^{-}\boldsymbol{d}_{syn}$ by invoking the same generalized inverse. Substituting $\boldsymbol{d}_{syn} = \boldsymbol{Am}_{syn}$ into this equation leads to $\hat{\boldsymbol{m}}_{syn} = \boldsymbol{G}^{-}\boldsymbol{Am}_{syn}$. Defining $\boldsymbol{R} = \boldsymbol{G}^{-}\boldsymbol{A}$ gives $\hat{\boldsymbol{m}}_{syn} = \boldsymbol{Rm}_{syn}$ where $\boldsymbol{R}$ is called the resolution matrix. The resolution matrix $\boldsymbol{R}$ explicitly describes in what way the model value in a particular cell depends on the values in all other cells; spatial resolution is a measure of the linear dependence between model parameters. The resolution matrix $\boldsymbol{R}$ is exactly the same as the one pertaining to the real data inversion. Starting from $\hat{\boldsymbol{m}} = \boldsymbol{G}^{-}\boldsymbol{d}$ and substituting $\boldsymbol{d} = \boldsymbol{Am_{true}} + \epsilon$, leads to $\hat{\boldsymbol{m}} = \boldsymbol{Rm_{true}} + \boldsymbol{G}^{-}\boldsymbol{\varepsilon}$. The term $\boldsymbol{G}^{-}\boldsymbol{\varepsilon}$ is caused by the effects of (unknown) data and theoretical errors and explicitly shows that data error affects a solution apart from resolution issues.

The resolution matrix $\boldsymbol{R}$ explicitly describes how the true mantle, $\boldsymbol{m_{true}}$ or $\boldsymbol{m}_{syn}$, is related to the tomographic model, $\hat{\boldsymbol{m}}$ or $\hat{\boldsymbol{m}}_{syn}$, respectively. Clearly, a perfectly resolved model has $\boldsymbol{R} = \boldsymbol{I}$, where $\boldsymbol{I}$ is the identity matrix. For large inverse problems the resolution matrix cannot be computed and this is where sensitivity analysis proves its value. By comparing $\hat{\boldsymbol{m}}_{syn}$ to $\boldsymbol{m}_{syn}$ one can arrive at estimates regarding spatial resolution and amplitude response. By adding synthetic noise $\boldsymbol{\varepsilon_{syn}}$, i.e. solving $\boldsymbol{d_{syn}} = \boldsymbol{Am} + \boldsymbol{\epsilon_{syn}}$, one can also assess the effect of data noise on the solution by computing $\boldsymbol{G}^{-}\boldsymbol{\varepsilon_{syn}}$, or by comparing sensitivity tests conducted with or without noise, leading to a more integral assessment of how the mantle structure $\boldsymbol{m_{true}}$ is mapped into a preferred model $\hat{\boldsymbol{m}}$. Examples of sensitivity tests for combined estimates of spatial resolution and noise are given in this paper (e.g. Fig. 3).

The choices made by the tomographer leading to a particular model $\hat{\boldsymbol{m}}$ cannot all be tested by inspecting the resolution matrix or by sensitivity analysis with synthetic models. Sensitivity analysis cannot test the assumptions and approximations that lead to the equation $\boldsymbol{d} = \boldsymbol{Am} + \epsilon$. This equation can only be used to study error propagation into the model and how well the preferred model is spatially resolved, which depends on the matrix $\boldsymbol{A}$, the assumptions made about the statistics of data errors, and on the additional regularisation constraints imposed on the model geometry. Sensitivity analysis for estimating image quality also has potential pitfalls if conclusions are drawn from tests with only a single synthetic model (Lévêque et al., 1993) but the risk of misinterpretation can be reduced considerably by analysing a wide range of synthetic models (e.g. Bijwaard et al., 1998). The basic requirement for a useful test is that a synthetic test model should contain structure to which the data are insensitive; formally, contain

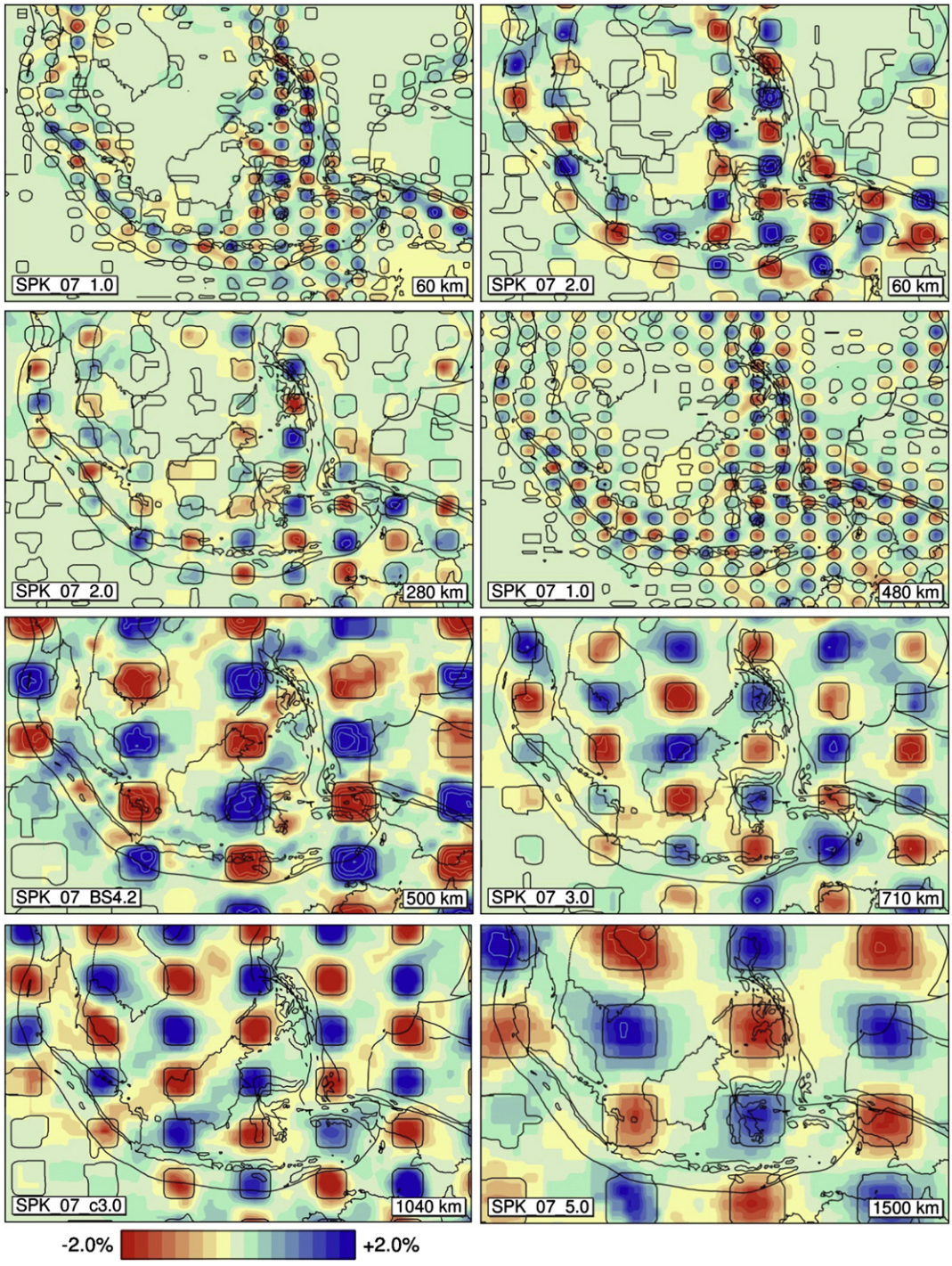


**Fig. 3.** Examples of sensitivity test results of imaging various synthetic block models. Black lines show coastlines and plate boundaries and the location of isolated synthetic blocks with seismic wave-speed anomaly amplitudes of +5% or −5% with respect to the 1-D reference model ak135 of Kennett et al. (1995). The input blocks can have an irregular shape, which is due to the parameterization of the tomographic model with cells of variable dimension. This is also the reason for the absence of synthetic blocks of a particular size in some parts of the model. The colours show the tomographic image of the input model using the same procedure as when real data are input. Gaussian noise was added to the synthetic data prior to tomographic inversion to attain a comparable similar variance reduction. More details can be found in Spakman et al. (1993) and Bijwaard et al. (1998). Comparison of 'input' and 'output' models leads to qualitative assessment of lack of spatial resolution. Lack of resolution can be detected where large amplitudes occur between the blocks, where block anomalies smear into the model, or when block anomalies are not recovered at all. The eight panels illustrate results at different depths and for different input block-models. The last number in the model label at the lower left of each panel gives the characteristic lateral spatial dimension of the input blocks in degrees, i.e. 1.0° at 60 km, 5.0° at 1500 km. The thickness of the blocks is usually half of this size. Note that a lateral distance of 5.0° at 1500 km depth (e.g., last panel) corresponds to ~400 km.

structure that is in the null space of the inverse problem. In that case the *lack* of resolution is always detected by sensitivity analysis. An obvious example of lack of resolution are the cells, or mantle regions, in the model that are not sampled by the seismic rays. More complex resolution artefacts lead to blurring of true mantle structure into larger structures with a different geometry. Blurring can also occur in specific directions only, i.e., smearing of true structure along a locally dominant orientation of seismic ray paths such as along the dip direction of a subducting slab. These resolution artefacts can all be detected by testing with proper synthetic models.

### 2.3. Seismic velocity anomalies

Seismic velocity is a material parameter depending on local elastic properties and density, which in turn depend on temperature, pressure, and composition (Cammarano et al., 2003; Deschamps and Trampert, 2003; Goes et al., 2000). Positive, or fast, velocity anomalies are often associated with the cold cratonic parts of continental lithosphere, with oceanic lithosphere, or with subducted lithosphere in the mantle. Conductive cooling of the lithosphere prior to subduction is the most important cause of the observed velocity contrast between subducted slabs and the ambient mantle. The low thermal conduction in the mantle explains why large volumes of subducted lithosphere remain detectable using tomography long after the lithosphere entered the trench even when subduction occurred hundreds of millions of years ago (e.g. van der Meer et al., 2010). Negative velocity anomalies are often correlated with higher temperatures in the mantle, which can be due to advective temperature transport (e.g. hot mantle upwelling), or may be locally generated (e.g. by partial melting in the mantle wedge above a subducting slab). Compositional effects are still difficult to assess, but play a role for the continental lithosphere (e.g. Lebedev and Nolet, 2003) and may be important for the deeper mantle (Trampert et al., 2004). Compositional effects are not considered dominant for most of the upper mantle above 400 km but can increase in importance below that depth (Cammarano et al., 2003). Applications of predictions of the effects of temperature and composition on seismic velocities to interpretation of imaged seismic velocities are still strongly hampered by the largely unknown error in the amplitudes of imaged seismic velocity anomalies that results from data noise, assumptions and approximations.

In this review paper, we are mostly concerned with the strong thermal anomalies associated with subducted lithosphere. We interpret positive velocity anomalies as images of subducted lithosphere, and negative velocity anomalies as reflections of relatively warmer mantle. P-wave velocity anomalies for the upper mantle vary from a few per cent at the top, in the first few hundreds of kilometres, to c. 1% in the transition zone, decreasing to c. 0.5% in the mid-mantle. According to Goes et al. (2005) this could correspond to a thermal anomaly in the range of 250°K (or 10–20% of ambient mantle temperature) for most depth ranges. Tomographic models based on S-wave data typically image velocity anomalies with amplitudes larger than those based on P-wave data by a factor ~1.7–2.0 which is generally due to a different dependence of S-waves on elastic parameters. The sensitivity of S-wave velocity to temperature anomalies is of the same sign as that of P-wave velocity. A discussion, pertaining to the SE Asian region, on the effects on seismic velocities of temperature and other quantities, such as composition, partial melting and volatiles, can be found in Lebedev and Nolet (2003).

### 2.4. Global mantle model UU-P07

Many tomographic studies based on cell parameterization of the mantle have been performed but differ in cell division, inversion and regularisation method, data treatment, amount of data, reference model, or in taking a regional or global approach. Rather than discussing different models for SE Asia, we present mantle structure from a detailed global mantle model which we use to illustrate mantle structure imaged in other tomographic studies as well as for developing some new interpretations of imaged structure. This model is the global P-wave velocity anomaly model UU-P07 of Amaru (2007) from which the evidence for subduction-related global lower mantle structure was presented by van der Meer et al. (2010, 2012). Several authors (e.g. Chertova et al., 2014; Schellart and Spakman, 2012; Schellart et al., 2009; van Benthem et al., 2013; van Hinsbergen et al., 2012) have used model UU-P07 in studies of regional mantle structure. It is the successor to the BSE model of Bijwaard et al. (1998) and is based on a similar treatment of travel-time data, mantle cell division and inversion approach. The main differences are in the use of more than twice as much data (c. 18 million P-wave type travel times), in a denser cell division of the mantle with lateral cell dimensions which are multiples of 0.5° with a minimum of 0.5° in regions of high ray sampling, and in the use of CRUST2.0 (Laske et al., 2013) as a crustal correction model. Details on how this model was constructed can be found in Amaru (2007). The cell parameterization is dependent on the local ray density with smaller cells placed in mantle volumes of higher ray density (Spakman and Bijwaard, 2001). In the subducted slab regions of SE Asia cell sizes are generally 0.5° or 1°. Cell dimensions also vary with depth. Cell thickness varies from 10 km in the crust, and is 50 km from the base of the crust down to 410 km, then 65 km down to 660 km, and then 100 km at the top of the lower mantle gradually increasing to 200 km in the mid mantle.

### 2.5. Display of tomographic images

In this paper we concentrate on the mantle structure of SE Asia associated with subduction along the Sunda–Banda arc, subduction in the region of Sulawesi, and on the origin of high velocity anomalies in the lower mantle beneath SE Asia and parts of the west Pacific. The imaged mantle structure of the region is presented in a number of figures and movies as Supplementary Data. Fig. 2 shows map view images at selected depths of the tomographic model UU-P07 (Amaru, 2007) for the SE Asian mantle. A complete sequence of such map view images is compiled as a movie file (SEA_UU-P07_mapview.mov; mmc1.mp4) showing depth slices for UU-P07 in the folder Mapview_depth slices_UU-P07. The P-wave velocity anomalies are plotted relative to the reference model ak135 of Kennett et al. (1995). Negative and positive anomalies correspond to regions where the seismic velocity is respectively lower or higher than the reference model value at the corresponding depth. Subducted slabs are marked by positive anomalies displayed with blue-to-green colours.

As discussed above, image blurring is assessed with sensitivity tests for spatial resolution with synthetic velocity models and examples are given in Fig. 3 and movies in the folder Resolution_movies (SVideo_Resolution_1.mov and SVideo_Resolution_2.mov; mmc2.mp4 and mmc3.mp4). The colour contouring in the figure and movies shows how synthetic anomalies of variable dimensions (solid line contours) and with alternating velocity amplitudes of $\pm 5\%$ are recovered in the tomographic inversion. The input blocks are separated by 0% anomalies, and in depths laterally shifted, which facilitates detecting anomaly smearing along locally dominant seismic ray orientations. Anomaly amplitudes are generally underestimated and local smearing effects illustrate limited resolution. These resolution tests also help identify larger regions where the tomographic model is essentially unresolved because of almost complete lack of data sampling the mantle, such as in the top 1000 km of the mantle under the Indian Ocean to the SW of Sumatra, and in the top 400 km under the core of Sundaland (Borneo, the Thai–Malay Peninsula and Indochina). Good spatial resolution at scales of 100 to 200 km is generally obtained in regions of the upper mantle where there are subducted slabs. In the lower mantle, resolution is generally good for all length scales between 200 to 700 km and anomaly smearing is mostly localised; where important for our analysis, we comment on the local resolution.

## 3. Mantle structure of SE Asia: larger scale patterns and early interpretations

The lithosphere of the continental region comprising the Sunda Shelf, Malay Peninsula, Borneo and Java Sea, shows negative seismic P-wave anomalies in all P-wave models. However, these negative seismic velocity anomalies are poorly resolved due to lack of sampling seismic rays. This region, inboard of the enclosing Sunda–Banda–Philippines subduction systems, is essentially the Sundaland continent (Hall and Morley, 2004) and is largely composed of continental

fragments added to Asia from the Triassic to the Cretaceous (e.g. Hall, 2012; Metcalfe, 2011, 2013). The UU-P07 model shows predominantly negative seismic anomalies in the top 100–150 km (Fig. 2 and SEA_UU-P07_mapview.mov; mmc1.mp4) with very limited, or even absent, spatial resolution under Sundaland (Fig. 3 and SVideo_Resolution_1.mov and SVideo_Resolution_2.mov; mmc2.mp4 and mmc3.mp4). Surface wave tomography studies have generally a better sampling of the top 100–150 km of SE Asia and invariably show negative seismic S-wave velocities in the top 100–150 km (Ritzwoller et al., 2002; Lebedev and Nolet, 2003; Shapiro et al., 2008; Ritsema et al., 2011; Schaeffer and Lebedev, 2013) Several of the models are shown in the movie Mapview_depth_slices_different_models/SEA_mapv_4mod.mov (mmc4.mp4). Although S-wave and P-wave velocities respond differently to temperature, composition and density, elevated temperatures lower both P- and S-wave velocities as discussed by Lebedev and Nolet (2003). Temperature effects are probably greater than compositional effects for the lithosphere and other possible causes for lowered seismic velocities such as partial melting, and presence of small amounts of volatiles such as water, or $CO_2$ which can be significant in many SE Asia hydrocarbon basins and may have a mantle origin (Imbus et al., 1998). All would point to a weakened continental lithosphere, or perhaps a partly absent lithospheric mantle.

Thermal weakening of the lithosphere may be a result of long-term Cenozoic subduction beneath continental SE Asia (e.g. Hall, 2002, 2012; Hamilton, 1979; Hutchison, 1989). Another local cause of thermal weakening could be plumes such as the interpreted Hainan plume (Lebedev and Nolet, 2003; Montelli et al., 2006) if the plume head had spread under a large part of Indochina. Intraplate Cenozoic volcanism is widespread in the Indochina–Hainan region (e.g. Barr and MacDonald, 1981; Hoang and Flower, 1998; Wang et al., 2001), particularly since the Middle Miocene, and has also been associated with the existence of the Hainan plume (e.g. Xu et al., 2012). Negative P-wave velocity anomalies are found in UU-P07 model under the Hainan region and Indochina to depths of 1900 km (Fig. 2 and SEA_UU-P07_mapview.mov; mmc1.mp4). At greater depths the negative anomaly can be traced ESE and it connects with the large low velocity region in the deepest mantle under the SW Pacific, which has been proposed to be a major plume generation region (Burke et al., 2008; Torsvik et al., 2006). A third possible contribution to the observed negative seismic velocity anomalies of the Sundaland lithosphere may result from the Triassic to Cretaceous amalgamation of continental blocks that make up much of SE Asia (Metcalfe, 2011, 2013; Hall, 2012; Hall and Sevastjanova, 2012). It is not clear whether these blocks retained their Gondwana mantle lithosphere, or lost it during their movement across the Tethys, during amalgamation with Asia, or perhaps shortly after.

Most of the earlier research focus in the region has been on the complex subduction systems bordering SE Asia along the Andaman–Sunda–Banda trench, along the eastern boundary with the Philippine Sea plate, and subduction zones internal to the region, e.g. North Sulawesi. The morphology of subducted slabs in the upper mantle around Indonesia and the Philippines has been quite well known from seismicity for many years (e.g. Cardwell and Isacks, 1978, 1981; Cardwell et al., 1980; Chiu et al., 1991; Hamburger et al., 1983; Hamilton, 1974, 1979; McCaffrey, 1988, 1989; Newcomb and McCann, 1987). Tomography has provided additional important insights. The most obvious feature of the upper mantle structure in the region is the prominent narrow positive velocity anomaly that can be traced from the Andaman Sea to the Banda Sea which is the product of subduction at the Sunda–Java trench and the former Banda trench (Fig. 2; SEA_UU-P07_mapview.mov; mmc1.mp4). In detail the structure of the subducted slab in the upper mantle is complex. There are several gaps, and prominent bends at depth, beneath Sumatra and the Banda region. Furthermore, there have been a number of suggestions concerning what happens to subducted slabs at the base of the upper mantle.

Fukao et al. (1992) used a global mantle approach focussed on the West Pacific and Indonesian region. They showed that the Java slab dips steeply in the lower part of the upper mantle and crosses the 660-km discontinuity into the lower mantle where the slab dips much less steeply, spreads laterally, and reaches depths up to 1200 km. They explained this using a model of Ringwood and Irifune (1988) by suggesting the subducted slab thickened and buckled to form a megalith above the 660-km discontinuity which then sank into the lower mantle because of its higher density. A similar mechanism for slab thickening was proposed by Das et al. (2000) in the Indonesian region although in their model the thickened slab dips steeply.

Puspito et al. (1993) presented a P-wave travel-time tomography model for the Indonesian region showing several of the main morphological features of slabs. They proposed that the western limb of the inverted U-shaped Molucca Sea plate (Hatherton and Dickinson, 1969) may penetrate into the lower mantle whereas the eastern limb beneath Halmahera reached a depth of about 400 km. They suggested there may be a remnant of an older subduction zone in the lower mantle below the Molucca Sea which they interpreted to be related to Miocene subduction below Sulawesi (Katili, 1978). Puspito et al. (1993) imaged the horseshoe-shaped positive velocity anomaly in the Banda arc, which Puspito and Shimazaki (1995) concluded did not penetrate into the lower mantle in contrast to the subducted Indian ocean slab further west beneath the eastern Sunda arc, which did. Puspito and Shimazaki (1995) also observed that a slab under the Andaman–Sumatra region could be traced deeper into the mantle (to 500 km) than indicated by seismicity (to 250 km).

Widiyantoro and van der Hilst (1996, 1997) produced the first model showing images of laterally continuous subduction along the entire Andaman–Sunda–Banda arc, and to the north under the Molucca Sea. Their major interpretation concerned the connection between the Andaman–Sunda–Banda slab in the upper mantle and the large lower mantle anomaly under SE Asia which they inferred to be one subducting system. They associated the lower mantle part with a Tethyan subduction system that can be traced to the Eastern Mediterranean (Bijwaard et al., 1998; Hafkenscheid et al., 2006; van der Hilst et al., 1997; van der Voo et al., 1999). To the west, under Sumatra, the upper and lower mantle anomalies appear disconnected in the transition zone, which was interpreted as slab detachment. However, this image of slab detachment in the transition zone under Sumatra has not been reproduced in later work (e.g. Bijwaard et al., 1998; Li and van der Hilst, 2010; Pesicek et al., 2008; Replumaz et al., 2004).

Widiyantoro and van der Hilst (1997) inferred an overall clockwise rotation between the upper mantle slab and the lower mantle slab which they linked to the Cenozoic northward advance of India, mid-ocean ridge collision with western Indonesia arcs and escape tectonics postulated for India–Asia collision. They suggested that this may also have caused a southward migration of the eastern Sunda slab explaining the observed kink between the upper and lower mantle Java slab. They tentatively suggested that there is probably a continuous slab in the seismic gap beneath East Java although they observed that the slab could be thinned.

Like earlier workers, Widiyantoro and van der Hilst (1997) contrasted penetration of the subducted slab beneath Java into the lower mantle with a flattening of the subducted slab further east in the transition zone to form a spoon-shape beneath the Banda arc. Their explanation for the shape of the Banda slab followed the 180-degree arc-bending hypothesis of Katili (1973, 1975) which they related to Pliocene collision of the Banda arc with Australia. They confirmed the inverted U-shape of subducted Molucca Sea lithosphere and proposed a steeper dip for the western limb beneath the Sangihe arc compared to the eastern limb below Halmahera, which they attributed to a westward movement of the entire slab system in the mantle.

Similar anomalies in the mantle under SE Asia are imaged in the global mantle model of Bijwaard et al. (1998), as shown in Rangin et al. (1999), Hafkenscheid et al. (2001) and Hall and Spakman (2002). Other global models support slab penetration into the lower

mantle under SE Asia (Fukao et al., 1992, 2001; Li and van der Hilst, 2010).

The morphology of the subducted slab below North Sumatra shows a conspicuous kink (Fig. 2) that has been a topic of considerable interest for many years. Page et al. (1979) and Fauzi et al. (1996) suggested there may be a slab tear beneath Sumatra, possibly linked to the Investigator Fracture Zone, which may be related to the Toba volcanic centre (Chesner, 1998, 2012; Chesner et al., 1991). Lange et al. (2010) also suggested the Investigator Fracture Zone may influence seismicity and presumably slab morphology. Widyantoro and van der Hilst (1996) recognised that the space-time evolution of slab structure beneath Sumatra was not understood and required further study. The Bijwaard et al. (1998) model and subsequent models of the Utrecht group display a clear lateral kink in the slab under NW Sumatra and several other studies have observed changes in orientation and dip of the subducted slabs between Sumatra and the Andaman segment (e.g. Kennett and Cummins, 2005; Richards et al., 2007; Shapiro et al., 2008). Pesicek et al. (2008, 2010) made a detailed study of this region and the lateral kink for which they favoured folding of the slab as an explanation. They also identified subducted slab material in the transition zone below Indochina not imaged in earlier studies but also visible in model UU-P07 (Fig. 2; SEA_UU-P07_mapview.mov; mmc1.mp4).

Hafkenscheid et al. (2001) and Gorbatov and Kennett (2003) showed similar slab geometries at the western end of the Sunda arc and they also showed the continuity of the Sumatra–Andaman slab. From a comparison of bulk-sound and shear velocity anomalies in the Sunda arc Gorbatov and Kennett (2003) interpreted an abrupt along-strike change in age of subducted lithosphere in the upper mantle below SE Sumatra which may also be reflected in a strong change in anisotropic directions mapped with SKS-splitting analysis (Hammond et al., 2010).

Beneath the Sunda arc Replumaz et al. (2004) interpreted upper and lower mantle anomalies based on a global tomography model by Kárason (2002). This model shows fragmented weak upper mantle slab anomalies delineating the Sunda arc and the Sumatra slab kink (Bijwaard and Spakman, 2000; Bijwaard et al., 1998; Hafkenscheid et al., 2001) although this is not discussed by Replumaz et al. (2004). Like Widiyantoro and van der Hilst (1997) they interpreted the lower mantle anomaly as having a Tethyan origin. They interpreted the strong northward turn of the modern Sunda arc subduction systems towards the Andaman region to be confined to the upper mantle, succeeding an older NW–SE trend of the interpreted deeper Tethys anomaly, as a development owing to the passage of India and concluded that the tomography fits the extrusion model of Replumaz and Tapponnier (2003).

Richards et al. (2007) appear to make the interpretation that the slabs imaged to great depth between western Indonesia and the Philippine Sea were all originally part of one single slab north of India and Australia and the slabs imaged now were all either torn from this or deformed. For instance, they proposed tearing between the Molucca Sea and Banda slabs as if these slabs had a common prior history. They follow the earlier interpretations by Widiyantoro and van der Hilst (1997) and Replumaz et al. (2004) that the deep Tethys anomaly is continuous with the deep mantle anomaly under SE Asia and tore at some point from the Andaman–Sumatra upper segment owing to the passage of the northward moving Indo–Australian plate, west of SE Asia. As discussed below we interpret several of these features in a different way.

Subducted slabs may be expected to deform in the mantle and tear (e.g. Chertova et al., 2014; Govers and Wortel, 2005; Lister et al., 2012; Richards et al., 2007; Rosenbaum et al., 2008; Spakman and Hall, 2010; Spakman and Wortel, 2004; Wortel and Spakman, 2000), and gaps or holes may be created in subducted slabs due to age differences in subducting plates, or as a result of subduction of features such as spreading centres or transform faults (e.g. Dickinson and Snyder, 1979; Thorkelson, 1996; van Wijk et al., 2001). Such features may be identified on the basis of seismicity although seismic gaps may have other causes. Several tears have been postulated in the SE Asian region, as summarised above, below Sumatra and eastern Indonesia, and other gaps in slabs have been suggested from distribution of seismicity or volcanic activity in the Banda region (e.g. Chamalaun and Grady, 1978; Das, 2004; McCaffrey, 1989; Sandiford, 2008), East Java (Hall et al., 2009; Widiyantoro et al., 2011), and the Flores region (Ely and Sandiford, 2010; Wheller et al., 1987). These and other observations of more regional nature are addressed further in the following sections.

## 4. Tectonic models

The geometry and position of plate boundaries is critical for interpreting velocity anomalies in the upper mantle. However, even for the present-day there is no agreement on how many plates there are and where their boundaries are. Bird (2003) has recognised 14 large plates and 38 small plates, the majority of which are in SE Asia and the western Pacific in the area of interest to this paper. At the surface it is impossible to draw continuously connected boundaries between major plates (India, Australia, Pacific, Philippine Sea) surrounding SE Asia, for example to join the Java trench to the Philippine trench, and the problem remains even if smaller and smaller plates are postulated. Particularly around the Philippines and eastern Indonesia trenches are shown on some tectonic maps where there is ambiguous or no evidence for subduction (e.g. Negros, Sulu, New Guinea trenches) and some trenches are often shown as connected when they clearly are not (e.g. Philippine to New Guinea trench). Much of the Banda–Molucca–Philippines–New Guinea region can be considered as a very broad diffuse plate boundary zone (Gordon, 1998), suture zone (Hall and Wilson, 2000) or orogen (Bird, 2003) in which there are no easily defined plates with deformation concentrated at plate boundaries.

If the present is complicated we can expect the past to have been equally complex. Since plate tectonics became the accepted paradigm there has been a myriad of reconstructions for the SE Asian region (e.g. Hamilton, 1979, 1988; Holloway, 1982; Silver et al., 1983a,b, 1985; Taylor and Hayes, 1983; Hall, 1987, 1996, 2002, 2012; Audley-Charles et al., 1988; Metcalfe, 1990, 2011, 2013; Smith and Silver, 1991; Ricou, 1994; Rangin et al., 1997; Villeneuve et al., 1998, 2010; Charlton, 2000; Replumaz and Tapponnier, 2003; Heine et al., 2004; Honza and Fujioka, 2004; Replumaz et al., 2004; Cloos et al., 2005; Heine and Muller, 2005; Hinschberger et al., 2005; Quarles van Ufford and Cloos, 2005; Hafkenscheid et al., 2006; Gaina and Muller, 2007; Whittaker et al., 2007; Keep and Haig, 2010; Harris, 2011; Gibbons et al., 2012, 2013; Whittaker et al., 2013; Zahirovic et al., 2014.) Relatively few of these can be easily tested, because most provide only a few maps, typically at widely spaced time intervals. Because of the number of models and reconstructions we have not attempted to compare different models. The reconstructions used in this paper are from Hall (2012) and were made using the ATLAS computer program (Cambridge Paleomap Services, 1993) and the plate motion model for the major plates of Hall (2002). The model uses the Indian-Atlantic hotspot frame of Müller et al. (1993) from 0 to 120 Ma and a palaeomagnetic reference frame before 120 Ma using poles provided by A.G. Smith (pers. comm., 2001). Information about the way in which the model was developed can be found in Hall (1996, 2002, 2012). Animations of the reconstructions that accompany Hall (2012) and Spakman and Hall (2010) can be downloaded from http://searg.rhul.ac.uk/FTP/tecto_2012/ or from http://dx.doi.org/10.1016/j.tecto.2012.04.021. Animations of earlier reconstructions from Hall (1996) and Hall (2002) can be found at http://searg.rhul.ac.uk/current_research/plate_tectonics/index.html.

We first describe the upper mantle structure, and then the lower mantle structure, which we interpret in the context of our reconstructions. We then discuss the principal features in the tomography that should be present or absent in different tectonic models.

## 5. Anomalies: upper mantle

For the most part, as reviewed in Section 4, the upper mantle has a relatively easily understood structure. There are several long linear high velocity anomalies that are broadly parallel to modern subduction zones which move away from the trenches on deeper depth slices consistent with subducted slabs dipping beneath over-riding plates. These are seen in depth slices (Fig. 2; SEA_UU-P07_mapview.mov; mmc1.mp4) and are also illustrated in movies showing Vertical_slices across the whole region (Vertical_slices/Slices_Whole region; mmc7.mp4 and mmc8.mp4) and in selected parts of the region in other subfolders in the folder Vertical_slices (mmc9.mp4 to mmc18.mp4).

### 5.1. Java–Sumba

The most obvious and longest feature in the upper mantle is the high velocity anomaly that follows the trace of the subduction zone from Sumatra to Banda (Figs. 2 and 4). Estimating the age at which the slab at the base of the upper mantle began to subduct is important for interpreting lower mantle structure but has some uncertainties. For example, there could have been variations in rates of subduction, and the very low dip of the slab between 0 and 100 km depth along the arc from Sumatra to Java could reflect an increase in the width of the volcanic arc-trench gap, meaning that the slab now at the base of the upper mantle passed the trench later than would be estimated from the total length now observed. However, whatever assumptions are made, all of the anomaly at the base of the upper mantle can be explained by Neogene subduction since between 24 Ma and 13 Ma, depending on location. Subduction has been active since the Eocene, from about 45 Ma, so this implies a significant length of lithosphere subducted in the early Neogene and Paleogene must contribute to the high velocity anomalies in the lower mantle.

The segment of the subduction zone from West Java to Sumba is the simplest (Figs. 2 and 4; SEA_UU-P07_mapview.mov; mmc1.mp4). Subduction is almost orthogonal, currently at a relative convergence rate of c. 7 cm/year (7.1 cm/year — NUVEL-1A; 6.3 mm/year — GPS velocity from Prawirodirdjo et al., 2010), and the volcanic arc-trench gap is about 300 km wide. The subducted slab dips north at about 20° between the trench and the volcanic arc and then dips more steeply at about 60–70° (Vertical_slices/Slices_Whole_regionSEA_UUP07_Sunda_Banda_sli.mov; mmc7.mp4), and may be locally overturned in the lowest part of the seismic zone (Schöffel and Das, 1999). Based on the length of the seismically active slab, observed rates of convergence at the Java trench, and plate reconstructions which imply similar longer-term average rates, the slab now at depths of 660 km would have passed the trench between 11 and 13 Ma (Fig. 5).

The steep dip of the slab from South Sumatra to Sumba may in part reflect its age. There are no magnetic anomalies on the Indian plate south of Java, probably because this part of the plate was formed during the Cretaceous magnetic quiet period. South of Bali the age of the ocean crust is between 154–134 Ma and south of South Sumatra is 100–78 Ma, and is overlain by a number of seamount provinces (Hoernle et al., 2011). Based on joint bulk-sound and shear wave velocity anomalies along the subducting slab Gorbatov and Kennett (2003) suggested an abrupt change in its age midway between West Sumatra and Bali (Fig. 6). This fits very well with the age change predicted by the reconstruction at the position of an former India–Australia transform fault (Hall, 2012).

Beneath East Java there is gap in seismicity between about 250 and 500 km. Although tomographic image resolution is not perfect, we infer from the spatial resolution tests (Fig. 3; SVideo_Resolution_1.mov and SVideo_Resolution_2.mov; mmc2.mp4 and mmc3.mp4) that seismic anomalies on the scale of this gap (up to c. 200 km) would be detectable which provides sufficient justification for exploring its origin. Tomography slices suggest that the East Java gap is not an aseismic section of the subduction zone but a hole in the slab

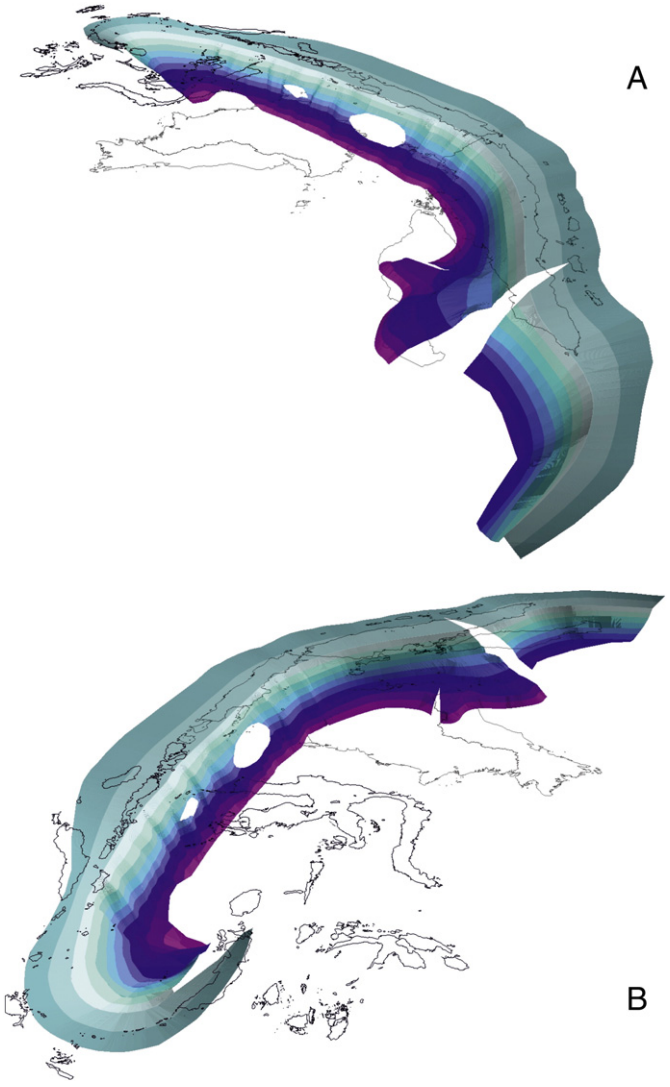


**Fig. 4.** Simplified 3-D figures showing the form of the subducted slab from Sumatra to Banda to depth of 600 km. Colour shades correspond to 50 km intervals. A. View looking approximately eastwards from west of Sumatra. B. View looking approximately westwards from east of Halmahera.

(Widiyantoro et al., 2011) which has an along-strike length of about 400 km (Figs. 4 and 5; Vertical_slices/Slices_Whole_region movies SEA_UUP07_Sunda_Banda_sli.mov; mmc7.mp4). Further east, there is a similar but smaller hole in the slab beneath east Sumbawa between about 200 and 400 km with an along-strike length of about 150 km long (Fig. 4). The cause of these features could be structural, e.g. a local absence or considerable thinning of lithospheric mantle, either already present as a lithosphere heterogeneity prior to subduction or created during subduction. It is less likely that lithospheric mantle with a strongly different composition or only locally thermally weakened lithosphere entered the trench could be an explanation for the tomographic images. Whatever the cause, they are interpreted to result from a positively buoyant crust/lithosphere that entered the trench and subducted with consequences for the tectonic evolution of East Java. Here we explore the possibility of a hole created during subduction.

Hall et al. (2009) suggested a hole was produced by blocking of subduction after buoyant thickened oceanic crust arrived at the trench south of East Java (Fig. 5). This object may have resembled the Roo Rise, which is beginning to subduct beneath East Java, and is currently causing deformation of the forearc and shallowing of the trench (Kopp et al., 2006; Shulgin et al., 2011). However, the object was not the Roo Rise, as sometimes suggested (e.g. Garwin, 2002; Simandjuntak and

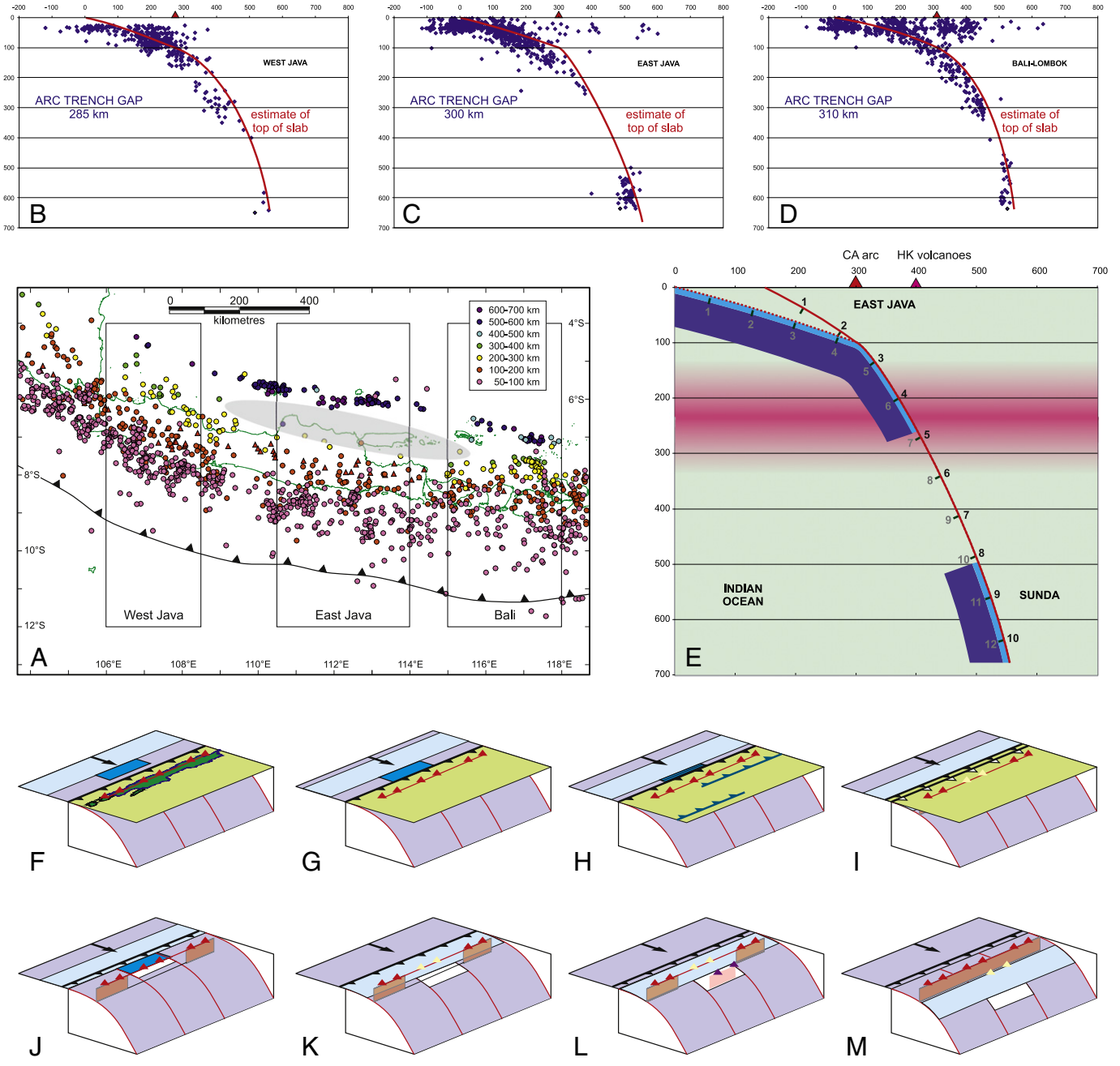


**Fig. 5.** Profiles across the slab subducted beneath Java showing interpreted hole in the slab and its inferred development. A. Map of seismicity with hypocentre depths below 50 km. B, C, D. Profiles across the selected areas of map A showing estimated position of the slab top and the prominent aseismic gap below East Java. E. Interpreted age (Ma) since slab entered trench based on the present trench position (dashed red line and grey numbers) and inferred position of trench assuming a sudden southward shift in its position (solid red line and black numbers) after blocking of subduction due to arrival of buoyant object at trench. Red filled triangle marks position of modern calc-alkaline arc (CA arc) and magenta filled triangle marks position of high-K volcanoes (HK volcanoes) north of the arc. F to I. Cartoons showing interpreted sequence of events as buoyant object (blue) arrived at trench, blocked subduction, leading to deformation on land in Java and southward jump in position of trench. J to M. Cartoons showing interpreted sequence of events with upper plate removed as blocking of subduction by buoyant object caused hole to form. As the hole passed beneath the volcanic arc normal calc-alkaline magmatism ceased as fluid flux from slab diminished and K-rich component was no longer diluted resulting in short period of high-K magmatism behind former arc. After hole was subducted to greater depths normal calc-alkaline magmatism resumed.

Barber, 1996; van der Werff et al., 1994), because the dimensions and position of the hole imply that it was created at about 8 Ma. The estimate of age is consistent with the timing of widespread thrusting in Java (Cross, 2013; Lunt, 2013; Lunt et al., 2009), which was followed by cessation of normal arc magmatism in East Java in the Late Miocene and resumption in the Late Pliocene (Cross, 2013). We suggest that a tear developed in the downgoing slab in front of the buoyant plateau which was unable to subduct. However, along the rest of the arc normal subduction continued, initiating the hole. This forced the plateau, forearc and arc to deform causing contraction, producing folding and thrusting in and south of Java island. Subduction later resumed behind the plateau, leaving a hole in the subducting slab, and leaving the deformed lithosphere beneath the widened forearc. The imaged depth extent of c. 200 km is likely to be an overestimate as local vertical sagging of the slab accommodated by vertical slab tearing directly below the hole may also have contributed to enlarging the hole and may have thickened the slab in the mantle transition zone. As the hole passed beneath the arc, and fluid flux from the subducting slab diminished, normal calc-alkaline volcanism ceased. The passage of a hole beneath East Java can explain the short-lived activity of K-rich volcanoes (Edwards

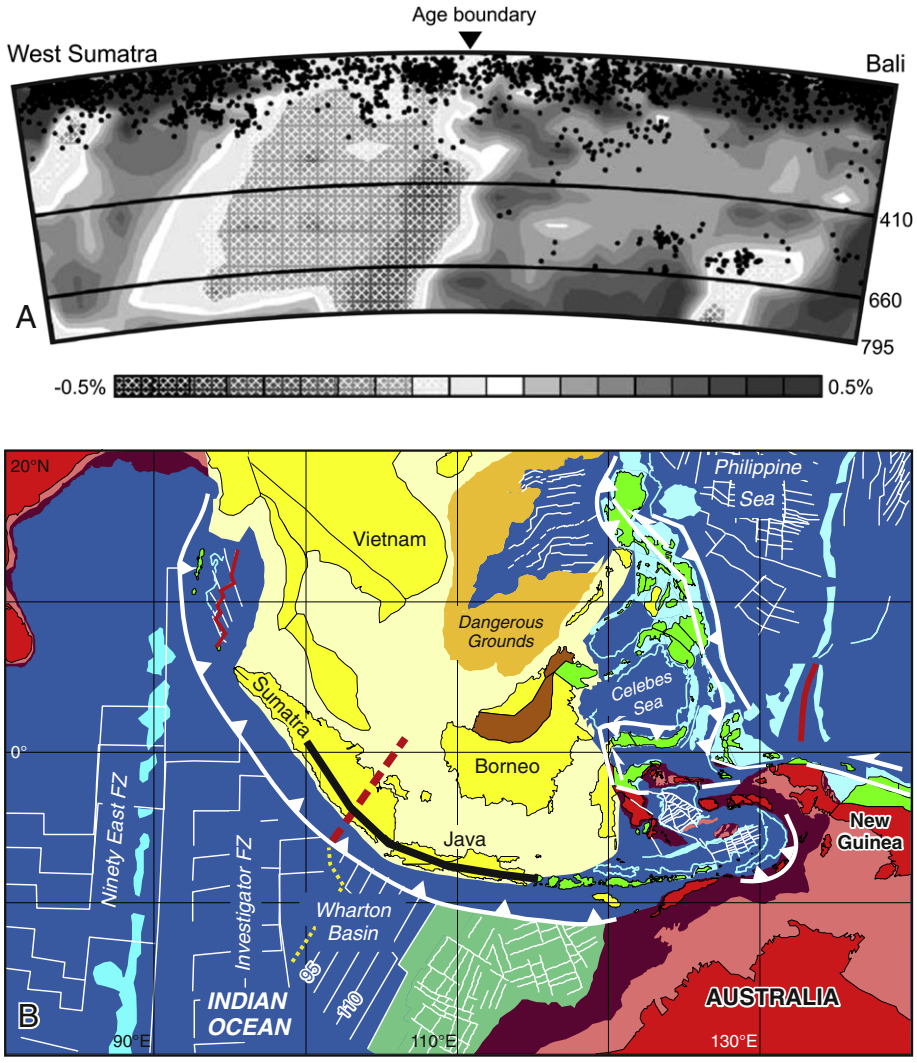


**Fig. 6.** A. Variation in bulk-sound speed and shear wave-speed anomalies along the slab subducted at the Sunda–Java trench zone correlated with interpreted age of the subducted lithosphere by Gorbatov and Kennett (2003). B. Present-day tectonic map showing position of inferred subducted India–Australia transform fault from Hall (2012) where there is a major change in age of the subducted lithosphere from Cretaceous in the east to Cenozoic in the west. Red dashed line is continuation of the transform in the subducted slab and black line is the approximate profile of the slab shown in A.

et al., 1991, 1994), now inactive, to the north of the calc-alkaline volcanoes of the modern arc and with greater depths to the Benioff zone. With the mantle wedge melt component 'switched off', K-rich melts, produced from a deeper mantle component that remained undiluted, dominated arc volcanism. As the hole became deeper, normal calc-alkaline volcanic activity resumed as the slab following the hole was subducted, the fluid flux was restored, and K-rich volcanism ceased. Reconstructing the entire slab (Fig. 4) shows that the slab hole is a relatively minor feature compared to the length and depth of the subducted slab from Sumatra to Sumba which makes it easier to comprehend how it formed and was subducted.

The Sumbawa hole may have developed in a similar way. There are young K-rich volcanoes (Turner et al., 2003) in northern Sumbawa also with greater depths to the Benioff zone than typical of the normal calc-alkaline arc. The smaller size and shallow depth of this hole suggests it was formed at about 4 Ma. The position of the volcanoes suggests that the hole could be related to an object fully subducted or to arrival of part of the Australian continental margin at the subduction zone.

There is a discontinuous zone of thrusts north of Wetar and Flores identified from marine geophysics (Silver et al., 1983a,b,c) which is often interpreted to mark a reversal of subduction polarity. A similar thrust zone is seen on many oil company seismic lines further west, to the north of Bali, that can be traced towards East Java. Widiyantoro et al. (2011) show tomographic images interpreted to indicate south-dipping back-arc lithosphere directly north of Bali. It is plausible that this feature is related to the south-dipping thrusts observed at the surface. However, although there is intense seismicity down to 100 km beneath the active arc in Flores and the inactive segment in Wetar, it is diffuse and there is no clear indication of the slab shape nor any obvious feature on the tomographic sections to show south-dipping subduction. If this is the beginning of polarity reversal the discontinuity of the thrust zone, and absence of a significant trench-like bathymetric feature, suggest that subduction has been initiated only recently, and will not continue for long since there is little oceanic lithosphere north of the arc to be subducted. North of Bali, with the exception of an E–W trough less than 1.5 km deep, the sea bed is mostly shallower than 0.5 km and is unlikely to be underlain by oceanic crust, and the deeper area north of Flores (>4 km) is very narrow. We therefore prefer the alternative interpretation offered by Widiyantoro and Fauzi (2005) that the seismicity reflects backthrusting within a complex backarc region related to the Pliocene collision of the Australian continental margin with SE Asia in the south Banda region.

### 5.2. Sumatra

Northwest of Java subduction becomes increasingly oblique beneath Sumatra and India–SE Asia relative motion is partitioned into trench-normal subduction and trench-parallel movement on the Sumatran and other strike-slip faults. There are a few hypocentres between 300 and 500 km below South Sumatra but further northwest there are no hypocentres below 300 km and therefore it is not possible to determine the subducted slab shape and length from seismicity. Recent tomographic studies (Pesicek et al., 2008, 2010) have significantly improved images of the subducted slab and beneath North Sumatra they interpret the slab to have the form of a large NNE- to NE-plunging fold. Our tomographic images (Vertical_slices/Slices_Whole_region movies SEA_UUP07_Sunda_Banda_sli.mov and SEA_UUP07_regional_sli.mov; mmc7.mp4 and mmc8.mp4) resemble those of Pesicek et al. (2008), although we have drawn Benioff zone contours slightly differently to them (Fig. 7). The tomographic slices show that the slab dip decreases significantly at about 1°N. South of this latitude the slab dips steeply and can be traced into the lower mantle but to the north the slab remains in the transition zone and can be followed to the NE (Fig. 4). The slab dip changes again north of 4°N. Fauzi et al. (1996) interpreted a bend in the slab between 1°N and 4°N based on hypocentres shallower than 200 km. This was interpreted as the northern limb of the fold by Pesicek et al. (2008, 2010) who identified a slab to depths of at least 530 km from tomographic images (Fig. 8).

An alternative interpretation to a fold limb is that of a NNE-trending tear in the slab (Fig. 8). We prefer this interpretation because west of our proposed tear the slab dips more steeply and about 800 km of subducted slab is imaged, whereas east of the tear the slab can be traced to about 550 km depth and much further to the NE, with a total length of about 1200 km. The tectonic reconstruction model suggests this length of slab was subducted in about 22–23 Ma; NUVEL1-A velocities would require 24 Ma and present-day GPS velocities of Prawirodirdjo et al. (2010) would require 27 Ma. The position of the postulated tear (Fig. 8) is now beneath the volcanic centre of Toba (Chesner, 1998, 2012; Chesner et al., 1991). Toba has been linked to subduction of the Investigator Fracture Zone on the Indian plate (e.g. Page et al., 1979), who suggested a tear at the fracture zone. Its cause could be a weakness due to the fracture zone which is being subducted subparallel to the postulated tear. In contrast, Fauzi et al. (1996) suggested there was no conclusive evidence of a tear in the slab but that high seismicity along the subducted portion of the Investigator Fracture Zone was the result of the intersection of the fracture zone and the bend in the slab where it is under compressive stress. Das et al. (2000) also suggested lateral compression and thickening would be produced in the Sunda slab as it subducts and encounters a barrier at the transition zone; beneath Sumatra lateral compression could result from deformation caused by the strong curvature of the subduction zone.

Whether or not a fold or tear interpretation is preferred there is an offset in the linear anomaly at depth (Fig. 7) which suggests a northward offset in the position of the Early Miocene trench from Central to North Sumatra. Unfortunately, the geological record of subduction-related volcanic activity (Crow, 2005) is not yet adequate to do more than speculate on the former position of the trench and more geological investigations of North Sumatra are required to identify this.

We have deliberately chosen not to discuss the mantle structure further north, from the Andaman Sea to Burma, because of its complexity which requires a more detailed analysis and longer discussion than can be provided here.

### 5.3. Banda

Between South Sumatra and Sumba tomographic images show a strong high velocity anomaly that can be traced from the seismically active slab to depths of approximately 1000 km and we consider that the subducted slab continues into the lower mantle. This is discussed further below. East of about 118°E (Fig. 9) the mantle structure changes. The deep high velocity anomaly is absent and in the Banda region seismicity defines a strongly curved Benioff zone known for many years (e.g. Bowin et al., 1980; Cardwell and Isacks, 1978; Hamilton, 1974, 1979). There have been two contrasting explanations for this seismicity: deformation of a single subducted slab or two different slabs subducted from north and south.

Tomographic images of the Banda slab show it is entirely confined to the upper mantle, and there is a c. 300 km wide flat-lying portion of the slab at the bottom of the upper mantle (Fig. 10). The slab has the form of a lithospheric fold that plunges west, that has been described as resembling a spoon-shape (Widiyantoro and van der Hilst, 1997) or the prow of a boat (Pownall et al., 2013). There is a prominent tear in the slab on its north side, beneath Buru and west Seram, that narrows eastwards. The contrast in mantle structure from west to east indicates a different history of subduction in the Java and Banda segments with major slab rollback in the Banda region. We have shown (Spakman and Hall, 2010) that the differences from east to west, and the shape of the Banda slab, can be explained by long-term subduction at the Java trench but that this subduction zone rolled back into a Jurassic oceanic embayment within the Australian continental margin only from about 15 Ma (Pownall et al., 2014) to form the Banda arc. We have a broadly similar conception of the 3-D shape of the subducted lithosphere to many others (e.g. Cardwell and Isacks, 1978; Das, 2004; McCaffrey, 1989; Richards et al., 2007) and support those who have advocated subduction of a single slab (e.g. Charlton, 2000; Hamilton, 1979; Milsom, 2001) but we differ from them in several ways. We consider that the Banda slab is not the simple continuation of a single long-lived subduction zone north of Australia, nor part of an even larger slab connected to Pacific subduction. It is the result of rollback into the Banda embayment located within the Australian continent which began when the northern boundary of the embayment became aligned with the Java trench. The lithospheric fold is not merely the result of rollback but has been tightened in a N–S direction by slab-mantle coupling. The Timor–Tanimbar–Seram Trough is not a subduction trench, nor a single continuous feature, and has a complex origin. As suggested by others, it is in places a flexural topographic expression of loading of the Australian continental margin during collision. Recent high resolution multibeam images and seismic lines crossing the Aru and Tanimbar Troughs show that in some places the trough is an inherited feature that pre-dates subduction (Hall, 2014). In addition, we have shown (Spakman and Hall, 2010) that the size of the high velocity Banda anomaly is greater than the area of the former Jurassic Banda embayment oceanic crust and we proposed that the lithospheric fold in the mantle also includes delaminated subcontinental lithosphere from the surrounding Australian margin. The Seram and Timor Troughs are located at the limit of delamination of the continental margin. Incidentally, although we consider that part of the folded high velocity Banda anomaly is sub-continental lithosphere we differ from some authors who have proposed that continental crust has subducted beneath the volcanic arc (Elburg et al., 2004; Fichtner et al., 2010; Hilton et al., 1992). In our view all of the chemical features suggested to indicate continental crust subduction can be accounted for by melting of continental crust basement of the Banda volcanic arc.

Various active tears in the slab have been proposed in the slab subducting under the Sumba–Aru segment from analysis of earthquake focal mechanisms (e.g. Das, 2004; Ely and Sandiford, 2010; McCaffrey et al., 1985; Sandiford, 2008) or tomography (Widiyantoro et al., 2011). These inferred tear zones are beyond the local resolution of tomographic model UU-P07. Slab tearing in the southern limb of the Banda slab may result from a combination of overriding motion of the Australian plate and resistance of the mantle to northward movement of the slab (Spakman and Hall, 2010). The complex spatial variation of focal mechanisms along the entire slab under the Banda Sea has been key information in developing arguments in support of the two-slab hypothesis (Cardwell and Isacks, 1978; Das, 2004). Our 2010 paper

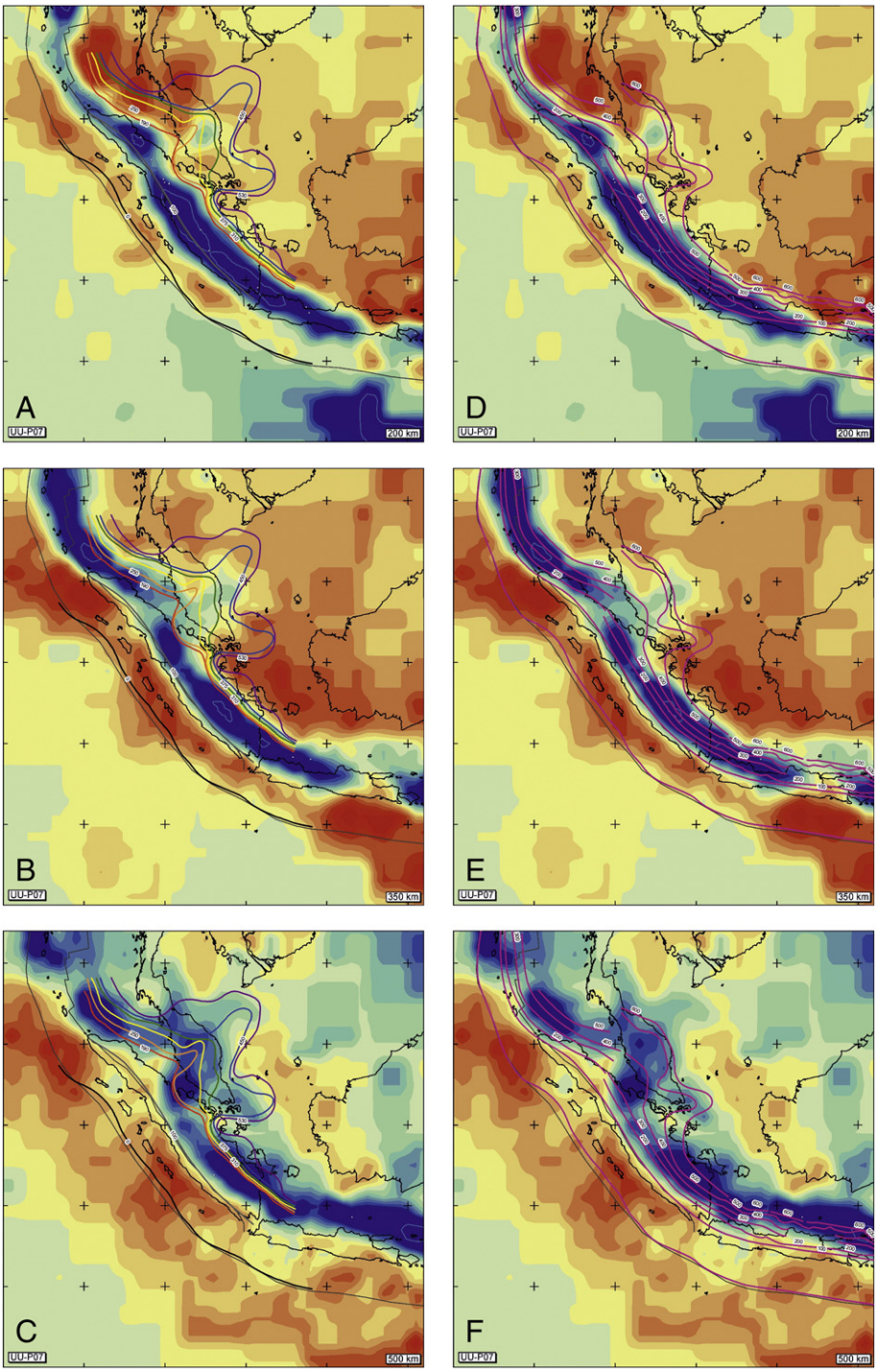


**Fig. 7.** A, B, C. Depth contours on subducted slab from Pesicek et al. (2008) overlain on depth slices at 200 km, 350 km and 500 km from UU-P07. D, E, F. Our interpreted depth contours on the subducted slab overlain on depth slices at 200 km, 350 km and 500 km from UU-P07.

advocated the importance of slab folding resulting from the interplay between regional plate motions, subduction, and slab-mantle coupling. We suggest that a next step forward could be a reassessment of focal mechanisms of the Banda slab based on a quantitative analysis of the stress-field in the slab as a function of regional plate motion and slab-mantle interaction by 3-D thermo-mechanical modelling. This may shed new light on the forcing of inferred slab tears in the southern segment, the absence of seismicity between 100 and 300 km beneath East Timor, and the complex seismicity elsewhere in the heavily deforming, perhaps even disintegrating, slab.

### 5.4. Molucca Sea-Sangihe

The Molucca Sea region is famous as the only present-day example of active arc–arc collision and the inverted U-shape of the subducted plate has been known for many years (e.g. Cardwell et al., 1980; Hall,

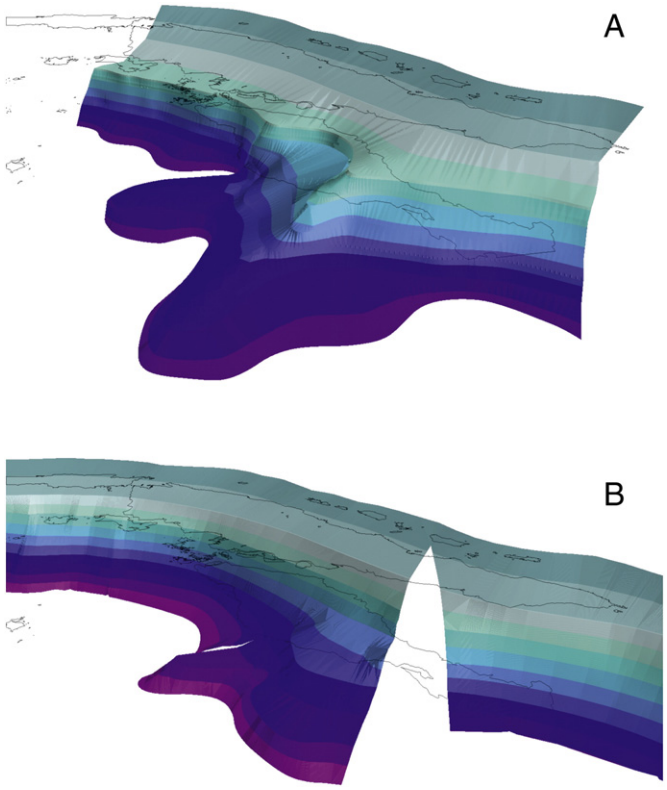


**Fig. 8.** Simplified 3-D figures showing form of the subducted slab beneath Sumatra to depth of 600 km viewed from the north. Colour shades correspond to 50 km intervals. A. Interpreted fold in Sumatra slab based on contours from Pesicek et al. (2008). B. Interpreted tears in Sumatra slab based on our depth contours from UU-P07.

1987; Hamilton, 1979; Hatherton and Dickinson, 1969; McCaffrey et al., 1980; Silver and Moore, 1978) with slabs dipping to west and east under the two active volcanic arcs of Sangihe and Halmahera on the west and east sides of the Molucca Sea. Although there are now no clear subduction trenches in the Molucca Sea because there is an elevated collision complex produced by the two converging arcs, there are two slabs subducting to west and east as explained above. We refer to the west-dipping part of the Molucca Sea plate traceable from seismicity to the base of the upper mantle beneath the Celebes Sea, as the Sangihe slab, and shorter east-dipping slab as the Halmahera slab (Fig. 11). The tomography slices show that neither slab penetrates into the lower mantle and the total length of subducted slab estimated from tomography and seismicity is in good agreement (Vertical_slices/Slices_Molucca_Sea/Molucca_sli.mov; mmc12.mp4). The Sangihe slab reaches the base of the upper mantle with an average dip of 45° indicating about 900–950 km of subducted slab. The Halmahera slab reaches 300 km with a similar average dip and has a length of about 400–450 km. Adding a flat section between the subduction hinges of 100–200 km indicates a total length of subducted lithosphere of about 1500 to 1600 km.

The length of the Molucca Sea slabs is of importance in reconstructing the Philippine Sea plate. The Molucca Sea plate (Hamilton, 1979; Moore and Silver, 1983) was once part of the Philippine Sea plate (Hall, 1987), but the Philippine Sea plate is surrounded by subduction zones and was therefore for many years omitted from global plate models using plate circuits with rotation poles determined by conventional methods based on spreading centres and transform faults. A model based on palaeomagnetic data from the Philippine Sea plate provided the basis for reconstructing eastern Indonesia and the western Pacific (Hall, 1996; Hall et al., 1995a,b,c). Palaeomagnetic data allow an estimate of rotation history and northward movement of the plate but these data alone only identify a zone within which Euler poles can lie (Hall et al., 1995a). Hall et al. (1995a,b,c) estimated a realistic position for the pole based on one additional geological condition — collision of the Halmahera arc with the Australian margin at about 25 Ma, after which Halmahera arc moved west by subduction of the Molucca Sea. The total amount of subduction was unknown and it was not expected that present-day seismicity would record it. The Halmahera arc was therefore reconstructed at the easternmost possible position on the Australian margin. The tomography slices indicate that the length of the seismically active slab is the total actually subducted, i.e. about 1500–1600 km, and is about 700 km less than postulated by Hall et al. (1995a,b,c) and used in the Hall (1996, 2002) model. Those models placed Halmahera at the eastern end of New Guinea in the Manus region at 25 Ma, whereas the length estimated from tomography indicates a position closer to the Bird's shoulder of western New Guinea. The 25 Ma reconstruction should thus look more like the Hall (1996, 2002) 15 Ma reconstruction. As discussed below, this suggestion is supported by observations of the lower mantle.

The position of the slabs in the mantle indicate that the Molucca Sea has moved in the later part of its history as an independent plate completely separate from all surrounding plates but subducting beneath both the Sangihe arc and the Halmahera arc. It is unlikely that subduction would have occurred simultaneously over a long period on both sides of the Molucca Sea. The simplest model that accounts for the present configuration is as follows. Subduction began on the west side under the Sangihe arc and was driven by Philippine Sea plate rotation at about 20 Ma. Up to 900 km of slab was subducted. At about 10 Ma subduction ceased on the Sangihe side and began on the Halmahera side. Continued motion of the Philippine Sea plate initiated volcanic activity in the Halmahera arc by 8 Ma (Baker and Malaihollo, 1996). 11–12 Ma volcanic rocks on Obi (Baker and Malaihollo, 1996; Ali et al., 2001), in the Bird's Head (Pieters et al., 1983), and western New Guinea (Weiland, 1999) are probably related to minor subduction within the northern New Guinea strike-slip zone. The Halmahera hinge rolled back rapidly until about 2 Ma when the arcs began to collide. During this period the Molucca Sea plate moved northwards pushed by Australia. Arc–arc collision has produced young volcanic activity from the eastern tip of North Sulawesi through Sangihe to Mindanao.

### 5.5. North Sulawesi trench subduction

The configuration of subducting slabs in the North Sulawesi region (Fig. 9) is possibly the most complex in the eastern Indonesian–Philippines region; if not the most complex it is certainly the most difficult to unravel. Movies that show different slices across the region are in the folders Vertical_slices/Slices_North_Sulawesi, Vertical_slices/Slices_Sula and Vertical_slices/Slices_Molucca_Sea (mmc13.mp4, mmc16.mp4, mmc12.mp4).

On the west side of the Molucca Sea is the west-dipping Sangihe slab (Fig. 11) traceable from seismicity to the base of the upper mantle and imaged clearly beneath the Celebes Sea by tomography (Vertical_slices/Slices_Molucca_Sea/Molucca_sli.mov; mmc12.mp4). Seismicity and tomography show that at depths below 400 km this slab is straight and strikes NNE. There is a second slab below the North Arm of Sulawesi, which we term the Celebes slab, that subducts Celebes Sea lithosphere southwards from the North Sulawesi trench (Fig. 11). The geometry of this system has been interpreted to result from rotation of the North Arm about a pole near the eastern end of the arm (Hamilton, 1979; Silver et al., 1983a,b,c). The subduction trench terminates at its eastern end, close to Manado, and at its western end terminates at the offshore continuation of the Palu–Koru Fault. In the central part of the subduction zone the subducted slab reaches a depth of just over 200 km, based on seismicity (Fig. 12). Palaeomagnetic evidence (Surmont et al., 1994) and GPS observations of rates of motion on the Palu–Koro Fault (Socquet et al., 2006) suggest this has been subducted in the last 5 Ma.

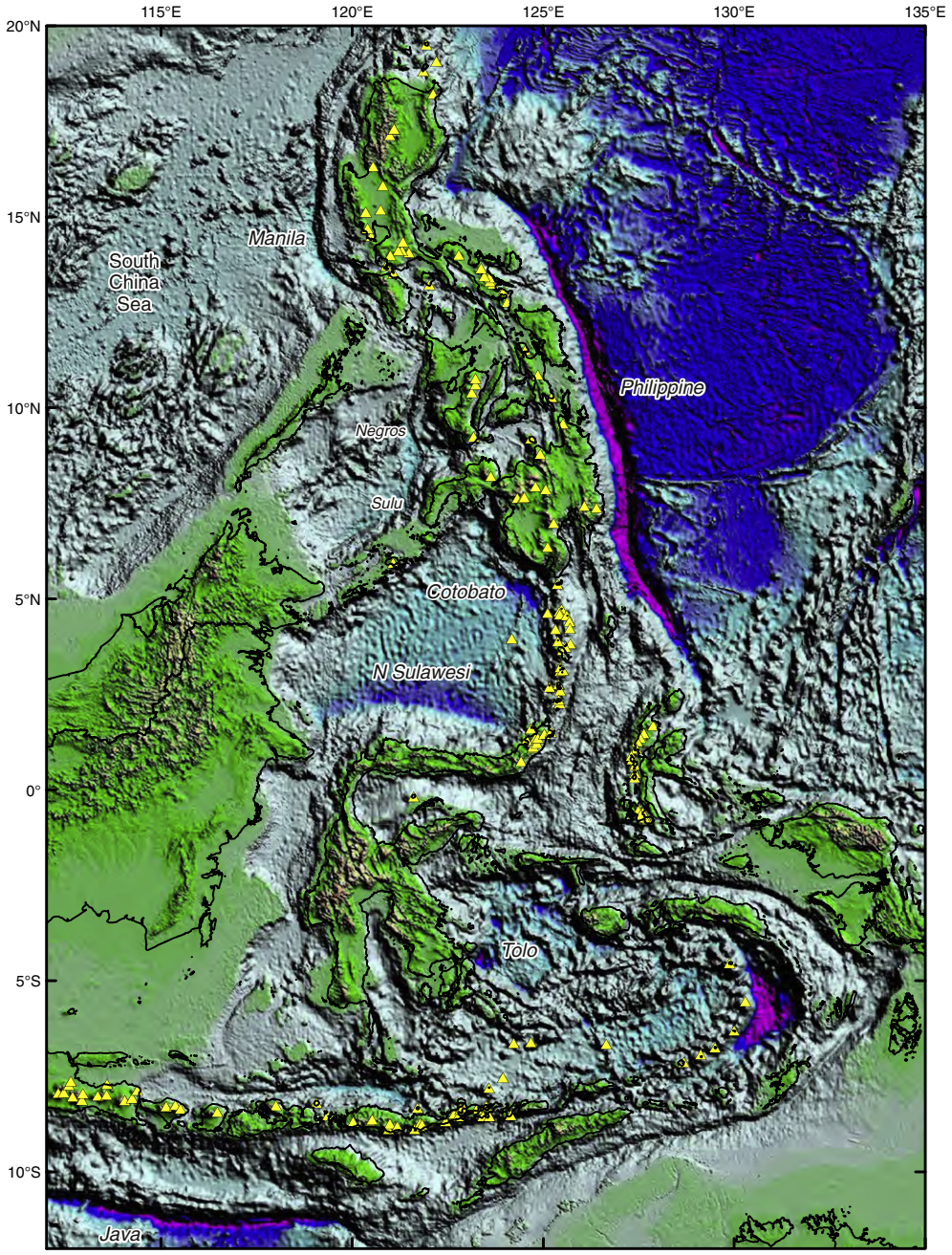


**Fig. 9.** Major trenches and troughs in Philippines to east Indonesia region discussed in the text.

Running approximately E–W from the central Molucca Sea ridge beneath the axis of Gorontalo Bay is a steep zone of earthquakes (Fig. 12). Mapping the slabs and their geometry from earthquake hypocentres is extremely difficult in this region because it is not possible to identify hypocentres with specific slabs. East of 123°E the hypocentres can be explained as marking the edge of the west-dipping Sangihe slab. Further west relatively few hypocentres are above the Sangihe slab. On different N–S profiles the hypocentres appear to define a vertical slab, in the central part of the bay near Una–Una the steep segment of a south-dipping slab, and on some sections a north-dipping slab. Gudmundsson and Sambridge (1998) produced a global regionalised mantle model by an automated process and the results are portrayed by Di Leo et al. (2012a,b) with slab identifications and contours in the Molucca Sea and North Sulawesi region. They considered all hypocentres to result from subduction of two slabs, the Sangihe slab and the Celebes slab, both of which bend through about 90° in the upper 200 km of the mantle beneath North Sulawesi. The Sangihe slab was traced in a similar way by Walpersdorf et al. (1998) and Kopp et al. (1999).

In the late 1990s almost nothing was known about Gorontalo Bay (Fig. 11), the area between the North and East Arms of Sulawesi, but in recent years a great deal has been learned from new fieldwork and dating on land, and from offshore oil industry exploration seismic and detailed multibeam bathymetric data. Based on these new data, the previously proposed slab shapes are difficult to reconcile with the geological observations. The 90° bend in the Celebes slab interpreted by Gudmundsson and Sambridge (1998) implies 150 km of subduction from the west, from the Makassar Strait of Palu–Koro Fault, for which there is no evidence. Seismicity indicates subduction was from the North Sulawesi trench and shows that the deepest seismicity of the Celebes slab is in its central part while suggesting diminishing slab length to the east and west consistent with the tomographic images.

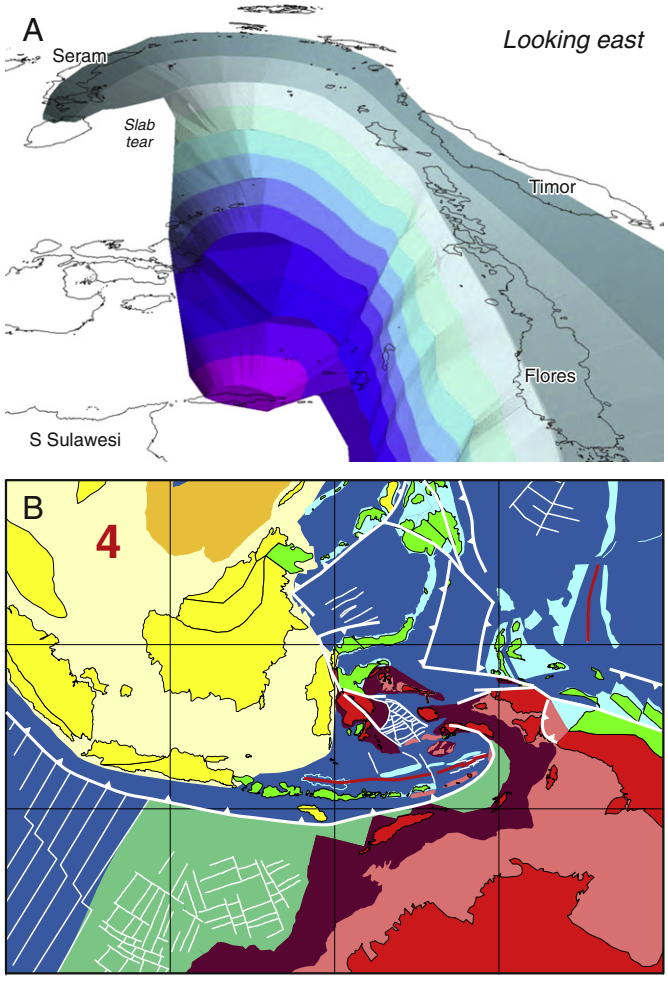


**Fig. 10.** Simplified 3-D figure showing form of the subducted slab beneath the Banda region to depth of 600 km viewed from the west. Colour shades correspond to 50 km intervals. The slab tear in interpreted to have propagated east as rollback into the Banda embayment proceeded. B. 4 Ma reconstruction from Spakman and Hall (2010) showing subduction zone rolling back into Banda embayment with trace of tear corresponding to zone of strike-slip faulting in west Seram.

The almost 90° bend in Sangihe slab interpreted by Gudmundsson and Sambridge (1998) is suggested by Walpersdorf et al. (1998) to join the Sangihe slab subducted from the east to a north-dipping slab joined to the northern edge of the Sula microcontinent. Based on hypocentres this requires the slab to increase in strike length at shallower depths, and be deformed most strongly at shallowest depths. Restoring the inferred subducted slab implies a major separation between the North Arm and the Sula Spur in the Late Miocene and Pliocene, whereas geological observations show they collided in the Early Miocene, emplacing the ophiolite on the Sula Spur, and since then have been close together. Recent studies of the offshore and onshore geology show that during the Late Miocene and Pliocene this region has extended rather than contracted (Advokaat et al., 2014; Hennig et al., 2012, 2014, in press; Pezzati et al., 2014a,b; Spencer, 2010, 2011). The Early Miocene suture zone is now overlain by a several kilometre thick sequence of almost undeformed sediments (Pholbud et al., 2012).

We suggest a new interpretation (Fig. 13) based on the earthquake hypocentres and tomography slices that is consistent with the geological observations. Rather than two slabs we explore the possibility of a slab dipping northwards, as previously proposed by others, but which we consider not to be part of the Sangihe slab but a separate third slab which we name the Sula slab. Silver et al. (1983a) tentatively suggested a north-dipping Benioff zone beneath Gorontalo Bay continuing north from the Sula microcontinental block. The recently acquired industry seismic lines support a north-dipping thrust interpretation north of the Sula Islands (Ferdian et al., 2010; Watkinson et al., 2011). It is also consistent with cross-sections drawn by Walpersdorf et al. (1998) although we interpret differently their postulated continuity of the Sangihe slab and our Sula slab. The Banda tectonic reconstruction (Hall, 2012; Spakman and Hall, 2010) shows how this situation could have evolved (http://dx.doi.org/10.1016/j.tecto.2012.04.021). Before collision of the Sula Spur and the North Arm in the Early Miocene there was a north-dipping slab subducting below the North Arm bounded by slab tears at its east and west ends (Fig. 14). The deeper part of this slab broke off after collision and sank into the lower mantle (as discussed below) leaving a short length of about 200 km still attached (Fig. 15). The tear at the eastern end became a new subduction zone at the west side of the Molucca Sea, and the Sangihe slab began to subduct westwards. Interaction with the nearby NW-subducting Sangihe slab (since c. 24 Ma) and S-subducting Celebes slab (since c. 5 Ma) may have affected the morphology of the Sula slab leading to steeper dips. At present, at shallow depths earthquakes could mark delamination of the lower continental lithosphere, as in the Banda arc. The deeper, vertical part of the Sula slab imaged in the tomography slices is currently almost aseismic.

The total length of the slab interpreted from the tomography slices is about 400 km (Fig. 13), of which up to half may be continental lithosphere, suggested by the observation that the overthrust Sula Spur continental crust may extend as far north as the North Arm of Sulawesi, based on zircon age data from young granites in the North Arm (Rudyawan et al., 2014). Thus, although it may be unusual to find a slab remnant still attached after collision, most of the slab did detach, leaving only a short hanging length of a few hundred kilometres. Recent slab detachment modelling (Duretz et al., 2011) shows that lithosphere older than ~80 Ma, as is the case here, can detach below ~300 km.

Our proposition of a third slab is tentative but consistent with the seismicity, recent geological evidence and the tectonic reconstruction. Moving an inactive slab of c. 200 km length hundreds of kilometres to the north in the last 20 Ma raises some geodynamic questions, although the much larger Molucca Sea plate must also have moved north by a similar amount as it subducted to the west and east. Thermo-mechanical modelling of 3-D slab evolution has helped constrain tectonic evolution models elsewhere (e.g. Chertova et al., 2014) and may contribute to assessing this proposal.

### 5.6. Philippines

For reasons of length we do not discuss the upper mantle structure of the West Pacific further north and east of the Philippines. Lallemand et al. (2001), Lin et al. (2004), Cheng (2009), Cheng et al. (2012), and Huang et al. (2014) are among many authors who have discussed tomography and complexities of reconstructions north of the Philippines. For the Philippines themselves, the history of the Philippine Sea plate is relevant, and modification of the reconstructions have been suggested above in the light of tomographic images that show the length of subducted Molucca Sea slabs. We consider that the tomographic images of the West Pacific support models suggesting Neogene rotation of the Philippine Sea plate (Mapview_movies/Philip_Sea_Plate.mov; mmc5.mp4). The eastern boundary of the plate is seen clearly to migrate eastwards during the past 15 Ma, the time corresponding to the depth of the slab imaged as far as the base of the upper mantle, with a flat section interpreted to record subduction since c. 20 Ma. The eastern and northern boundaries of the plate have been discussed by Miller and Kennett (2006) and Miller et al. (2006) who suggested modifications of previous reconstructions for the past 25 Ma based on Euler poles estimated from earthquake slip vectors, observed GPS velocities, and data from the NUVEL-1 and -1A global plate motion models. It is difficult to see how such data can be used much beyond the recent past as all are measurements of present-day plate

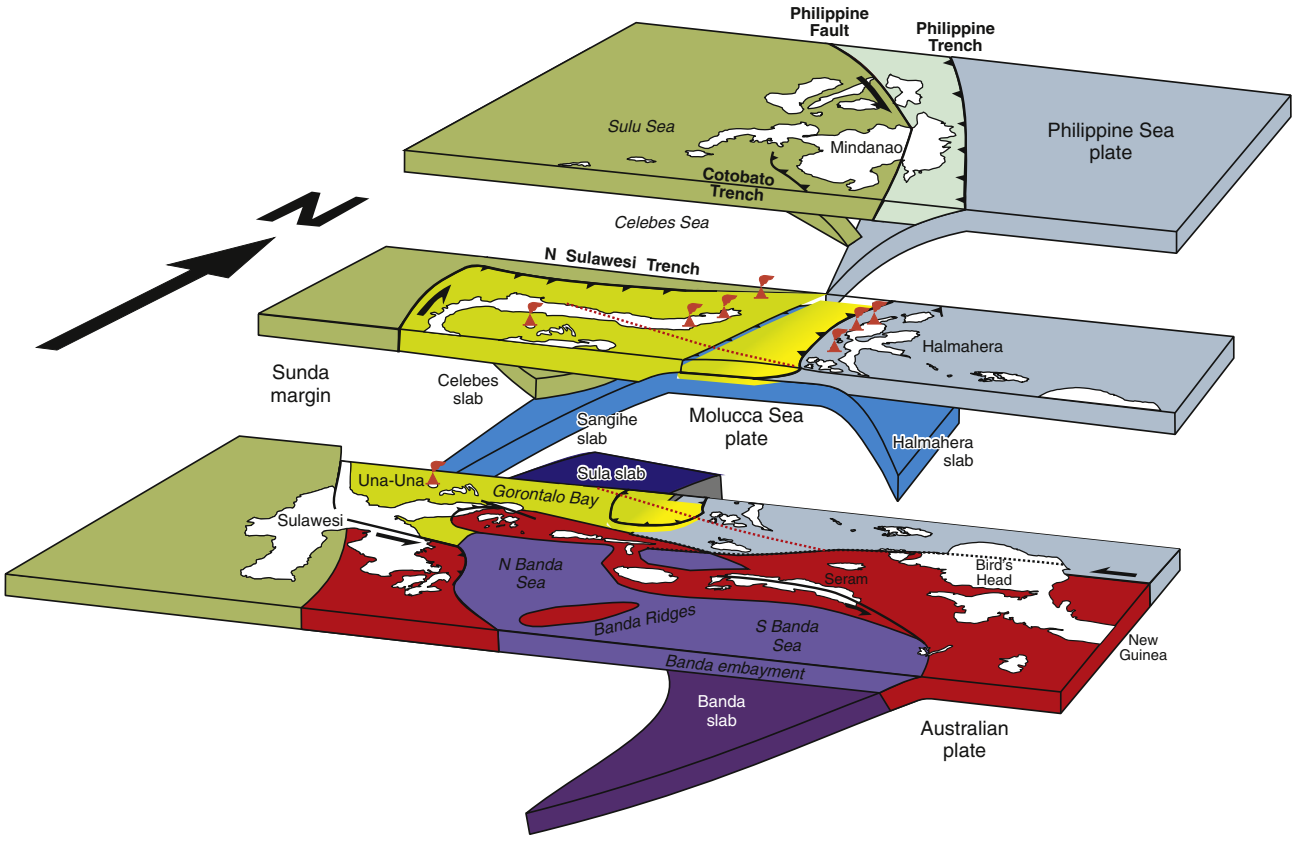


**Fig. 11.** 3-D cartoon showing principal subduction zones in the southern Philippines and east Indonesia region. Dashed red line is inferred northern limit of subducted continental crust of the Sula Spur which extends beneath part of the Sulawesi North Arm.

motions, and it has been shown that the present-day Philippine Sea plate rotation pole (Seno et al., 1993) cannot account for the motion of the plate before 5 Ma recorded by palaeomagnetic data (Hall et al., 1995a,b,c). Nonetheless Miller et al. (2006) concluded their reconstruction confirmed the basic characteristics of models by previous workers (Hall, 2002; Hall et al., 1995b,c; Seno and Maruyama, 1984; Seno et al., 1993) and used the rotation poles of Hall et al. (1995c) for their reconstructions older than 5 Ma. We suggest the history of the Philippine Sea plate before c. 20 Ma is recorded in the lower mantle as discussed further below.

None of the tomographic studies have been concerned with the western boundary of the Philippine Sea plate in the Philippines and further south in eastern Indonesia (Fig. 9). At the south of the Philippines the Cotobato trench on the SW side of Mindanao has no clear tomographic expression, as expected from its short length and lack of seismicity below about 100 km, suggesting a trench that is just beginning. The Negros trench, often shown on tectonic maps on the west side of the central Philippines, has no tomographic or seismic expression. On the east side of the Philippines there is little or no indication of a slab subducting from the Philippine trench, again consistent with the lack of a seismically well-defined slab and relatively recent (Pliocene or younger) initiation of subduction. Cardwell et al. (1980) identified the key features of subduction geometry, and larger and better located seismic data sets (Engdahl et al., 1998; ISC, 2015) including events acquired since their study have not changed the picture they interpreted. A slab subducting from the Philippine trench can be traced to little more than 100 km depth between 15°N and 3°N and cannot be identified more clearly from the tomographic sections (Vertical_slices/Slices_Philippines/Philippines_sli.mov; mmc14.mp4). This is surprising considering how well defined the Philippine trench is, and its great depth of more than 9 km east of Mindanao. It is however, consistent with absence of obvious volcanoes associated with subduction at the Philippine trench; volcanoes in the southern and central Philippines appear to be associated with the Philippine fault, or have no obvious link to any slabs subducting below the western Philippines, except in Luzon (Fig. 9). Subduction at the Philippine trench is young and the partitioning of oblique subduction into trench-normal subduction and strike-slip motion on the Philippine fault may reflect re-use of a much older strike-slip fault zone. Long lived strike-slip faulting in the Philippines has been discussed by many authors (e.g. Karig, 1983; Karig et al., 1986; Pubellier et al., 1991; Quebral et al., 1996; Rutland, 1968; Stephan et al., 1986; Yumul et al., 2004).

The northern part of the Sangihe slab is clearly identified from hypocentres beneath Mindanao in a position consistent with the tectonic reconstruction (Vertical_slices/Slices_Molucca_Sea/Molucca_sli.mov and Mapview_movies/SEA_east_mapv.mov; mmc12.mp4 and mmc6.mp4). At the north end of the Philippines, beneath Luzon, the South China Sea slab subducted at the Manila trench can be identified to about 300 km depth from seismicity and a little deeper from the tomography slices (Mapview_movies/Manila_sli.mov; mmc11.mp4). Between them, is a complex pattern of high velocity anomalies, which are at different depths, mainly below 200 km, mostly aseismic, and vary in their dip. There is a particularly large and strong steep-dipping anomaly beneath the central Philippines at depths between 200 and 600 km (Mapview_movies/SEA_east_mapv.mov; mmc6.mp4). The tectonic reconstruction simplifies this region and shows a number of different subduction zones on the east and west side of the Philippines linked intermittently by strike-slip faults, in part reflecting the difficulty of understanding and reconstructing such a complex region (e.g. Queano et al., 2007; Rangin, 1991; Rangin et al., 1991; Yumul et al., 2008, 2009) based on present knowledge. Tomographic models have not yet provided the detail needed to help unravel this complexity but as they

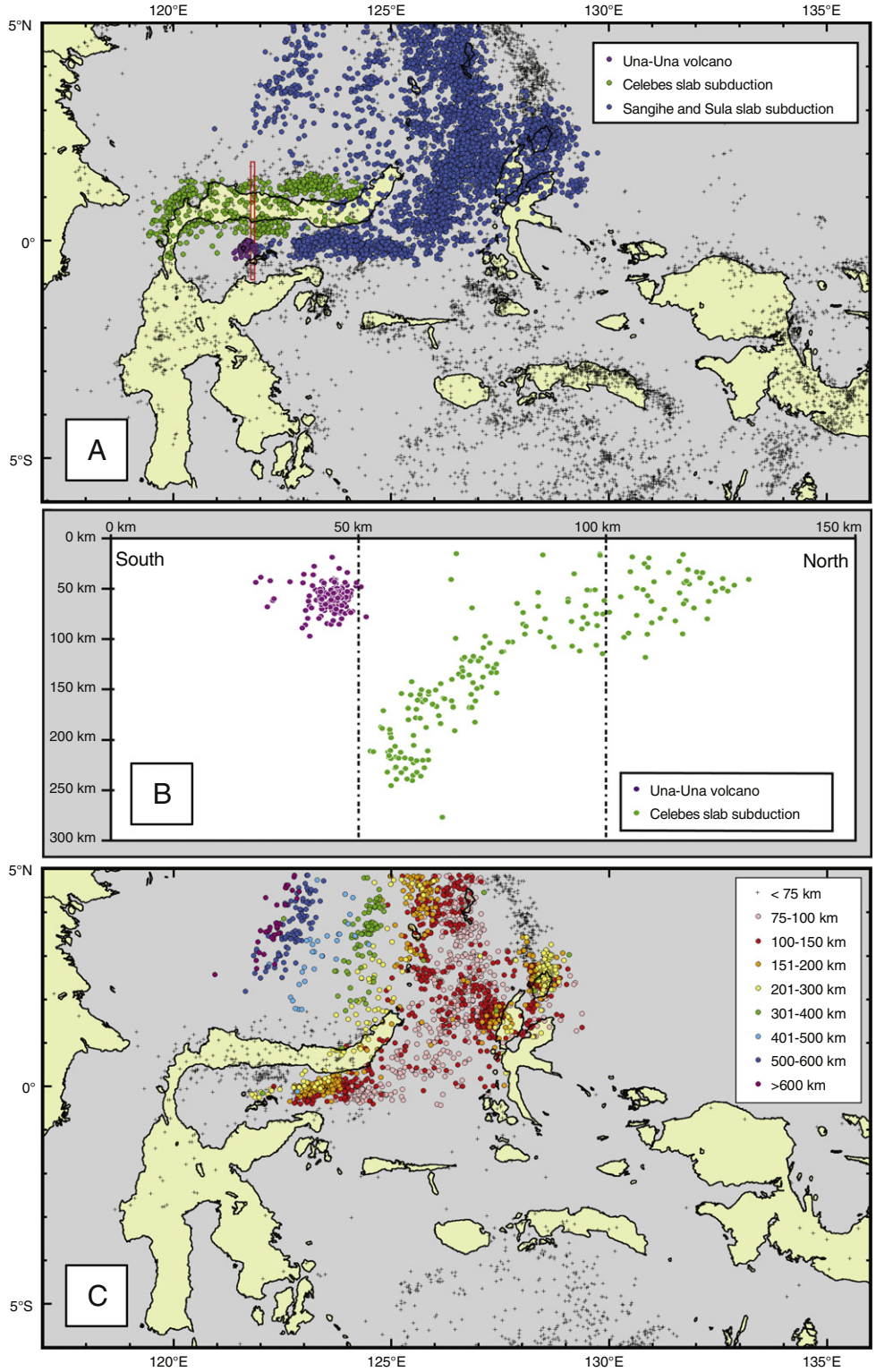


**Fig. 12.** Seismicity and subducted slabs in the North Sulawesi and Molucca Sea region modified from Cottam et al. (2011). A. Hypocentres interpreted to be related to subduction of Celebes slab from North Sulawesi trench. Hypocentres shown in purple were all related to 1983 eruption of Una–Una volcano. B. Profile on red box shown in A showing slab dipping south from North Sulawesi trench to depth of c. 250 km. Note the Una–Una hypocentres are all south of the dipping slab. C. Hypocentre depths in the region. Note the very abrupt termination of deeper seismicity at approximately W–E line in centre of Gorontalo Bay between the East and North Arms of Sulawesi. Almost all events south of this line have depths less than 50 km.

support models that include significant rotation of the Philippine Sea plate, this implies a complex strike-slip dominated mobile belt at its western side, rather than simple northward translation during the Cenozoic.

Below the South China Sea and possibly traceable beneath the northern Philippines is a broad flat lying high velocity anomaly in the transition zone (Fig. 2; Mapview_movies/Philip_Sea_Plate.mov; mmc5.mp4). There is nothing in our tectonic reconstruction, nor to our knowledge in any other reconstruction, that accounts for this anomaly. Our tentative hypothesis is that this is an anomaly produced during a much earlier episode of subduction than any other anomaly in the upper mantle of the region, which can all be related to Cenozoic

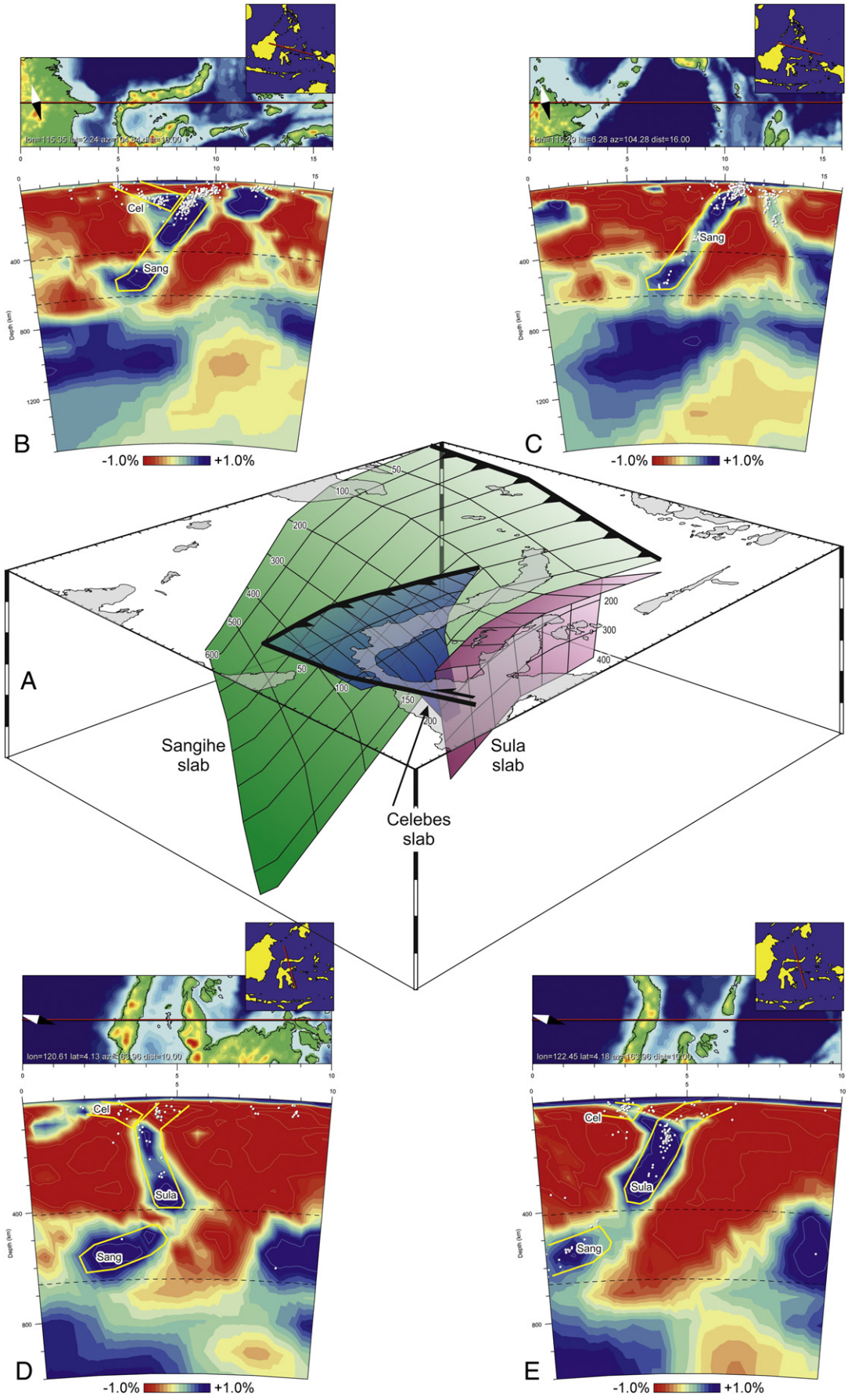
B
Cel
Sang
Depth (km)
-1.0% +1.0%
C
Sang
-1.0% +1.0%
A
Sangihe slab
Sula slab
Celebes slab
D
Cel
Sula
Sang
-1.0% +1.0%
E
Cel
Sula
Sang
-1.0% +1.0%

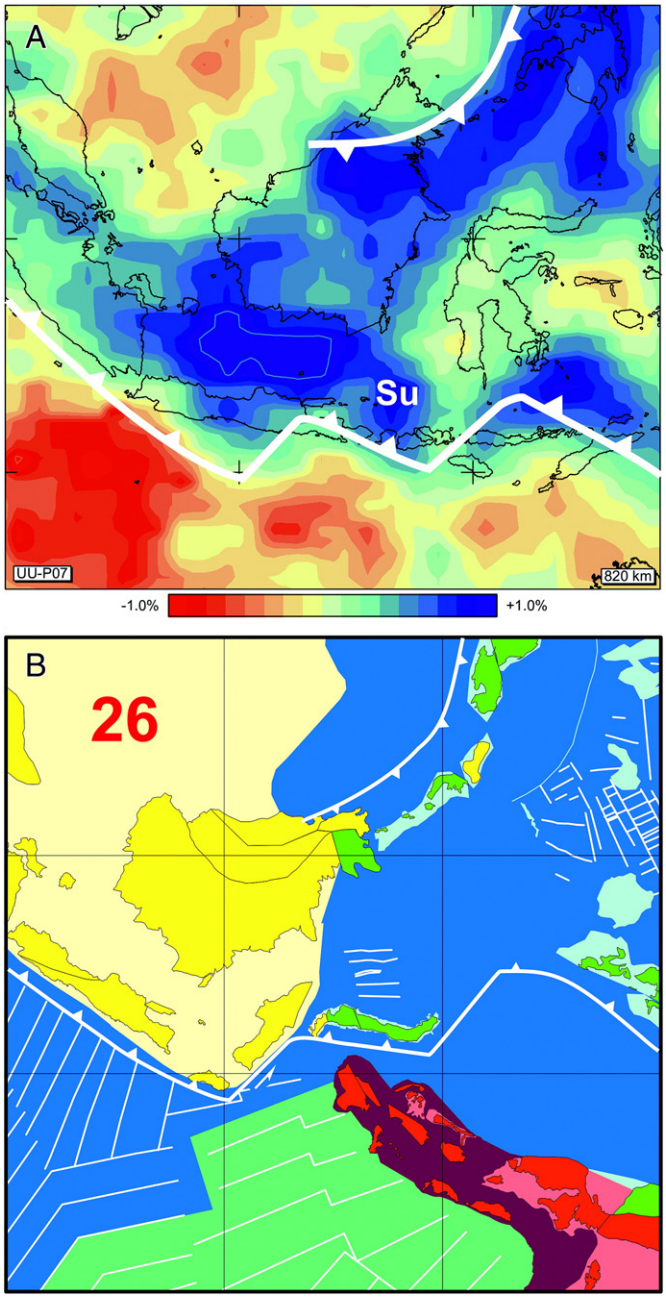


**Fig. 14.** A. Depth slice at 820 km from UU-P07 showing high velocity anomalies. Su is the interpreted slab subducted beneath the North Arm of Sulawesi which broke off after collision at c. 24 Ma between Sula Spur and North Arm. B. Reconstruction at 26 Ma for the Banda region shortly before collision of Sula Spur and Sulawesi North Arm from Spakman and Hall (2010).

subduction. In a study of the SW Pacific (Hall and Spakman, 2002, 2003) we suggested that large flat anomalies that are identified there could have been produced during major episodes of subduction rollback and could remain in the transition zone for very long periods before entering the lower mantle. A candidate in the western Pacific for major rollback, possibly associated with flat slab subduction, that could have left a wide flat anomaly, is the west-directed Mesozoic subduction beneath the Asian margin. This subduction was marked by granite magmatism from Vietnam to East China and terminated in the Cretaceous at about 80–90 Ma (e.g. Li and Li, 2007; Nguyen et al., 2004; Zhou and Li, 2000).

### 5.7. North Borneo to Sulu Sea

In the northern part of the area of interest of this paper, beneath the South China Sea and its margins, there are no obvious anomalies in the upper mantle at depths less than 500 km but this is an area with very little resolution as indicated by the resolution tests (Fig. 3; SVideo_Resolution_1.mov and SVideo_Resolution_2.mov; mmc2.mp4 and mmc3.mp4). However, based on the resolution tests it should be possible to image subducted slabs in the upper parts of the upper mantle beneath the Sulu Sea from the Philippines as far west as northern Borneo. There is a relatively large anomaly beneath northern Borneo at depths between 100 and 250 km (Fig. 2) but this is on the edge of the area with limited or inadequate resolution so this feature could be an artefact. Regional surface wave tomography (Tang and Zheng, 2013) shows high velocities in the lithosphere suggesting the anomaly is real. Assuming it is not an artefact, a possible explanation for this feature is a slab subducted northwards from the Celebes Sea in the Middle and Late Miocene (c. 15 to 5 Ma), now broken off, which created the Sulu arc (Cottam et al., 2013; Hall, 2013). However, if this was the case it would be expected that the slab would be imaged beneath the Sulu Sea and it is not (Vertical_slices/Slices_Sulu/Sulu_sli.mov and Vertical_slices/Slices_Proto_SCS/Proto_SCS_sli.mov; mm17.mp4 and mmc15.mp4). The anomaly is directly beneath Mt Kinabalu which is a granite pluton emplaced between 8–7 Ma (Cottam et al., 2010) and rapidly exhumed during the Late Miocene to Early Pliocene (Cottam et al., 2013). An alternative explanation is that the anomaly represents a thickened lithosphere beneath northern Borneo, formed during collision of the Dangerous Grounds microcontinental block with the Sabah–Cagayan volcanic arc, which has recently detached and is sinking into the mantle below Mt Kinabalu (Cottam et al., 2013).

The absence of a high velocity anomaly beneath the Sulu Sea is surprising since there is a volcanic arc, the Sulu arc, between Sabah and the Zamboanga peninsula of Mindanao, although there is no seismicity and little other geological or geophysical evidence to support active or recent subduction. Hamilton (1979) suggested both south- and north-directed subduction beneath the now inactive arc at different times since the Oligocene, and many tectonic maps show a Sulu trench on the north side of the Sulu arc. On Sabah, Middle to Upper Miocene volcanic rocks are typical calc-alkaline arc products (Chiang, 2002) interpreted as the result of north-directed subduction. However, ODP drilling results (Rangin and Silver, 1991; Silver and Rangin, 1991; Silver et al., 1991) show no oceanic crust was produced in the Sulu Sea in what would have been the backarc of this north-directed subduction, and the maximum extension between Palawan and the Sulu arc during the Miocene was less than 200 km. If this was entirely the result of subduction rollback (Hall, 2013) the length of subducted slab could have been very small, and would be no deeper than about 150 km. Plio–Pleistocene volcanic rocks are chemically different from the Miocene volcanics in Mindanao (Sajona et al., 1996, 2000), the Sulu arc (Castillo and Solidum, 2002) and Sabah (Macpherson et al., 2010). The differences have been attributed to melting of a subducted slab (Sajona et al., 1996, 2000), an interpretation excluded by later workers. Castillo and Solidum (2002) proposed that the mantle already contained an enriched component that melted during later subduction whereas Macpherson et al. (2010) suggested that Plio–Pleistocene magmatism was not subduction-related but resulted from upwelling

**Fig. 13.** A. 3-D cartoon showing interpreted slabs in the North Sulawesi and Molucca Sea region. This portrays the upper surfaces of the three slabs. B: approximately E–W slice across the southern end of the Molucca Sea plate which obliquely intersects the south-dipping Celebes slab. C: approximately E–W slice across the northern part of the Molucca Sea plate showing the Sangihe and Halmahera slabs. D, E: NNW–SSE slices crossing Gorontalo Bay which cut the south-dipping Celebes slab and the sub-vertical Sula slab (south-dipping and overturned in the west and steeply north-dipping further east). The Sangihe slab is cut very obliquely in the transition zone.

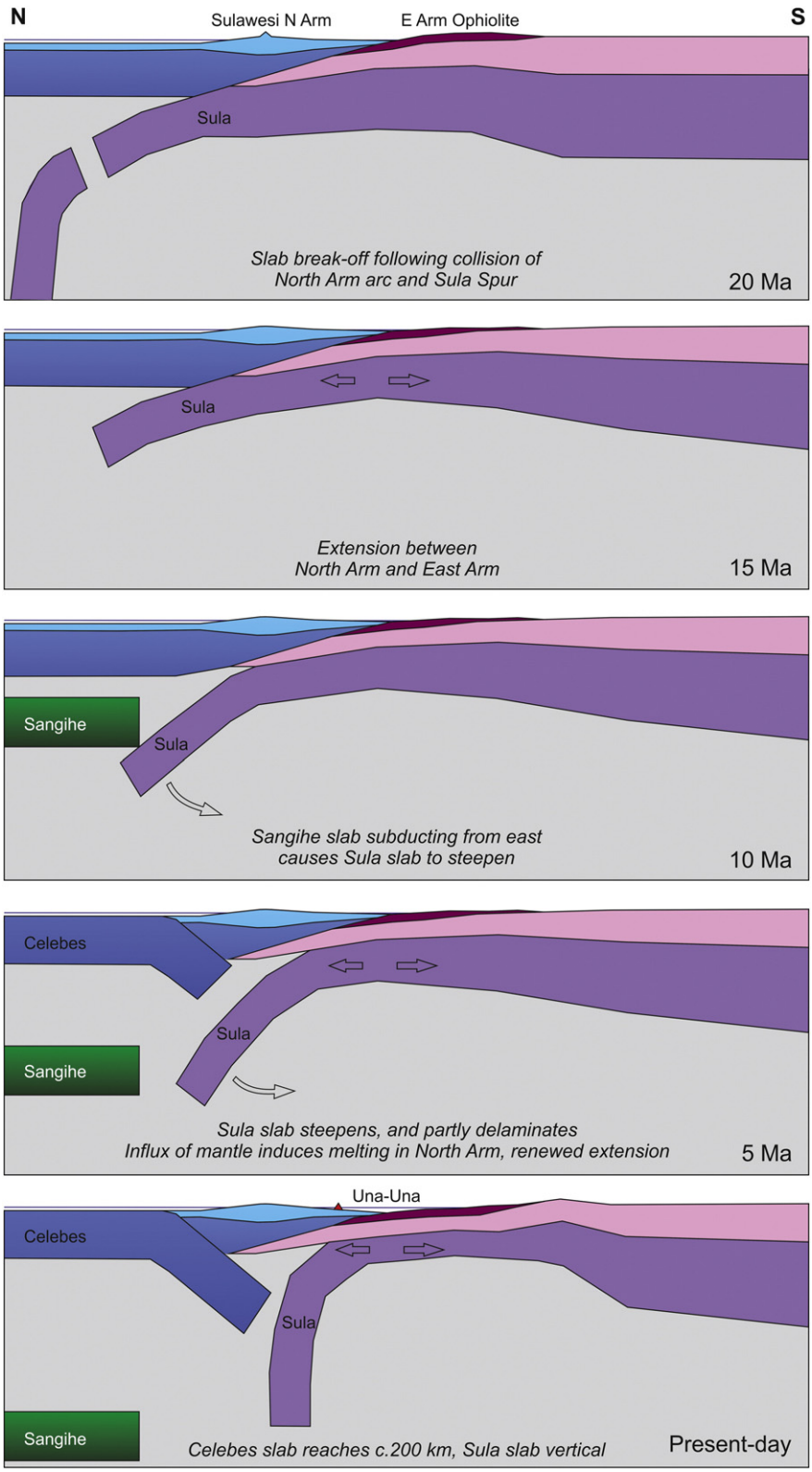


**Fig. 15.** Inferred development of Sula slab following collision of Sula Spur and Sulawesi North Arm. By 20 Ma oceanic lithosphere has broken off and at present day is in the lower mantle (Fig. 14). Extension at 15 Ma was associated with beginning of Banda rollback further SE. By 10 Ma Sangihe slab is subducting from the Molucca Sea to the east into the plane of the section and contributes to steepening of Sula slab. Subduction of Celebes Sea lithosphere beneath the North Arm and steepening of dip of Sula slab begins delamination of Sula Spur contributing to extension and rapid subsidence of Gorontalo Bay, and magmatism in North Arm. Celebes slab has now reached depth of c. 200 km beneath Gorontalo Bay, and Una–Una volcano is product of localised melting accompanying crustal thinning and delamination of Sula Spur as Sula slab becomes vertical.

of OIB-like domains in the upper mantle into lithospheric thin spots formed during earlier Miocene subduction. Therefore, the absence of any high velocity anomalies beneath the Sulu Sea is interpreted here to reflect a very short length of slab subducted in the Miocene, with younger volcanism unrelated to subduction, and possibly reflecting extension (Hall, 2013). In passing it is also worth reiterating that the

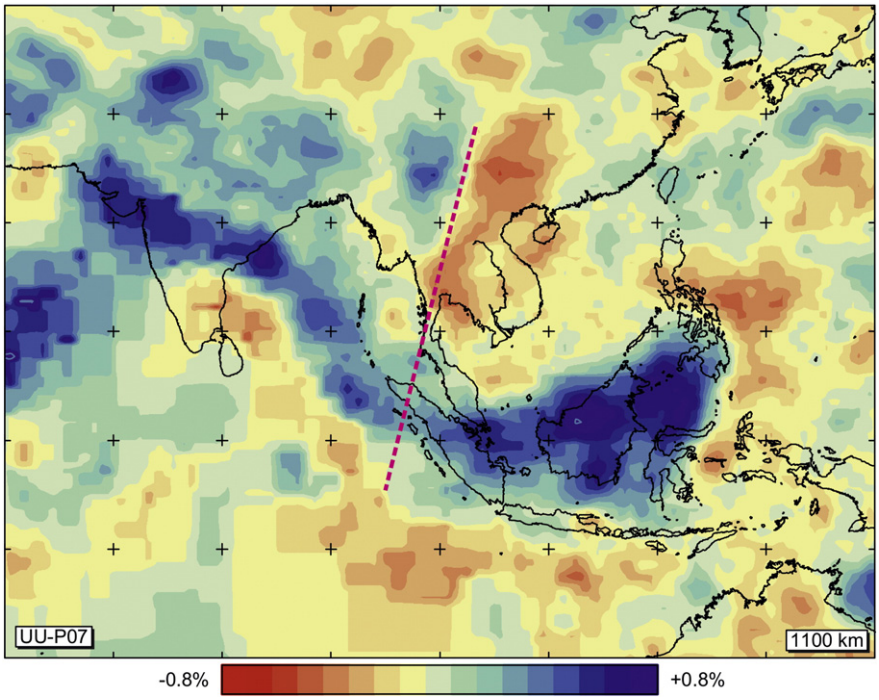


**Fig. 16.** 1100 km depth slice of UU-P07 showing change in lower mantle structure from west to east. Linear anomalies west of 110°E record Mesozoic and early Cenozoic Tethyan subduction north of India, later overridden by India. Broad deep anomaly below Indonesia east of 110°E records Cenozoic subduction.

so-called Negros and Sulu trenches often shown on the east and southeast side of the Sulu Sea (Fig. 9) have no seismically-defined, nor tomographically imaged, slab associated with them, and seismic lines crossing them show nothing more than shallow thrusting.

## 6. Anomalies: lower mantle

Tomography studies showed some years ago that there is a different structure in the lower mantle compared to the upper mantle beneath SE Asia (e.g. Bijwaard et al., 1998; Hafkenscheid et al., 2001, 2006; Widiyantoro and van der Hilst, 1997). Furthermore, the deep structure changes from west to east (Fig. 16). Recent tomography models (UU-P07 used here; Li et al., 2008) show that what was previously imaged in earlier models as a broad and deep anomaly below SE Asia has a clearer internal structure and we argue below that many of the features can be identified with older subduction zones recognised in the tectonic reconstructions.

### 6.1. Sunda–Java–Banda

West of about 110°E there are several broadly NW–SE linear high velocity anomalies interpreted first by van der Voo et al. (1999) as different subducted Tethyan slabs now over-ridden by India (Fig. 16) trending roughly NW–SE. The prominent southern linear anomaly is now accepted to mark an early Cenozoic India–arc collision (e.g. Aitchison and Davis, 2004; Aitchison et al., 2007; Hall, 2012; Hall et al., 2008; Jagoutz et al., 2015; van Hinsbergen et al., 2012). This anomaly dips steeply southwards and can be traced eastwards beneath North Sumatra, where it strikes approximately E–W, below the north-dipping Sunda slab (Fig. 17).

East of about 110°E under SE Asia instead of linear anomalies there is broad high velocity anomaly trending roughly NE–SW which is particularly prominent between 800 and 1100 km. This anomaly can be seen on lower mantle depth slices (Fig. 2; SEA_UU-P07_mapview.mov; mmc1.mp4) to have an internal structure. We interpret there to be several parts to this anomaly which represent different subduction zones (Fig. 18). The first of these is north of Java where the anomaly strikes E–W and can be traced with steep dip to about 900 km and then less steeply to about 100 km below southern Borneo just south of the equator. Volcanic activity related to this subduction began at about 42 Ma in East Java (Smyth et al., 2007, 2008) and West Java (Clements and Hall, 2011; Clements et al., 2012). The position of the deep anomaly is consistent with the Java trench remaining relatively fixed in a mantle reference frame during the Cenozoic.

Further east, positive anomalies in the lower mantle between Timor and Sulawesi at depths between c. 700 and 950 km are interpreted as remnants of the slab that subducted under the North Arm of Sulawesi prior to the Early Miocene collision with the Australian Sula Spur (Fig. 14). Slab detachment and vertical sinking following this collision fits the present-day lower mantle position of the slab remnant in the reconstructions of Spakman and Hall (2010) and Hall (2012).

### 6.2. North Borneo–Proto-South China Sea

On the 800 km depth slice (Fig. 18) the two parts of the deep anomaly are separated but below 900 km to depths of about 1100 km they merge (Fig. 2). The lower mantle anomaly north of the equator can be traced from below central Borneo with a SW–NE strike to 15°N under the central Philippines. We suggest this SW–NE striking anomaly is the Proto-South China Sea which subducted SE-wards from 45 to 20 Ma beneath North Borneo and the Cagayan arc, now southeast of Palawan. Subduction beneath Borneo, and rotation of Borneo, was suggested many years ago based on pioneering palaeomagnetic studies (Haile, 1979, 1981), and incorporated in the earliest plate tectonic models for the South China Sea (Holloway, 1982; Taylor and Hayes, 1980, 1983) which also included a then unnamed Proto-South China Sea. Fuller et al. (1999) reviewed the palaeomagnetic evidence and concluded there had been rigid plate rotation of much of Kalimantan, Sarawak and southern Sabah of about 50° CCW between 30 and 10 Ma, and attributed this to convergence between Australia and SE Asia.

Nonetheless, the size and subduction history of the Proto-South China Sea remain controversial (e.g. Cullen, 2010, 2014; Cullen et al., 2010; Hall, 1996, 2002; Rangin et al., 1999; Replumaz and Tapponnier, 2003; Replumaz et al., 2004). Tang and Zheng (2013) interpreted

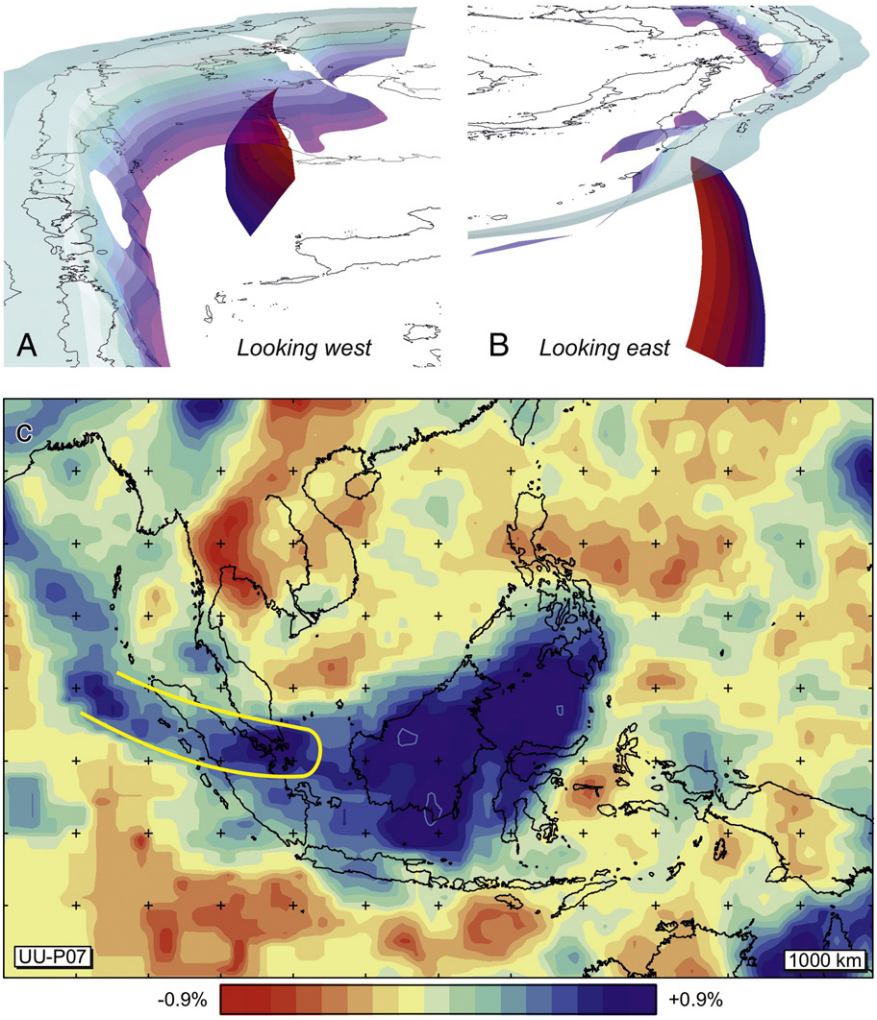


**Fig. 17.** A. 3-D images showing the Tethyan slab at depth below the Sunda slab. Below Sumatra the Sunda slab is in the upper mantle but further SE below South Sumatra and Java the subducted slab penetrates the lower mantle. Below Java and Sumatra the part of the slab at depths greater than 600 km is omitted for clarity. B. 1000 km depth slice of UU-P07 showing the eastern end of the elongate Tethyan anomaly and the broad deep anomaly below Indonesia east of 110°E which is due to Cenozoic subduction.

regional surface wave tomography to show a Proto-South China Sea slab of 500 km length in the upper mantle beneath northern Borneo which is longer than estimated by Rangin et al. (1999) but smaller than interpreted by the Hall (1996, 2002, 2012) reconstructions. The P-wave tomography has poor resolution in this region, as discussed above, and we do not see this feature in the upper mantle (Vertical_slices/Slices_Proto_SCS/Proto_SCS_sli.mov; mmc15.mp4). However, we suggest that those looking for the Proto-South China Sea directly beneath Borneo are looking in the wrong place because of the rotation of Borneo and SE margin of Sundaland. Fig. 18 shows a tectonic reconstruction for 30 Ma compared to a tomography depth slice at 800 km. In the lower mantle the P-wave tomography images show an anomaly with a lateral extent consistent with a wide Proto-South China Sea in the Paleogene which narrowed and terminated towards the SW, and a position consistent with a large Neogene rotation of Borneo, all features of the tectonic reconstructions (Hall, 1996, 2002, 2012). We suggest this anomaly in the lower mantle, like almost all other velocity anomalies to depths of c. 1200 km, is a slab subducted before subduction ceased at about 20 Ma and represents the Proto-South China Sea.

### 6.3. Philippine Sea plate margins 40–25 Ma north and south sides

The anomalies in the lower mantle below the Philippines and southern part of the Philippine Sea plate have a very different orientation and position to inferred Neogene and modern-day subduction zones. East of the interpreted Proto-South China Sea discussed above, there are several broadly linear anomalies that strike ESE, most clearly seen at 800 km but visible on depth slices from 760 to 900 km. On the other hand, these anomalies are in a position consistent with subduction at the margins of the Philippine Sea plate, and beneath the North Arm of Sulawesi. All of the main subduction zones (Proto-South China Sea, North Arm of Sulawesi, south side of Philippine Sea plate, north side of Philippine Sea plate) were stationary during the interval between 40 and 25–15 Ma which was a period of no rotation of the Philippine Sea plate, based on palaeomagnetic data (Hall et al., 1995a,b,c). The tectonic reconstruction for 30 Ma, in the middle of this period, is compared to the tomography depth slice at 800 km in Fig. 18. Most anomalies are in good agreement with the reconstructed positions of the major subduction zones. There is one north-south anomaly beneath the Philippines for which we currently have no explanation. It is parallel to, and east of, the Proto-South China Sea slab and appears to be traceable to greater depths (Fig. 18A). It suggests a more complex subduction history at the Paleogene NW side of the Philippine Sea plate, which could include either double or opposed subduction zones, for which there may be evidence in complex geology of the Philippines.

North of the Philippine Sea plate a subduction zone was interpreted on the reconstructions (Fig. 18B) in the Paleogene from approximately Luzon to Japan. There is no tomographic support for

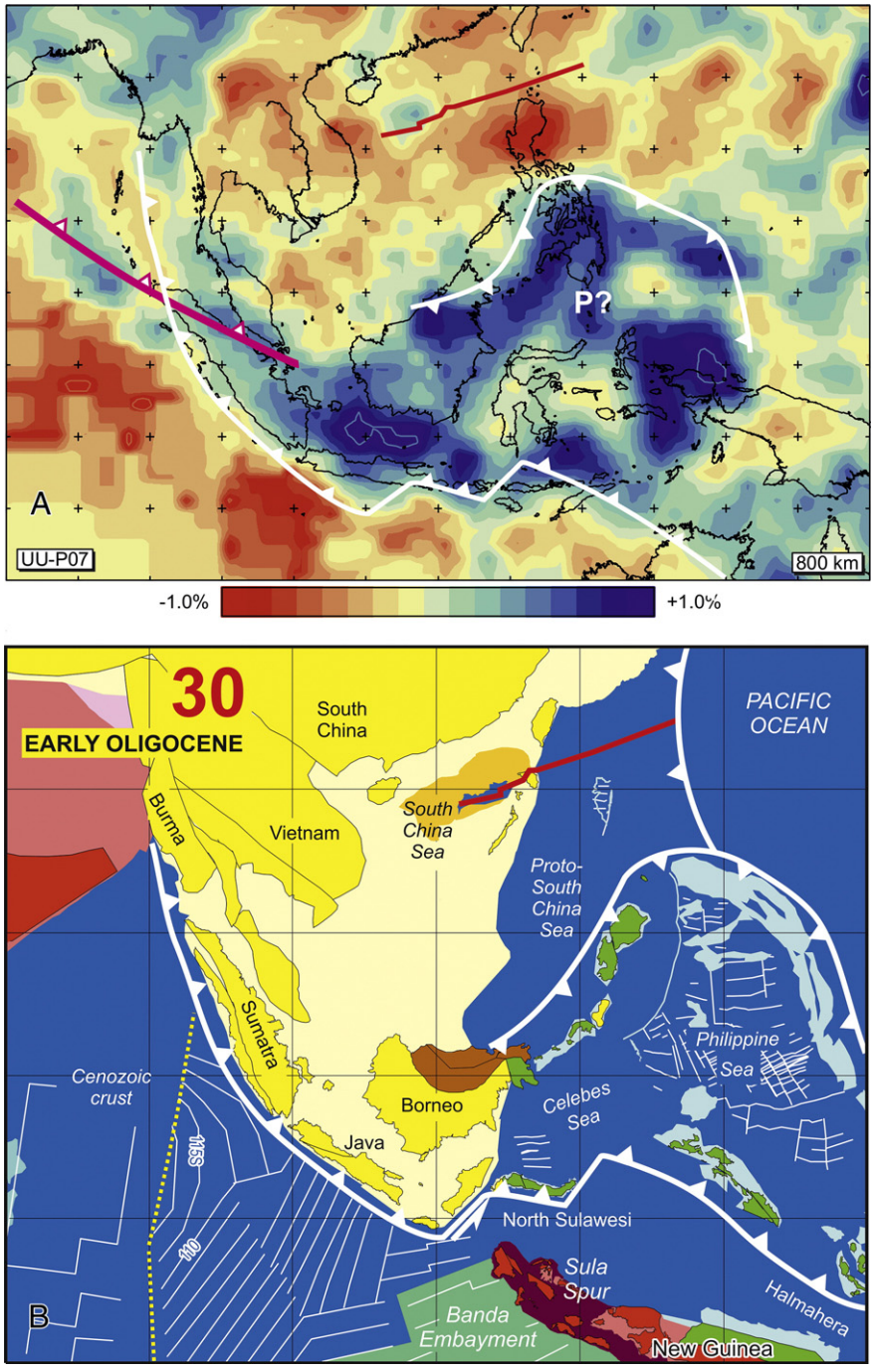


**Fig. 18.** A. Depth slice at 800 km from UU-P07 showing high velocity anomalies. Tethyan linear anomaly marked with magenta line interpreted to record northward subduction north of India in Late Cretaceous and early Cenozoic. Anomalies east of about 110°E are interpreted as the result of subduction since 45 Ma. Symbol P? marks a linear feature in the deep anomaly that could represent a subduction zone not in tectonic model. B. Reconstruction at 30 Ma from Hall (2012) showing interpreted subduction zones. Sunda-Java trench subduction, Proto-South China Sea subduction, subduction below North Sulawesi–East Philippines, and subduction below NE side of Philippine Sea plate all fit well with position of high velocity anomalies in lower mantle. There is no evidence from tomography to support the interpreted subduction at the east side of the Pacific, north of the Philippine Sea plate.

this. West-directed subduction beneath Japan during the Paleogene is commonly interpreted (e.g. Lewis and Byrne, 2003; Maruyama et al., 1997; Taira, 2001) although it may have ceased at times (von Huene et al., 1982) but where subduction boundaries were to the south of Japan in unknown. Resolution in the mantle beneath the Pacific is poor, but it is possible that the subduction boundary of the Kula or Pacific plates continued southwards to join the east end of the Philippine Sea plate where there is a weak high velocity anomaly trending northwards (Fig. 18A).

## 7. Discussion: tomography and tectonic models

Based on the premise that positive seismic P-wave velocity anomalies in the mantle are primarily the product of subduction, the tomographic images of the mantle from UU-P07 record subduction beneath the SE Asian region to depths of approximately 1600 km. As explained above the anomalies in the upper mantle mainly record subduction during the last 10 to 25 Ma, depending on the region considered. Based on our tectonic model we interpret virtually all features seen in upper

mantle and lower mantle to depths of at least 1200 km to be the result of Cenozoic subduction.

### 7.1. Upper mantle: results from tomography

In Section 3 we reviewed previous interpretations of tomographic models. The quality and resolution of recent models has improved but in general there are few significant differences between them and the majority of high velocity anomalies in the upper mantle can be linked to present subduction zones. We conclude that most anomalies record Neogene subduction mostly younger than suggested by some previous authors (e.g. Li and van der Hilst, 2010).

For the Sunda–Java subduction zone we postulate a tear rather than a fold in the slab beneath Sumatra, and like Widiyantoro et al. (2011) we infer there are holes in the slab below East Java and Flores–Sumbawa which are interpreted to result from buoyant obstacles on the subducting plate. Our interpretation of slab geometry from Sunda to Banda is similar to that of Richards et al. (2007), but we differ in particular from them and earlier workers in our interpretation of the development of the Banda region. The crucial differences are the recognition that the Banda subduction began only in the last 15 Ma, and the geometry of the slab reflects the shape of the pre-existing Banda embayment, and Neogene eastwards rollback into the embayment while the Australian plate moved northward.

Beneath Sulawesi we propose a new interpretation of slab geometry consistent with seismicity, tomographic images and recently acquired geological observations that suggests a third slab. From the Molucca Sea northwards into the Philippines region the subducted slabs are segmented, and several subduction zones are not imaged because of the short slab lengths consistent with their young age (Cotobato trench, Philippine trench, Celebes Sea subduction beneath the Sulu arc). The oldest subduction zone in the Philippines region that can be connected to a modern trench is the slab subducting eastwards from the Manila Trench. However, high velocity anomalies in lower part of the upper mantle suggest a subduction history more complex than shown in model reconstructions.

There is a broad positive velocity anomaly in the transition zone (400–650 km) below the South China Sea with weak amplitudes which is not explained by any tectonic model. We tentatively suggest this could be a possible remnant of a flat slab section from a westward-directed Cretaceous subduction zone at the Pacific margin. If correct, this would imply this slab has been in the mantle in this position since about 80–90 Ma and would be the oldest subduction system that is identifiable beneath SE Asia.

### 7.2. Lower mantle: results from tomography

The UU-P07 model resolves more structure in the lower mantle than seen in previous models. We suggest this can now identify subduction zones which mainly pre-date about 15 Ma.

Previous interpretations of the lower mantle high velocity anomaly beneath SE Asia have invariably proposed a single anomaly linked to the Tethyan anomalies which can be traced to the Eastern Mediterranean. We propose a separation of this huge SE Asia anomaly from the Tethys anomaly. The most prominent, and southern, Tethyan linear anomaly extends beneath Sumatra at depths below c. 850 km but only to about 110°E. To the east of this there are several parts to the broad anomaly at depths from 800 to 1100 km. There is a Java trench-related part (NE-directed subduction from 45 to 15 Ma), a Sula subduction zone, subduction at the Philippine Sea plate margins, and a Proto-South China slab which were subducted between 45 and 25 Ma.

Below Java the steep anomaly in the upper mantle passes through and overlaps the deep flatter anomaly which extends further south. This is what would be expected based on the tectonic model (Hall, 2012) which shows advance of the subduction hinge between 25 and 15 Ma as a result of Borneo (SE Sundaland) rotation. From about 1200 km to greater depths the anomaly becomes NE–SW oriented — explained as NW-directed subduction from 65 to 50 Ma in the tectonic model. This deep anomaly disappears by about 1500 km and suggests that the oldest subduction being seen is latest Cretaceous (c. 65 Ma). The tectonic model predicts no subduction beneath the region from 90 Ma so no high velocity anomaly is expected at depths greater than about 1500 km.

As explained by Spakman and Hall (2010) the deep mantle structure changes further east below the Banda region where the folded slab in the upper mantle cannot be traced into the lower mantle. Unlike several previous authors we therefore do not identify Tethyan subduction zones below the Banda region. In the lower mantle below the Banda Sea and into the West Pacific north of New Guinea there are remnants of 45 to 25 Ma subduction, including the broken off Sula slab, subduction below the East Philippines (Fig. 18) and Halmahera (Hall and Spakman, 2002, 2003).

### 7.3. Key points concerning tectonic models

For the Neogene the tomographic images broadly confirm the subduction history that is inferred from present trenches and geological observations. However, the improving resolution of the tomographic models now makes it possible to link the subduction history to geological observations of the upper crust. Thus, the holes interpreted in subducted slabs, arc deformation, and changes in arc magma chemistry can now be linked for areas like East Java, and plausibly interpreted in other areas such as Sumbawa–Flores. Age variations in the subducted slabs can be identified (Gorbatov and Kennett, 2003) and are consistent with predictions of our tectonic model. The boundary between Cretaceous and much younger Cenozoic crust is now beneath SE Sumatra. Tomography shows this is where slab dip begins to change from very steep below Java (Cretaceous crust subducted) to much less steep below Sumatra in areas where there are few hypocentres. The relative age of the subducted slab may have contributed to the way in which the subducted slab has deformed.

A significantly improved understanding of the Banda arc evolution has been acquired with the aid of tomographic models, supporting the one-slab model and deformation of the subducted slab in the upper mantle first proposed by Hamilton (1979), and linking surface deformation to slab-mantle interaction. In this region the resolution of the tomographic models can also exclude some tectonic interpretations, such as the Miocene initiation of faulting at the Tarera–Aiduna fault, accompanied by subduction of several hundred kilometres of oceanic lithosphere (Hinschberger et al., 2005) which should be clearly visible in tomography sections. Beneath Sulawesi, tomography can rule out suggestions of major east-directed subduction on the east side of the Makassar Straits and, as we have shown above, can also suggest new tectonic interpretations in areas of complex seismicity and deformation.

For subduction before the Cenozoic the lower mantle tomography does not greatly aid tectonic interpretation because most high velocity anomalies are due to Cenozoic subduction. However, the change in lower mantle structure west and east of 110°E implies a major change in subduction history north of India compared to that north of Australia. If subduction beneath Indonesia had been continuous during the Mesozoic, as often suggested, we would expect the lower mantle anomalies to be traceable to much greater depths. In our view, this therefore favours the tectonic reconstruction (Hall, 2012) in which subduction ceased for a period from about 90 Ma to 45 Ma and accounts for the absence of a high velocity anomaly associated with subduction at the Java trench deeper than about 1600 km.

We discussed various features of the SE Asia region, centred on Borneo, in an earlier paper (Hall et al., 2008) and concluded that some tectonic interpretations of the region could not be distinguished using the tomographic images. However, the resolution of the tomographic models has significantly improved since then and we have argued above that lower mantle structure can now be interpreted in terms of

several different subduction zones, including the Proto-South China Sea. We therefore suggest that simplified models which include a single rigid block for SE Asia, that rotated clockwise due to indentation of Asia by India (e.g. Replumaz and Tapponnier, 2003; Replumaz et al., 2004), do not account for the complexities of lower mantle structure imaged by tomography under SE Asia. Furthermore, the identification of the Proto-South China Sea subduction zone also supports the counter-clockwise rotation of Borneo and the SE corner of Sundaland following Australia–SE Asia collision in the Early Miocene.

## 8. Conclusions

SE Asia is geologically a particularly complex region and remains relatively understudied because of difficulties of access, vegetation and climate. It is important because it is a region in which the active tectonic processes that are more advanced in older mountain belts can be observed and for which numerous tectonic models have been proposed, many of which are speculative and difficult to assess. The abundant seismicity of the region means that high-resolution tomographic models can be developed and the subduction history of the region interpreted. We have focused on assessment of independent models of tectonic evolution and mantle structure concerned with the region and we conclude that there is now significant convergence between them. The tectonic model can explain many of the key features of the tomography, and the tomography has in many parts of the region offered new insights into tectonic interpretations.

The next steps are to modify the tectonic reconstructions in some parts in the light of the tomographic models, and also to reconsider some features that are unexplained (e.g. high velocity anomaly in the transition zone below the South China Sea, details of upper and lower mantle structure below the Philippines). In several areas improved resolution of the tomography would aid tectonic interpretation, and thermo-mechanical modelling of 3-D slab evolution may help constrain tectonic evolution models.

## Acknowledgments

WS acknowledges support by the Netherlands Research Centre for Integrated Solid Earth Science (ISES) and support by the Research Council of Norway through its Centres of Excellence funding scheme, project number 223272. RH thanks the SE Asia Research Group and its members at Royal Holloway, funded over many years by a changing consortium of oil companies, and support at times from the Royal Society, the London University Central Research Fund, and the Natural Environment Research Council. We thank Tim Horscroft for his encouragement and patience during the preparation of this paper.

## Appendix A. Supplementary data

Supplementary data to this article can be found online at as mov files at http://searg.rhul.ac.uk/FTP/tecto_2015/ or mp4 files at http://dx.doi.org/10.1016/j.tecto.2015.07.003.

## References

Advokaat, E., Hall, R., White, L., Armstrong, R., Kohn, B., BouDagher-Fadel, M., 2014. Neogene extension and exhumation in NW Sulawesi. AGU Fall Meeting December 2014, San Francisco.

Aitchison, J.C., Davis, A.M., 2004. Evidence for the multiphase nature of the India–Asia collision from the Yarlung Tsangpo suture zone, Tibet. In: Malpas, J., Fletcher, C.J.N., Ali, J.R., Aitchison, J.C. (Eds.), Aspects of the Tectonic Evolution of China. Geological Society of London Special Publication 226, pp. 217–233.

Aitchison, J.C., Ali, J.R., Davis, A.M., 2007. When and where did India and Asia collide? J. Geophys. Res. 112, B05423. http://dx.doi.org/10.1029/2006JB004706.

Aki, K., Christoffersson, A., Husebye, E.S., 1977. Determination of the three-dimensional seismic structure of the lithosphere. J. Geophys. Res. 82, 277–296.

Ali, J.R., Hall, R., Baker, S.J., 2001. Palaeomagnetic data from a Mesozoic Philippine Sea Plate ophiolite on Obi Island. Eastern Indonesia. J. Asian Earth Sci. 19, 535–546.

Amaru, M.L., 2007. Global travel time tomography with 3-D reference models. Utrecht University (PhD Thesis).

Anderson, D.L., 2007. New Theory of the Earth. Cambridge University Press, New York (384 pp.).

Audley-Charles, M.G., Ballantyne, P.D., Hall, R., 1988. Mesozoic–Cenozoic rift-drift sequence of Asian fragments from Gondwanaland. Tectonophysics 155, 317–330.

Baker, S., Malaihollo, J., 1996. Dating of Neogene igneous rocks in the Halmahera region: arc initiation and development. In: Hall, R., Blundell, D.J. (Eds.), Tectonic Evolution of SE Asia. Geological Society of London Special Publication 106, pp. 499–509.

Barr, S.M., Macdonald, A.S., 1981. Geochemistry and geochronology of Late Cenozoic basalts of Southeast Asia. Geol. Soc. Am. Bull. 92, 1069–1142.

Bijwaard, H., Spakman, W., 2000. Nonlinear global P-wave tomography by iterated linearized inversion. Geophys. J. Int. 141, 71–82.

Bijwaard, H., Spakman, W., Engdahl, E.R., 1998. Closing the gap between regional and global travel time tomography. J. Geophys. Res. 103, 30055–30078.

Bird, P., 2003. An updated digital model of plate boundaries. Geochem. Geophys. Geosyst. 4, 1027. http://dx.doi.org/10.1029/2001gc000252.

Bock, Y., Prawirodirdjo, L., Genrich, J.F., Stevens, C.W., McCaffrey, R., Subarya, C., Puntodewo, S.S.O., Calais, E., 2003. Crustal motion in Indonesia from Global Positioning System measurements. J. Geophys. Res. 108, 2367. http://dx.doi.org/10.1029/2001JB000324.

Bowin, C., Purdy, G.M., Johnston, C., Shor, G., Lawver, L., Hartono, H.M.S., Jezek, P., 1980. Arc-continent collision in the Banda Sea region. Am. Assoc. Pet. Geol. Bull. 64, 868–918.

Burke, K., Steinberger, B., Torsvik, T.H., Smethurst, M.A., 2008. Plume generation zones at the margins of large low shear velocity provinces on the core–mantle boundary. Earth Planet. Sci. Lett. 265, 49–60.

Cammarano, F., Goes, S., Vacher, P., Giardini, D., 2003. Inferring upper-mantle temperatures from seismic velocities. Phys. Earth Planet. Inter. 138, 197–222.

Cambridge Paleomap Services, 1993. ATLAS version 3.3. Cambridge Paleomap Services, P.O. Box 246, Cambridge, U.K.

Cardwell, R.K., Isacks, B.L., 1978. Geometry of the subducted lithosphere beneath the Banda Sea in eastern Indonesia from seismicity and fault plane solutions. J. Geophys. Res. 83, 2825–2838.

Cardwell, R.K., Isacks, B.L., 1981. A review of the configuration of the lithosphere subducted beneath the eastern Indonesia and Philippine islands. In: Barber, A.J., Wiryosujono, S. (Eds.), The Geology and Tectonics of Eastern Indonesia. Geological Research and Development Centre, Bandung, Special Publication 2, pp. 31–47.

Cardwell, R.K., Isacks, B.L., Karig, D.E., 1980. The spatial distribution of earthquakes, focal mechanism solutions and subducted lithosphere in the Philippines and northeast Indonesian islands. In: Hayes, D.E. (Ed.), The Tectonic and Geologic Evolution of Southeast Asian Seas and IslandsGeophysical Monograph 23. American Geophysical Union, Washington, D.C., pp. 1–35.

Castillo, P.R., Solidum, R.U., 2002. Origin of high field strength element enrichment in the Sulu Arc, southern Philippines, revisited. Geology 30, 707–710.

Chamalaun, F.H., Grady, A., 1978. The tectonic development of Timor: a new model and its implications for petroleum exploration. Aust. Petrol. Explor. Assoc. J. 18, 102–108.

Charlton, T.R., 2000. Tertiary evolution of the Eastern Indonesia collision complex. J. Asian Earth Sci. 18, 603–631.

Cheng, W.-B., 2009. Tomographic imaging of the convergent zone in Eastern Taiwan — a subducting forearc sliver revealed? Tectonophysics 466, 170–183.

Cheng, W.B., Hsu, S.K., Chang, C.H., 2012. Tomography of the southern Taiwan subduction zone and possible emplacement of crustal rocks into the forearc mantle. Glob. Planet. Chang. 90–91, 20–28.

Chertova, M.V., Spakman, W., Geenen, T., van den Berg, A.P., van Hinsbergen, D.J.J., 2014. Underpinning tectonic reconstructions of the western Mediterranean region with dynamic slab evolution from 3-D numerical modeling. J. Geophys. Res. 119, 5876–5902. http://dx.doi.org/10.1002/2014jb011150.

Chesner, C.A., 1998. Petrogenesis of the Toba Tuffs, Sumatra, Indonesia. J. Petrol. 39, 397–438.

Chesner, C.A., 2012. The Toba caldera complex. Quat. Int. 258, 5–18.

Chesner, C.A., Rose, W.I., Deino, A., Drake, R., Westgate, J.A., 1991. Eruptive history of Earth's largest Quaternary caldera (Toba, Indonesia) clarified. Geology 19, 200–203.

Chiang, K.K., 2002. Geochemistry of the Cenozoic Igneous Rocks of Borneo and Tectonic Implications (Ph.D. Thesis), University of London (364 pp.).

Chiu, J.M., Isacks, B.L., Cardwell, R.K., 1991. 3-D Configuration of subducted lithosphere in the Western Pacific. Geophys. J. Int. 106, 99–111.

Clements, B., Hall, R., 2011. A record of continental collision and regional sediment flux for the Cretaceous and Palaeogene core of SE Asia: implications for early Cenozoic palaeogeography. J. Geol. Soc. 168, 1187–1200.

Clements, B., Sevastjanova, I., Hall, R., Belousova, E., Griffin, W., Pearson, N., 2012. Detrital zircon U-Pb age and Hf-isotope perspective on sediment provenance and tectonic models in SE Asia. In: Rasbury, T., Hemming, S., Riggs, N. (Eds.), Mineralogical and Geochemical Approaches to Provenance. Geological Society of America Special Paper 487, pp. 37–61.

Cloos, M., Sapiie, B., Quarles van Ufford, A., Weiland, R.J., Warren, P.Q., McMahon, T.P., 2005. Collisional delamination in New Guinea: the geotectonics of subducting slab breakoff. Geol. Soc. Am. Spec. Pap. 400 (48 pp.).

Cottam, M.A., Hall, R., Sperber, C., Armstrong, R., 2010. Pulsed emplacement of the Mount Kinabalu Granite, North Borneo. J. Geol. Soc. Lond. 167, 49–60.

Cottam, M.A., Hall, R., Forster, M., Boudagher Fadel, M., 2011. Basement character and basin formation in Gorontalo Bay, Sulawesi, Indonesia: new observations from the Togian Islands. In: Hall, R., Cottam, M.A., Wilson, M.E.J. (Eds.), The SE Asian gateway: history and tectonics of Australia–Asia collision. Geological Society of London Special Publication 355, pp. 177–202.

Cottam, M.A., Hall, R., Sperber, C., Kohn, B.P., Forster, M.A., Batt, G.E., 2013. Neogene rock uplift and erosion in Northern Borneo: evidence from the Kinabalu granite, Mount Kinabalu. J. Geol. Soc. Lond. 170, 817–831.

Cross, L., 2013. Neogene Evolution of Java. University of London (PhD Thesis).
Crow, M.J., 2005. Chapter 8: tertiary volcanicity. In: Barber, A.J., Crow, M.J., Milsom, J.S. (Eds.), Sumatra: Geology, Resources and Tectonic Evolution. Geological Society London Memoir 31, pp. 98–119.
Cullen, A.B., 2010. Transverse segmentation of the Baram–Balabac Basin, NW Borneo: refining the model of Borneo's tectonic evolution. Pet. Geosci. 16, 3–29.
Cullen, A., 2014. Nature and significance of the West Baram and Tinjar Lines, NW Borneo. Mar. Pet. Geol. 51, 197–209.
Cullen, A.B., Reemst, P., Henstra, G., Gozzard, S., Ray, A., 2010. Rifting of the South China Sea: new perspectives. Pet. Geosci. 16, 273–282.
Das, S., 2004. Seismicity gaps and the shape of the seismic zone in the Banda Sea region from relocated hypocentres. J. Geophys. Res. 109, B12303. http://dx.doi.org/10.1029/2004JB003192.
Das, S., Schoffel, H.-J., Gilbert, F., 2000. Mechanism of slab thickening near 670 km under Indonesia. Geophys. Res. Lett. 27, 831–834.
DeMets, C., Gordon, R.G., Argus, D.F., Stein, S., 1990. Current plate motions. Geophys. J. Int. 101, 425–478.
DeMets, C., Gordon, R.G., Argus, D.F., 2010. Geologically current plate motions. Geophys. J. Int. 181, 1–80.
Deschamps, F., Trampert, J., 2003. Mantle tomography and its relation to temperature and composition. Phys. Earth Planet. Inter. 140, 277–291.
Di Leo, J.F., Wookey, J., Hammond, J.O.S., Kendall, J.M., Kaneshima, S., Inoue, H., Yamashina, T., Harjadi, P., 2012a. Deformation and mantle flow beneath the Sangihe subduction zone from seismic anisotropy. Phys. Earth Planet. Inter. 194–195, 38–54.
Di Leo, J.F., Wookey, J., Hammond, J.O.S., Kendall, J.M., Kaneshima, S., Inoue, H., Yamashina, T., Harjadi, P., 2012b. Mantle flow in regions of complex tectonics: insights from Indonesia. Geochem. Geophys. Geosyst. 13. http://dx.doi.org/10.1029/2012gc004417.
Dickinson, W.R., Snyder, W.S., 1979. Geometry of subducted slabs related to San Andreas transform. J. Geol. 87, 609–627.
Duretz, T., Gerya, T.V., May, D.A., 2011. Numerical modelling of spontaneous slab breakoff and subsequent topographic response. Tectonophysics 502, 244–256.
Edwards, C., Menzies, M., Thirlwall, M., 1991. Evidence from Muriah, Indonesia, for the interplay of supra-subduction zone and intraplate processes in the genesis of potassic alkaline magmas. J. Petrol. 32, 555–592.
Edwards, C.M.H., Menzies, M.A., Thirlwall, M.F., Morris, J.D., Leeman, W.P., Harmon, R.S., 1994. The transition to potassic alkaline volcanism in island arcs: the Ringgit–Besar Complex, East Java, Indonesia. J. Petrol. 35, 1557–1595.
Elburg, M.A., van Bergen, M.J., Foden, J.D., 2004. Subducted upper and lower continental crust contributes to magmatism in the collision sector of the Sunda–Banda arc, Indonesia. Geology 32, 41–44.
Ely, K.S., Sandiford, M., 2010. Seismic response to slab rupture and variation in lithospheric structure beneath the Savu Sea, Indonesia. Tectonophysics 483, 112–124.
Engdahl, E.R., van der Hilst, R., Buland, R., 1998. Global teleseismic earthquake relocation with improved travel times and procedures for depth determination. Bull. Seismol. Soc. Am. 88, 722–743.
Fauzi, McCaffrey, R., Wark, D., Sunaryo, Prih Haryadi, P.Y., 1996. Lateral variation in slab orientation beneath Toba Caldera, northern Sumatra. Geophys. Res. Lett. 23, 443–446.
Ferdian, F., Watkinson, I.M., Hall, R., 2010. A structural re-evaluation of the North Banggai–Sula area, eastern Sulawesi. Proceedings Indonesian Petroleum Association, 34th Annual Convention, IPA10-G-009 1-20.
Fichtner, A., de Wit, M., van Bergen, M., 2010. Subduction of continental lithosphere in the Banda Sea region: Combining evidence from full waveform tomography and isotope ratios. Earth Planet. Sci. Lett. 297, 405–412.
Fichtner, A., Trampert, J., Cupillard, P., Saygin, E., Taymaz, T., Capdeville, Y., Villaseñor, A., 2013. Multiscale full waveform inversion. Geophys. J. Int. http://dx.doi.org/10.1093/gji/ggt118.
Fukao, Y., Obayashi, M., Inoue, H., Nenbai, M., 1992. Subducting slabs stagnant in the mantle transition zone. J. Geophys. Res. 97, 4809–4822.
Fukao, Y., Widiyantoro, S., Obayashi, M., 2001. Stagnant slabs in the upper and lower mantle transition region. Rev. Geophys. 39, 291–323.
Fuller, M., Ali, J.R., Moss, S.J., Frost, G.M., Richter, B., Mahfi, A., 1999. Paleomagnetism of Borneo. J. Asian Earth Sci. 17, 3–24.
Gaina, C., Muller, D., 2007. Cenozoic tectonic and depth/age evolution of the Indonesian gateway and associated back-arc basins. Earth-Sci. Rev. 83, 177–203.
Garwin, S., 2002. The geologic setting of intrusion-related hydrothermal systems near the Batu Hijau porphyry copper-gold deposit, Sumbawa, Indonesia. In: Goldfarb, R.J., Nielsen, R.L. (Eds.), Integrated Methods for Discovery: Global Exploration in the Twenty-First Century. Society of Economic Geologists Special Publication 9, pp. 333–366.
Gibbons, A.D., Barckhausen, U., van den Bogaard, P., Hoernle, K., Werner, R., Whittaker, J.M., Müller, R.D., 2012. Constraining the Jurassic extent of Greater India: tectonic evolution of the West Australian margin. Geochem. Geophys. Geosyst. 13, Q05W13. http://dx.doi.org/10.1029/2011gc003919.
Gibbons, A.D., Whittaker, J.M., Müller, R.D., 2013. The breakup of East Gondwana: assimilating constraints from Cretaceous ocean basins around India into a best-fit tectonic model. J. Geophys. Res. 118, 808–822. http://dx.doi.org/10.1002/jgrb.50079.
Goes, S., Govers, R., Vacher, P., 2000. Shallow mantle temperatures under Europe from P and S wave tomography. J. Geophys. Res. 105, 11153–11169. http://dx.doi.org/10.1029/1999jb900300.
Goes, S., Simons, F.J., Yoshizawa, K., 2005. Seismic constraints on temperature of the Australian uppermost mantle. Earth Planet. Sci. Lett. 236, 227–237.
Gorbatov, A., Kennett, B.L.N., 2003. Joint bulk-sound and shear tomography for Western Pacific subduction zones. Earth Planet. Sci. Lett. 210, 527–543.
Gordon, R.G., 1998. The plate tectonic approximation: plate nonrigidity, diffuse plate boundaries, and global plate reconstructions. Annu. Rev. Earth Planet. Sci. 26, 615–642.
Govers, R., Wortel, M.J., 2005. Lithosphere tearing at STEP faults: response to edges of subduction zones. Earth Planet. Sci. Lett. 236, 505–523.
Gudmundsson, O., Sambridge, M., 1998. A regionalized upper mantle (RUM) seismic model. J. Geophys. Res. 103, 7121–7136.
Hafkenscheid, E., Buiter, S.J.H., Wortel, M.J.R., Spakman, W., Bijwaard, H., 2001. Modelling the seismic velocity structure beneath Indonesia: a comparison with tomography. Tectonophysics 333, 35–46.
Hafkenscheid, E., Wortel, M.J.R., Spakman, W., 2006. Subduction history of the Tethyan region derived from seismic tomography and tectonic reconstructions. J. Geophys. Res. 111, B08401. http://dx.doi.org/10.1029/2005jb003791.
Haile, N.S., 1973. The recognition of former subduction zones in Southeast Asia. In: Tarling, D.H., Runcorn, S.K. (Eds.), Implications of continental drift to the Earth Sciences 2. Academic Press, London, pp. 885–891.
Haile, N.S., 1979. Rotation of Borneo microplate completed by Miocene: palaeomagnetic evidence. Warta Geol. Geol. Soc. Malays. Newsl. 5, 19–22.
Haile, N.S., 1981. Paleomagnetism of southeast and East Asia. In: McElhinny, M.W., Valencio, D.A. (Eds.), Palaeoreconstruction of the Continents. American Geophysical Union, Geodynamic Series 2, pp. 129–135.
Hall, R., 1987. Plate boundary evolution in the Halmahera region, Indonesia. Tectonophysics 144, 337–352.
Hall, R., 1996. Reconstructing Cenozoic SE Asia. In: Hall, R., Blundell, D.J. (Eds.), Tectonic Evolution of SE Asia. Geological Society of London Special Publication 106, pp. 153–184.
Hall, R., 2002. Cenozoic geological and plate tectonic evolution of SE Asia and the SW Pacific: computer-based reconstructions, model and animations. J. Asian Earth Sci. 20, 353–434.
Hall, R., 2012. Late Jurassic–Cenozoic reconstructions of the Indonesian region and the Indian Ocean. Tectonophysics 570–571, 1–41.
Hall, R., 2013. Contraction and extension in Northern Borneo driven by subduction rollback. J. Asian Earth Sci. 76, 399–411.
Hall, R., 2014. Towards Understanding the Sunda and Banda Arcs. AGU Fall Meeting December 2014, San Francisco, T51D-06.
Hall, R., Morley, C.K., 2004. Sundaland basins. In: Clift, P., Wang, P., Kuhnt, W., Hayes, D.E. (Eds.), Continent-Ocean Interactions within the East Asian Marginal SeasGeophysical Monograph 149. American Geophysical Union, Washington, D.C., pp. 55–85.
Hall, R., Sevastjanova, I., 2012. Australian crust in Indonesia. Aust. J. Earth Sci. 59, 827–844.
Hall, R., Spakman, W., 2002. Subducted slabs beneath the eastern Indonesia-Tonga region: insights from tomography. Earth Planet. Sci. Lett. 201, 321–336.
Hall, R., Spakman, W., 2003. Mantle structure and tectonic evolution of the region north and east of Australia 22. Geological Society of Australia Special Publication 22 and Geological Society of America Special Paper 372, pp. 361–381.
Hall, R., Wilson, M.E.J., 2000. Neogene sutures in eastern Indonesia. J. Asian Earth Sci. 18, 787–814.
Hall, R., Ali, J.R., Anderson, C.D., 1995a. Cenozoic motion of the Philippine Sea Plate — paleomagnetic evidence from eastern Indonesia. Tectonics 14, 1117–1132.
Hall, R., Ali, J.R., Anderson, C.D., Baker, S.J., 1995b. Origin and motion history of the Philippine Sea Plate. Tectonophysics 251, 229–250.
Hall, R., Fuller, M., Ali, J.R., Anderson, C.D., 1995c. The Philippine Sea Plate: magnetism and reconstructions. In: Taylor, B., Natland, J. (Eds.), Active Margins and Marginal Basins of the Western Pacific. American Geophysical Union, Geophysical Monograph 88, pp. 371–404.
Hall, R., van Hattum, M.W.A., Spakman, W., 2008. Impact of India–Asia collision on SE Asia: the record in Borneo. Tectonophysics 451, 366–389.
Hall, R., Cross, L., Clements, B., Spakman, W., 2009. Neogene subduction beneath Java: slab tearing, arc deformation and arc magmatism, and their causes. SAGE 2009: Southeast Asian Gateway Evolution Conference, Royal Holloway University of London, UK.
Hamburger, M.W., Cardwell, R.K., Isacks, B.L., 1983. Seismotectonics of the northern Philippine Island Arc. In: Hayes, D.E. (Ed.), The Tectonic and Geologic Evolution of Southeast Asian Seas and Islands, Part 2Geophysical Monograph 27. American Geophysical Union, Washington, D.C., pp. 1–22.
Hamilton, W., 1974. Earthquake map of the Indonesian Region. U.S. Geological Survey, Miscellaneous Investigations Series Map I-875-C.
Hamilton, W., 1979. Tectonics of the Indonesian region. U.S. Geological Survey Professional Paper 1078 (345 pp.).
Hamilton, W., 1988. Plate tectonics and island arcs. Geol. Soc. Am. Bull. 100, 1503–1527.
Hamilton, W., 2007. Driving mechanism and 3-D circulation of plate tectonics. In: Sears, J.W., Harms, T.A., Evenchick, C.A. (Eds.), Whence the Mountains? Inquiries into the Evolution of Orogenic Systems. Geological Society of America Special Paper 433, pp. 1–25.
Hammond, J.O.S., Wookey, J., Kaneshima, S., Inoue, H., Yamashina, T., Harjadi, P., 2010. Systematic variation in anisotropy beneath the mantle wedge in the Java–Sumatra subduction system from shear-wave splitting. Phys. Earth Planet. Inter. 178, 189–201.
Harris, R., 2011. The nature of the Banda Arc–continent collision in the Timor region. In: Brown, D., Ryan, P.D. (Eds.), Arc-Continent CollisionFrontiers in Earth Sciences. Springer-Verlag Berlin, Heidelberg, pp. 163–211.
Hatherton, T., Dickinson, W.R., 1969. The relationship between andesitic volcanism and seismicity in Indonesia, the Lesser Antilles, and other island arcs. J. Geophys. Res. 74, 5301–5310.
Heine, C., Muller, R.D., 2005. Late Jurassic rifting along the Australian North West Shelf: margin geometry and spreading ridge configuration. Aust. J. Earth Sci. 52, 27–39.
Heine, C., Muller, D., Gaina, C., 2004. Reconstructing the lost Eastern Tethys Ocean Basin: convergence of the SE Asian margin and marine gateways. In: Clift, P., Wang, P., Kuhnt, W., Hayes, D.E. (Eds.), Continent–Ocean Interactions within the East Asian Marginal SeasGeophysical Monograph 149. American Geophysical Union, Washington, D.C., pp. 37–54.

Hennig, J., Hall, R., Watkinson, I., Forster, M., 2012. Timing and mechanisms of exhumation in west Central Sulawesi, Indonesia. AGU Fall Meeting, San Francisco.
Hennig, J., Advokaat, E., Rudyawan, A., Hall, R., 2014. Large sediment accumulations and major subsidence offshore; rapid uplift on land: consequences of extension of Gorontalo Bay and northern Sulawesi. Proceedings Indonesian Petroleum Association, 38th Annual Convention, IPA14-G-304 1-16.
Hennig, J., Hall, R., Armstrong, R., 2015. U-Pb zircon geochronology of rocks from west Central Sulawesi, Indonesia: extension-related metamorphism and magmatism during the early stages of mountain building. Gondwana Res. (in press), http://dx/doi.rg/10.1016/j.gr.2014.12.012.
Hilton, D.R., Hoogewerff, J.A., van Bergen, M.J., Hammerschmidt, K., 1992. Mapping magma sources in the east Sunda–Banda arcs, Indonesia: constraints from Helium isotopes. Geochim. Cosmochim. Acta 56, 851–859.
Hinschberger, F., Malod, J.-A., Rehault, J.-P., Villeneuve, M., Royer, J.-Y., Burhanuddin, S., 2005. Late Cenozoic geodynamic evolution of eastern Indonesia. Tectonophysics 404, 91–118.
Hoang, N., Flower, M., 1998. Petrogenesis of Cenozoic basalts from Vietnam: implication for origins of a 'diffuse igneous province'. J. Petrol. 39, 369–395.
Hoernle, K., Hauff, F., Werner, R., van den Bogaard, P., Gibbons, A.D., Conrad, S., Müller, R.D., 2011. Origin of Indian Ocean Seamount Province by shallow recycling of continental lithosphere. Nat. Geosci. 4, 883–887. http://dx.doi.org/10.1038/ngeo1331.
Holloway, N.H., 1982. North Palawan block, Philippines — its relation to Asian mainland and role in evolution of South China Sea. Am. Assoc. Pet. Geol. Bull. 66, 1355–1383.
Honza, E., Fujioka, K., 2004. Formation of arcs and backarc basins inferred from the tectonic evolution of Southeast Asia since the Late Cretaceous. Tectonophysics 384, 23–53.
Huang, H.-H., Wu, Y.-M., Song, X., Chang, C.-H., Lee, S.-J., Chang, T.-M., Hsieh, H.-H., 2014. Joint Vp and Vs tomography of Taiwan: implications for subduction-collision orogeny. Earth Planet. Sci. Lett. 392, 177–191.
Humphreys, E., Clayton, R.W., 1988. Adaptation of back projection tomography to seismic travel time problems. J. Geophys. Res. 93, 1073–1085.
Hutchison, C.S., 1989. Geological evolution of South-East Asia. Oxford Monographs on Geology and Geophysics 13. Clarendon Press (376 pp.).
Imbus, S.W., Katz, B.J., Urwongse, T., 1998. Predicting $CO_2$ occurrence on a regional scale: Southeast Asia example. Org. Geochem. 29, 325–345.
ISC, 2015. EHB Bulletin. http://www.isc.ac.uk/ehbbulletin/.
Jagoutz, O., Royden, L., Holt, A.F., Becker, T.W., 2015. Anomalously fast convergence of India and Eurasia caused by double subduction. Nat. Geosci. 8, 475–478.
Kárason, H., 2002. Constraints on mantle convection from seismic tomography and flow modeling. Massachusetts Institute of Technology, Cambridge, MA (PhD Thesis).
Karig, D.E., 1983. Accreted terranes in the northern part of the Philippine archipelago. Tectonics 2, 211–236.
Karig, D.E., Sarewitz, D.R., Haeck, G.D., 1986. Role of strike-slip faulting in the evolution of allochthonous terranes in the Philippines. Geology 14, 852–855.
Katili, J.A., 1973. On fitting certain geological and geophysical features of the Indonesian island arc to the new global tectonics. In: Coleman, P.J. (Ed.), The Western Pacific: Island arcs, Marginal Seas, Geochemistry. University of Western Australia Press, Perth, pp. 287–305.
Katili, J.A., 1975. Volcanism and plate tectonics in the Indonesian island arcs. Tectonophysics 26, 165–188.
Katili, J.A., 1978. Past and present geotectonic position of Sulawesi, Indonesia. Tectonophysics 45, 289–322.
Keep, M., Haig, D.W., 2010. Deformation and exhumation in Timor: distinct stages of a young orogeny. Tectonophysics 483, 93–111.
Kennett, B.L., Cummins, P.R., 2005. The relationship of the seismic source and subduction zone structure for the 2004 December 26 Sumatra–Andaman earthquake. Earth Planet. Sci. Lett. 239, 1–8.
Kennett, B.L.N., Engdahl, E.R., Buland, R., 1995. Constraints on seismic velocities in the Earth from travel times. Geophys. J. Int. 122, 108–124.
Kopp, C., Flueh, E.R., Neben, S., 1999. Rupture and accretion of the Celebes Sea crust related to the North-Sulawesi subduction: combined interpretation of reflection and refraction seismic measurements. J. Geodyn. 27, 309–325.
Kopp, H., Flueh, E.R., Petersen, C.J., Weinrebe, W., Wittwer, A., Scientists, M., 2006. The Java margin revisited: Evidence for subduction erosion off Java. Earth Planet. Sci. Lett. 242, 130–142.
Lallemand, S., Font, Y., Bijwaard, H., Kao, H., 2001. New insights on 3-D plates interaction near Taiwan from tomography and tectonic implications. Tectonophysics 335, 229–253.
Lange, D., Tilmann, F., Rietbrock, A., Collings, R., Natawidjaja, D.H., Suwargadi, B.W., Barton, P., Henstock, T., Ryberg, T., 2010. The fine structure of the subducted Investigator Fracture Zone in western Sumatra as seen by local seismicity. Earth Planet. Sci. Lett. 298, 47–56.
Laske, G., Masters, G., Reif, C., 2013. CRUST 2.0 A New Global Crustal Model at 2x2 Degrees. http://igppweb.ucsd.edu/~gabi/crust2.html.
Lebedev, S., Nolet, G., 2003. Upper mantle beneath Southeast Asia from S velocity tomography. J. Geophys. Res. 108. http://dx.doi.org/10.1029/2000JB000073.
Lee, T.-Y., Lawver, L.A., 1995. Cenozoic plate reconstruction of Southeast Asia. Tectonophysics 251, 85–138.
Lévêque, J.-J., Rivera, L., Wittlinger, G., 1993. On the use of the checker-board test to assess the resolution of tomographic inversions. Geophys. J. Int. 115, 313–318.
Lewis, J.C., Byrne, T.B., 2003. History of metamorphic fluids along outcrop-scale faults in a Paleogene accretionary prism, SW Japan: implications for prism-scale hydrology. Geochem. Geophys. Geosyst. 4, 9007. http://dx.doi.org/10.1029/2002gc000359.
Li, Z.X., Li, X.H., 2007. Formation of the 1300-km-wide intracontinental orogen and postorogenic magmatic province in Mesozoic South China: a flat-slab subduction model. Geology 35, 179–182.
Li, C., van der Hilst, R.D., 2010. Structure of the upper mantle and transition zone beneath Southeast Asia from traveltime tomography. J. Geophys. Res. 115, B07308. http://dx.doi.org/10.1029/2009jb006882.
Li, C., van der Hilst, R.D., Engdahl, E.R., Burdick, S., 2008. A new global model for P wave speed variations in Earth's mantle. Geochem. Geophys. Geosystems. 9, 5. http://dx.doi.org/10.1029/2007GC001806.
Lin, J.-Y., Hsu, S.-K., Sibuet, J.-C., 2004. Melting features along the western Ryukyu slab edge (northeast Taiwan): tomographic evidence. J. Geophys. Res. 109, B12402. http://dx.doi.org/10.1029/2004jb003260.
Lister, G.S., White, L.T., Hart, S., Forster, M.A., 2012. Ripping and tearing the rolling-back New Hebrides slab. Aust. J. Earth Sci. 59, 899–911.
Lunt, P., 2013. The Sedimentary Geology of Java. Indonesian Petroleum Association.
Lunt, P., Burgon, G., Baky, A., 2009. The Pemali Formation of Central Java and equivalents: indicators of sedimentation on an active plate margin. J. Asian Earth Sci. 34, 100–113.
Macpherson, C.G., Chiang, K.K., Hall, R., Nowell, G.M., Castillo, P.R., Thirlwall, M.F., 2010. Plio-Pleistocene intra-plate magmatism from the southern Sulu Arc, Semporna peninsula, Sabah, Borneo: implications for high-Nb basalt in subduction zones. J. Volcanol. Geotherm. Res. 190, 25–38.
Maruyama, S., Isozaki, Y., Kimura, G., Terabayashi, M., 1997. Paleogeographic maps of the Japanese Islands: plate tectonic synthesis from 750 Ma to the present. Island Arc 6, 121–142.
McCaffrey, R., 1988. Active tectonics of the eastern Sunda and Banda Arcs. J. Geophys. Res. 93, 15163–15182.
McCaffrey, R., 1989. Seismological constraints and speculations on Banda Arc tectonics. Neth. J. Sea Res. 24, 141–152.
McCaffrey, R., 1996. Slip partitioning at convergent plate boundaries of SE Asia. In: Hall, R., Blundell, D.J. (Eds.), Tectonic Evolution of SE Asia. Geological Society of London Special Publication 106, pp. 3–18.
McCaffrey, R., Silver, E.A., Raitt, R.W., 1980. Crustal structure of the Molucca Sea collision zone, Indonesia. In: Hayes, D.E. (Ed.), The tectonic and geologic evolution of Southeast Asian seas and islands, part 1. American Geophysical Union, Geophysical Monographs Series 23, pp. 161–178.
McCaffrey, R., Molnar, P., Roecker, S., Joyodiwiryo, Y., 1985. Microearthquake seismicity and fault plane solutions related to arc-continent collision in the eastern Sunda Arc, Indonesia. J. Geophys. Res. 90, 4511–4528.
Metcalfe, I., 1990. Allochthonous terrane processes in Southeast Asia. Phil. Trans. R. Soc. London A331, 625–640.
Metcalfe, I., 2011. Tectonic framework and Phanerozoic evolution of Sundaland. Gondwana Res. 19, 3–21.
Metcalfe, I., 2013. Gondwana dispersion and Asian accretion: tectonic and palaeogeographic evolution of eastern Tethys. J. Asian Earth Sci. 66, 1–33.
Miller, M.S., Kennett, B.L.N., 2006. Evolution of mantle structure beneath the northwest Pacific: evidence from seismic tomography and paleogeographic reconstructions. Tectonics 25, TC4002. http://dx.doi.org/10.1029/2005TC001909.
Miller, M.S., Kennett, B.L.N., Toy, V.G., 2006. Spatial and temporal evolution of the subducting Pacific plate structure along the western Pacific margin. J. Geophys. Res. 111, B02401. http://dx.doi.org/10.1029/2005JB003705.
Milsom, J., 2001. Subduction in eastern Indonesia: how many slabs? Tectonophysics 338, 167–178.
Montelli, R., Nolet, G., Dahlen, F.A., Masters, G., 2006. A catalogue of deep mantle plumes: new results from finite-frequency tomography. Geochem. Geophys. Geosyst. 7. http://dx.doi.org/10.1029/2006gc001248.
Moore, G.F., Silver, E.A., 1983. Collision processes in the northern Molucca Sea. In: Hayes, D.E. (Ed.), The Tectonic and Geologic Evolution of Southeast Asian Seas and Islands, Part 2. American Geophysical Union, Geophysical Monograph 27, pp. 360–372.
Müller, R.D., Royer, J.-Y., Lawver, L.A., 1993. Revised plate motions relative to hotspots from combined Atlantic and Indian Ocean hotspot tracks. Geology 21, 275–278.
Newcomb, K.R., McCann, W.R., 1987. Seismic history and seismotectonics of the Sunda Arc. J. Geophys. Res. 92, 421–440.
Nguyen, T.T.B., Satir, M., Siebel, W., Chen, S., 2004. Granitoids in the Dalat zone, southern Vietnam: age constraints on magmatism and regional geological implications. Int. J. Earth Sci. 93, 329–340.
Nolet, G., 2008. A Breviary of Seismic Tomography: Imaging the Interior of the Earth and Sun. Cambridge University Press (344 pp.).
Page, B.N.G., Bennett, J.D., Cameron, N.R., Bridge, D.M., Jeffrey, D.H., Keats, W., Thaib, J., 1979. A review of the main structural and magmatic features of northern Sumatra. J. Geol. Soc. Lond. 136, 569–579.
Pesicek, J.D., Thurber, C.H., Widiyantoro, S., Engdahl, E.R., DeShon, H.R., 2008. Complex slab subduction beneath northern Sumatra. Geophys. Res. Lett. 35. http://dx.doi.org/10.1029/2008GL035262.
Pesicek, J.D., Thurber, C.H., Widiyantoro, S., Zhang, H., DeShon, H.R., Engdahl, E.R., 2010. Sharpening the tomographic image of the subducting slab below Sumatra, the Andaman Islands and Burma. Geophys. J. Int. 182, 433–453.
Pezzati, G., Hall, R., Burgess, P., Perez-Gussinye, M., 2014a. Pliocene core complex exhumation on land and rapid subsidence in Gorontalo Bay, Sulawesi (Indonesia). AGU Fall Meeting December 2014, San Francisco.
Pezzati, G., Hall, R., Burgess, P., Perez-Gussinye, M., 2014b. The Poso Basin in Gorontalo Bay, Sulawesi: extension related to core complex formation on land. Proceedings Indonesian Petroleum Association, 38th Annual Convention, IPA14-G-297 1-12.
Pholbud, P., Hall, R., Advokaat, E., Burgess, P., Rudyawan, A., 2012. A new interpretation of Gorontalo Bay, Sulawesi. Proceedings Indonesian Petroleum Association, 36th Annual Convention, IPA12-G-039 1-23.
Pieters, P.E., Pigram, C.J., Trail, D.S., Dow, D.B., Ratman, N., Sukamto, R., 1983. The stratigraphy of western Irian Jaya. Bull. Geol. Res. Dev. Cent. Bandung 8, 14–48.

Pownall, J.M., Hall, R., Watkinson, I.M., 2013. Extreme extension across Seram and Ambon, eastern Indonesia: evidence for Banda slab rollback. Solid Earth 4, 277–314.
Pownall, J.M., Hall, R., Armstrong, R.A., Forster, M.A., 2014. Earth's youngest known ultrahigh-temperature granulites discovered on Seram, eastern Indonesia. Geology 42, 279–282.
Prawirodirdjo, L., McCaffrey, R., Chadwell, C.D., Bock, Y., Subarya, C., 2010. Geodetic observations of an earthquake cycle at the Sumatra subduction zone: role of interseismic strain segmentation. J. Geophys. Res. 115, B03414. http://dx.doi.org/10.1029/2008jb006139.
Pubellier, M., Quebral, R., Rangin, C., Deffontaines, B., Müller, C., Butterlin, J., Manzano, J., 1991. The Mindanao Collision Zone: a soft collision event with a continuous Neogene strike-slip setting. J. SE Asian Earth Sci. 6, 239–248.
Puspito, N.T., Shimazaki, K., 1995. Mantle structure and seismotectonics of the Sunda and Banda arcs. Tectonophysics 251, 215–228.
Puspito, N.T., Yamanaka, Y., Miyatake, T., Shimazaki, K., Hirahara, K., 1993. Three-dimensional P-wave velocity structure beneath the Indonesian region. Tectonophysics 220, 175–192.
Quarles van Ufford, A., Cloos, M., 2005. Cenozoic tectonics of New Guinea. Am. Assoc. Pet. Geol. Bull. 89, 119–140.
Queano, K.L., Ali, J.R., Milsom, J., Aitchison, J.C., Pubellier, M., 2007. North Luzon and the Philippine Sea Plate motion model: Insights following paleomagnetic, structural, and age-dating investigations. J. Geophys. Res. 112, B05101. http://dx.doi.org/10.1029/2006JB004506.
Quebral, R., Rangin, C., Pubellier, M., 1996. The onset of movement on the Philippine Fault in eastern Mindanao: a transition from collision to strike-slip environment. Tectonics 15, 713–726.
Rangin, C., 1991. The Philippine Mobile Belt: a complex plate boundary. J. SE Asian Earth Sci. 6, 209–220.
Rangin, C., Silver, E.A., 1991. Neogene tectonic evolution of the Celebes Sulu basins; new insights from Leg 124 drilling. In: Silver, E.A., Rangin, C., von Breymann, M.T., et al. (Eds.), Proceedings of the Ocean Drilling Program, Scientific Results 124, pp. 51–63.
Rangin, C., Stephan, J.F., Butterlin, J., Bellon, H., Muller, C., Chorowicz, J., Baladad, D., 1991. Collision Néogène d'arcs volcaniques dans le centre des Philippines. Stratigraphie et structure de la chaîne d'Antique: Ile de Panay. Bull. Géol. Soc. Fr. 162, 465–477.
Rangin, C., Maury, R.C., Polvé, M., Bellon, H., Priadi, B., Soeria-Atmadja, R., Cotten, J., Joron, J.L., 1997. Eocene to Miocene back-arc basin basalts and associated island arc tholeiites from northern Sulawesi (Indonesia): implications for the geodynamic evolution of the Celebes basin. Bull. Soc. Geol. Fr. 168, 627–635.
Rangin, C., Spakman, W., Pubellier, M., Bijwaard, H., 1999. Tomographic and geological constraints on subduction along the eastern Sundaland continental margin (South-East Asia). Bull. Soc. Geol. Fr. 170, 775–788.
Rawlinson, N., Fichtner, A., Sambridge, M., Young, M.K., 2014. Seismic tomography and the assessment of uncertainty. Adv. Geophys. 55, 1–76.
Replumaz, A., Tapponnier, P., 2003. Reconstruction of the deformed collision zone between India and Asia by backward motion of lithospheric blocks. J. Geophys. Res. 108. http://dx.doi.org/10.1029/2001JB000661.
Replumaz, A., Karason, H., van der Hilst, R.D., Besse, J., Tapponnier, P., 2004. 4-D evolution of SE Asia's mantle from geological reconstructions and seismic tomography. Earth Planet. Sci. Lett. 221, 103–115.
Richards, S., Lister, G., Kennett, B., 2007. A slab in depth: three-dimensional geometry and evolution of the Indo-Australian plate. Geochem. Geophys. Geosyst. 8. http://dx.doi.org/10.1029/2007GC001657.
Ricou, L.E., 1994. Tethys reconstructed — plates, continental fragments and their boundaries since 260 Ma from Central America to Southeastern Asia. Geodin. Acta 7, 169–218.
Ringwood, A.E., Irifune, T., 1988. Nature of the 650 km seismic discontinuity: implications for mantle dynamics and differentiation. Nature 331, 131–136.
Ritsema, J., Deuss, A., van Heijst, H.J., Woodhouse, J.H., 2011. S40RTS: a degree-40 shear-velocity model for the mantle from new Rayleigh wave dispersion, teleseismic traveltime and normal-mode splitting function measurements. Geophys. J. Int. 184, 1223–1236.
Ritzwoller, M.H., Shapiro, N.M., Barmin, M.P., Levshin, A.L., 2002. Global surface wave diffraction tomography. J. Geophys. Res. 107, 2335. http://dx.doi.org/10.1029/2002jb001777.
Rosenbaum, G., Gasparon, M., Lucente, F.P., Peccerillo, A., Miller, M.S., 2008. Kinematics of slab tear faults during subduction segmentation and implications for Italian magmatism. Tectonics 27. http://dx.doi.org/10.1029/2007TC002143.
Rudyawan, A., Hall, R., White, L., 2014. Neogene extension of the central north Arm of Sulawesi, Indonesia. AGU Fall Meeting December 2014, San Francisco.
Rutland, R.W.R., 1968. A tectonic study of part of the Philippine Fault zone. Q. J. Geol. Soc. Lond. 123, 293–325.
Sajona, F., Maury, R.C., Bellon, H., Cotten, J., Defant, M., 1996. High field strength element enrichment of Pliocene-Pleistocene island arc basalts, Zamboanga Peninsula, Western Mindanao (Philippines). J. Petrol. 37, 693–726.
Sajona, F.G., Maury, R.C., Pubellier, M., Leterrier, J., Bellon, H., Cotten, J., 2000. Magmatic source enrichment by slab-derived melts in a young post-collision setting, central Mindanao (Philippines). Lithos 54, 173–206.
Sandiford, M., 2008. Seismic moment release during slab rupture beneath the Banda Sea. Geophys. J. Int. 174, 659–671.
Sandwell, D.T., Smith, W.H.F., 2009. Global marine gravity from retracked Geosat and ERS-1 altimetry: ridge segmentation versus spreading rate. J. Geophys. Res. 114, B01411. http://dx.doi.org/10.1029/2008JB006008.
Schellart, W.P., Spakman, W., 2012. Mantle constraints on the plate tectonic evolution of the Tonga–Kermadec–Hikurangi subduction zone and the South Fiji Basin region. Aust. J. Earth Sci. 59, 933–952.
Schaeffer, A.J., Lebedev, S., 2013. Global shear-speed structure of the upper mantle and transition zone. Geophysical Journal International 194, 417–449.
Schellart, W.P., Kennett, B.L.N., Spakman, W., Amaru, M., 2009. Plate reconstructions and tomography reveal a fossil lower mantle slab below the Tasman Sea. Earth Planet. Sci. Lett. 278, 143–151.
Schöffel, H.-J., Das, S., 1999. Fine details of the Wadati–Benioff zone under Indonesia and its geodynamic implications. J. Geophys. Res. 104, 13101–13114.
Seno, T., Maruyama, S., 1984. Palaeogeographic reconstruction and origin of the Philippine Sea. Tectonophysics 102, 53–84.
Seno, T., Stein, S.A., Gripp, A.E., Demets, C.R., 1993. A model for the motion of the Philippine Sea plate consistent with NUVEL-1. J. Geophys. Res. 98, 17941–17948.
Shapiro, N.M., Ritzwoller, M.H., Engdahl, E.R., 2008. Structural context of the Great Sumatra–Andaman Islands earthquake. Geophys. Res. Lett. 35, L05301. http://dx.doi.org/10.1029/2008GL033381.
Shulgin, A., Kopp, H., Mueller, C., Planert, L., Lueschen, E., Flueh, E.R., Djajadihardja, Y., 2011. Structural architecture of oceanic plateau subduction offshore Eastern Java and the potential implications for geohazards. Geophys. J. Int. 184, 12–28.
Siebert, L., Simkin, T., 2002. Volcanoes of the World: an Illustrated Catalog of Holocene Volcanoes and their Eruptions. Smithsonian Institution, Global Volcanism Program Digital Information Series, GVP-3 (http://www.volcano.si.edu/world/).
Silver, E.A., Moore, J.C., 1978. The Molucca Sea collision zone, Indonesia. J. Geophys. Res. 83, 1681–1691.
Silver, E.A., Rangin, C., 1991. Leg 124 tectonic synthesis. In: Silver, E.A., Rangin, C., von Breymann, M.T., et al. (Eds.), Proceedings of the Ocean Drilling Program, Scientific Results 124, pp. 3–9.
Silver, E.A., McCaffrey, R., Joyodiwiryo, Y., Stevens, S., 1983a. Ophiolite emplacement and collision between the Sula platform and the Sulawesi island arc, Indonesia. J. Geophys. Res. 88, 9419–9435.
Silver, E.A., McCaffrey, R., Smith, R.B., 1983b. Collision, rotation, and the initiation of subduction in the evolution of Sulawesi, Indonesia. J. Geophys. Res. 88, 9407–9418.
Silver, E.A., Reed, D., McCaffrey, R., Joyodiwiryo, Y., 1983c. Back arc thrusting in the eastern Sunda arc, Indonesia: a consequence of arc-continent collision. J. Geophys. Res. 88, 7429–7448.
Silver, E.A., Gill, J.B., Schwartz, D., Prasetyo, H., Duncan, R.A., 1985. Evidence of submerged and displaced continental borderland, north Banda Sea, Indonesia. Geology 13, 687–691.
Silver, E.A., Rangin, C., von Breymann, M.T., et al., 1991. Proc. Ocean Drill. Program Sci. Results 124.
Simandjuntak, T.O., Barber, A.J., 1996. Contrasting tectonic styles in the Neogene orogenic belts of Indonesia. In: Hall, R., Blundell, D.J. (Eds.), Tectonic Evolution of SE Asia. Geological Society of London Special Publication 106, pp. 185–201.
Simons, W.J.F., Socquet, A., Vigny, C., Ambrosius, B.A.C., Abu, S.H., Promthong, C., Subarya, C., Sarsito, D.A., Matheussen, S., Morgan, P., 2007. A decade of GPS in Southeast Asia: Resolving Sundaland motion and boundaries. J. Geophys. Res. 112, B06420.
Smith, R.B., Silver, E.A., 1991. Geology of a Miocene collision complex, Buton, eastern Indonesia. Geol. Soc. Am. Bull. 103, 660–678.
Smyth, H.R., Hamilton, P.J., Hall, R., Kinny, P.D., 2007. The deep crust beneath island arcs: inherited zircons reveal a Gondwana continental fragment beneath East Java, Indonesia. Earth Planet. Sci. Lett. 258, 269–282.
Smyth, H.R., Hall, R., Nichols, G.J., 2008. Cenozoic volcanic arc history of East Java, Indonesia: the stratigraphic record of eruptions on an active continental margin. In: Draut, A.E., Clift, P.D., Scholl, D.W. (Eds.), Formation and Applications of the Sedimentary Record in Arc Collision Zones. Geological Society of America Special Paper 436, pp. 199–222.
Socquet, A., Simons, W., Vigny, C., McCaffrey, R., Subarya, C., Sarsito, D., Ambrosius, B., Spakman, W., 2006. Microblock rotations and fault coupling in SE Asia triple junction (Sulawesi, Indonesia) from GPS and earthquake slip vector data. J. Geophys. Res. 111, B08409. http://dx.doi.org/10.1029/2005JB003963.
Spakman, W., Van der Lee, S., Van der Hilst, R.D., 1993. Travel-time tomography of the European-Mediterranean mantle down to 1400km. Phys. Earth. Planet. Int. 79, 3–74.
Spakman, W., Bijwaard, H., 2001. Optimization of cell parameterizations for tomographic inverse problems. Pure Appl. Geophys. 158, 1401–1423.
Spakman, W., Hall, R., 2010. Surface deformation and slab-mantle interaction during Banda Arc subduction rollback. Nat. Geosci. 3, 562–566.
Spakman, W., Nolet, G., 1988. Imaging algorithms, accuracy and resolution in delay time tomography. In: Vlaar, N.J., Nolet, G., Wortel, M.J.R., Cloetingh, S.A.P.L. (Eds.), Mathematical Geophysics. D. Reidel, Dordrecht, pp. 155–188.
Spakman, W., Wortel, R., 2004. A tomographic view on Western Mediterranean geodynamics. In: Cavazza, W., Roure, F., Spakman, W., Stampfli, G.M., Ziegler, P.A. (Eds.), The TRANSMED Atlas. The Mediterranean Region from Crust to Mantle. Springer Berlin, Heidelberg, pp. 31–52.
Spencer, J.E., 2010. Structural analysis of three extensional detachment faults with data from the 2000 Space-Shuttle Radar Topography Mission. GSA Today 20. http://dx.doi.org/10.1130/GSATG59A.
Spencer, J.E., 2011. Gently dipping normal faults identified with Space Shuttle radar topography data in central Sulawesi, Indonesia, and some implications for fault mechanics. Earth Planet. Sci. Lett. 308, 267–276.
Stephan, J.K., Blanchet, R., Rangin, C., Pelletier, B., Letouzey, J., Muller, C., 1986. Geodynamic evolution of the Taiwan-Luzon-Mindoro Belt since the Late Eocene. Tectonophysics 125, 245–268.
Surmont, J., Laj, C., Kissal, C., Rangin, C., Bellon, H., Priadi, B., 1994. New paleomagnetic constraints on the Cenozoic tectonic evolution of the North Arm of Sulawesi, Indonesia. Earth Planet. Sci. Lett. 121, 629–638.
Taira, A., 2001. Tectonic evolution of the Japanese island arc system. Annu. Rev. Earth Planet. Sci. 29, 109–134.
Tang, Q., Zheng, C., 2013. Crust and upper mantle structure and its tectonic implications in the South China Sea regions. J. Asian Earth Sci. 63, 510–525.

Taylor, B., Hayes, D.E., 1980. The tectonic evolution of the South China Sea Basin. In: Hayes, D.E. (Ed.), The tectonic and geologic evolution of Southeast Asian seas and islands. American Geophysical Union, Geophysical Monographs Series 23, pp. 89–104.
Taylor, B., Hayes, D.E., 1983. Origin and history of the South China Sea Basin. In: Hayes, D.E. (Ed.), The tectonic and geologic evolution of Southeast Asian seas and islands, Part 2. American Geophysical Union, Geophysical Monographs Series 27, pp. 23–56.
Thorkelson, D.J., 1996. Subduction of diverging plates and the principles of slab window formation. Tectonophysics 255, 47–63.
Torsvik, T.H., Smethurst, M.A., Burke, K., Steinberger, B., 2006. Large igneous provinces generated from the margins of the large low-velocity provinces in the deep mantle. Geophys. J. Int. 167, 1447–1460.
Trampert, J., Deschamps, F., Resovsky, J., Yuen, D., 2004. Probabilistic tomography maps chemical heterogeneities throughout the lower mantle. Science 306, 853–856.
Turner, S., Foden, J., George, R., Evans, P., Varne, R., Elburg, M., Jenner, G., 2003. Rates and processes of potassic magma evolution beneath Sangeang Api Volcano, East Sunda Arc, Indonesia. J. Petrol. 44, 491–515.
van Benthem, S., Govers, R., Spakman, W., Wortel, R., 2013. Tectonic evolution and mantle structure of the Caribbean. J. Geophys. Res. 118, 3019–3036. http://dx.doi.org/10.1002/jgrb.50235.
van der Hilst, R.D., Spakman, W., 1989. Importance of the reference model in linearized tomography and images of subduction below the Caribbean plate. Geophys. Res. Lett. 16, 1093–1096.
van der Hilst, R.D., Widiyantoro, S., Engdahl, E.R., 1997. Evidence for deep mantle circulation from global tomography. Nature 386 (6625), 578–584.
van der Meer, D.G., Spakman, W., van Hinsbergen, D.J.J., Amaru, M.L., Torsvik, T.H., 2010. Towards absolute plate motions constrained by lower-mantle slab remnants. Nat. Geosci. 3, 36–40.
van der Meer, D.G., Torsvik, T.H., Spakman, W., van Hinsbergen, D.J.J., Amaru, M.L., 2012. Intra-Panthalassa Ocean subduction zones revealed by fossil arcs and mantle structure. Nat. Geosci. 5, 215–219.
van der Voo, R., Spakman, W., Bijwaard, H., 1999. Tethyan subducted slabs under India. Earth Planet. Sci. Lett. 171, 7–20.
van der Werff, W., Kusnida, D., Prasetyo, H., van Weering, T.C.E., 1994. Origin of the Sumba forearc basement. Mar. Pet. Geol. 11, 363–374.
van Hinsbergen, D.J.J., Lippert, P.C., Dupont-Nivet, G., McQuarrie, N., Doubrovine, P.V., Spakman, W., Torsvik, T.H., 2012. Greater India Basin hypothesis and a two-stage Cenozoic collision between India and Asia. Proc. Natl. Acad. Sci. 109, 7659–7664.
van Wijk, J.W., Govers, R., Furlong, K.P., 2001. Three-dimensional thermal modeling of the California upper mantle: a slab window vs. stalled slab. Earth Planet. Lett. 186, 175–186.
Villeneuve, M., Rehault, J.P., Cornee, J.J., Honthaas, C., Gunawan, W., 1998. Geodynamic evolution of eastern Indonesia from the Eocene to the Pliocene. C.R. Acad. Sci. Ser. Paris Sci. Terre Planets 327, 291–302.
Villeneuve, M., Martini, R., Bellon, H., Réhault, J.-P., Cornée, J.-J., Bellier, O., Burhannuddin, S., Hinschberger, F., Honthaas, C., Monnier, C., 2010. Deciphering of six blocks of Gondwanan origin within Eastern Indonesia (South East Asia). Gondwana Res. 210, 420–437.
von Huene, R., Langseth, M., Nasu, N., Okada, H., 1982. A summary of Cenozoic tectonic history along the IPOD Japan Trench transect. Geol. Soc. Am. Bull. 93, 829–846.
Walpersdorf, A., Rangin, C., Vigny, C., 1998. GPS compared to long-term geologic motion of the north arm of Sulawesi. Earth Planet. Sci. Lett. 159, 47–55.
Wang, J.-H., Yin, A., Harrison, T.M., Grove, M., Zhang, Y.-Q., Xie, G.-H., 2001. A tectonic model for Cenozoic igneous activities in the eastern Indo–Asian collision zone. Earth Planet. Sci. Lett. 188, 123–133.
Watkinson, I.M., Hall, R., Ferdian, F., 2011. Tectonic re-interpretation of the Banggai–Sula–Molucca Sea margin, Indonesia. In: Hall, R., Cottam, M.A., Wilson, M.E.J. (Eds.), The SE Asian gateway: history and tectonics of Australia–Asia collision. Geological Society of London Special Publication 355, pp. 203–224.
Weiland, R.J., 1999. Emplacement of the Irian Ophiolite and Unroofing of the Ruffaer Metamorphic Belt of Irian Jaya, Indonesia PhD Thesis, University of Texas at Austin (525 pp.).
Wheller, G.E., Varne, R., Foden, J.D., Abbott, M.J., 1987. Geochemistry of Quaternary volcanism in the Sunda–Banda Arc, Indonesia, and three-component genesis of island-arc basaltic magmas. J. Volcanol. Geotherm. Res. 32, 137–160.
Whittaker, J.M., Müller, R.D., Sdrolias, M., Heine, C., 2007. Sunda–Java trench kinematics, slab window formation and overriding plate deformation since the Cretaceous. Earth Planet. Sci. Lett. 255, 445–457.
Whittaker, J.M., Williams, S.E., Müller, R.D., 2013. Revised tectonic evolution of the Eastern Indian Ocean. Geochem. Geophys. Geosyst. 14, 1891–1909. http://dx.doi.org/10.1002/ggge.20120.
Widiyantoro, S., Fauzi, 2005. Note on seismicity of the Bali convergent region in the eastern Sunda Arc, Indonesia. Aust. J. Earth Sci. 52, 379–383.
Widiyantoro, S., van der Hilst, R.D., 1997. Mantle structure beneath Indonesia inferred from high-resolution tomographic imaging. Geophys. J. Int. 130, 167–182.
Widiyantoro, S., Gorbatov, A., Kennett, B.L.N., Fukao, Y., 2000. Improving global shear wave traveltime tomography using three-dimensional ray tracing and iterative inversion. Geophys. J. Int. 141, 747–758.
Widiyantoro, S., Pesicek, J.D., Thurber, C.H., 2011. Subducting slab structure below the eastern Sunda Arc inferred from non-linear seismic tomographic imaging. In: Hall, R., Cottam, M.A., Wilson, M.E.J. (Eds.), The SE Asian gateway: history and tectonics of Australia–Asia collision. Geological Society of London Special Publication 355, pp. 139–155.
Widyantoro, S., van der Hilst, R.D., 1996. Structure and evolution of lithospheric slab beneath the Sunda Arc, Indonesia. Science 171, 1566–1570.
Wortel, M.J.R., Spakman, W., 2000. Subduction and slab detachment in the Mediterranean–Carpathian region. Science 290, 1910–1917.
Xu, Y., Wei, J., Qiu, H., Zhang, H., Huang, X., 2012. Opening and evolution of the South China Sea constrained by studies on volcanic rocks: Preliminary results and a research design. Chin. Sci. Bull. 57, 3150–3164.
Yumul Jr., G.P., Dimalanta, C.B., Tamayo, R.A., Maury, R.C., Bellon, H., Polvé, M., Maglambayan, V.B., Querubin, C.L., Cotten, J., 2004. Geology of the Zamboanga Peninsula, Mindanao, Philippines: an enigmatic South China continental fragment? Geol. Soc. Lond. Spec. Publ. 226, 289–312.
Yumul Jr., G.P., Dimalanta, C.B., Maglambayan, V.B., Marquez, E.J., 2008. Tectonic setting of a composite terrane: a review of the Philippine island arc system. Geosci. J. 12, 7–17.
Yumul Jr., G.P., Dimalanta, C.B., Marquez, E.J., Queaño, K.L., 2009. Onland signatures of the Palawan microcontinental block and Philippine mobile belt collision and crustal growth process: A review. J. Asian Earth Sci. 34, 610–623.
Zahirovic, S., Seton, M., Müller, R.D., 2014. The Cretaceous and Cenozoic tectonic evolution of Southeast Asia. Solid Earth 5, 227–273.
Zhou, X.M., Li, W.X., 2000. Origin of Late Mesozoic igneous rocks in Southeastern China: implications for lithosphere subduction and underplating of mafic magmas. Tectonophysics 326, 269–287.
Zhu, H., Bozdag, E., Peter, D., Tromp, J., 2012. Structure of the European upper mantle revealed by adjoint tomography. Nat. Geosci. 5, 493–498.